The A. & M. College of Texas

Department of

OCEANOGRAPHY AND METEOROLOGY

Research Conducted through the

Texas A & M Research Foundation

COLLEGE STATION, TEXAS

CHARACTERISTICS OF DEEP-SEA ANCHOR CABLES IN STRONG OCEAN CURRENTS

Basil W. Wilson

Research conducted under Bureau of Ships, Fundamental Hydromechanics Research Program NS 715-102, administered by the David Taylor Model Basin, U. S. Navy; Contract No. N onr 2119(02)

A. & M. Project 204
Reference 61-3-6

TECHNICAL REPORT
No. 204-3
February, 1961

THE AGRICULTURAL AND MECHANICAL COLLEGE OF TEXAS
Department of Oceanography and Meteorology
College Station, Texas

Research Conducted Through The
Texas A. & M. Research Foundation

CHARACTERISTICS OF DEEP-SEA ANCHOR CABLES IN STRONG OCEAN CURRENTS

Basil W. Wilson
Principal Investigator

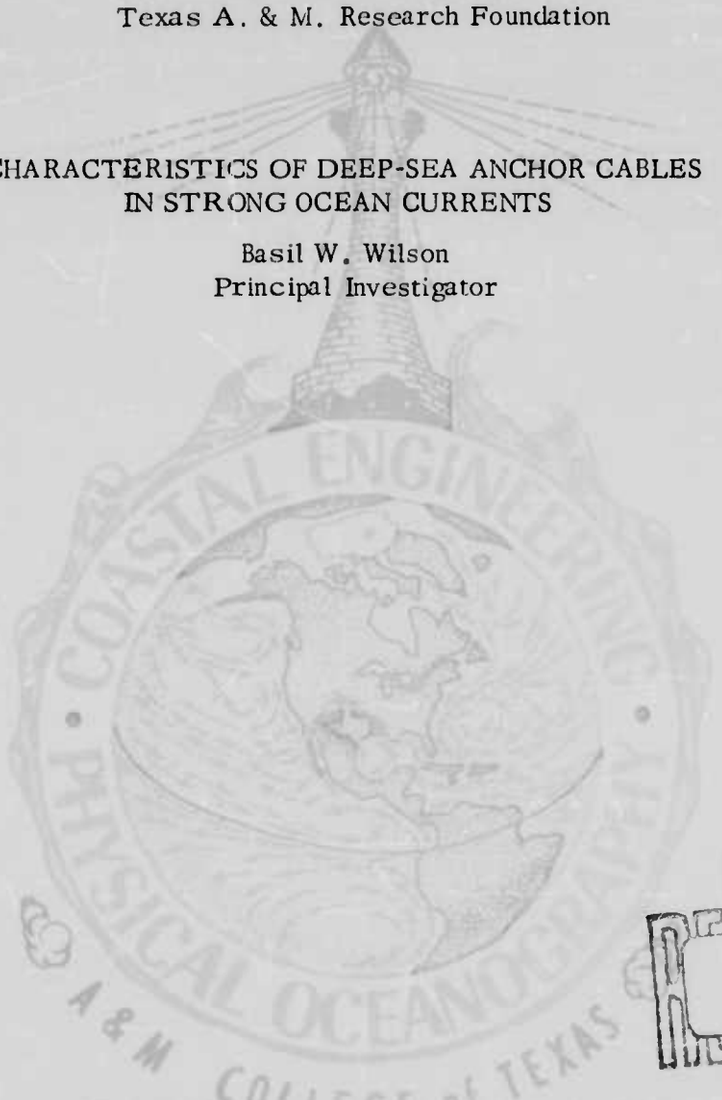

Project 204 is supported by the Bureau of Ships
Fundamental Hydromechanics Research Program NS 715-102
administered by the David Taylor Model Basin, U. S. Navy
Contract No. N onr 2119(02)
and by
The South African Railways and Harbours Administration
Technical Report No. 204-3
A & M Project 204 - Reference 61-1T

February, 1961

PREFACE

This report and its companion (No. 204-3A) investigate a second phase of study of the problem of deep-sea mooring of ships and other objects in winds, waves and currents and are direct sequels to Report No. 204-1 in this series. The mathematical tools developed in the latter report are here applied in evolving the characteristics of steel wire and nylon fiber mooring cables, used under realistic conditions in the deep-sea (nominal depth 12,000 ft), where strong ocean currents prevail. Almost any contingency of mooring situation is included in the number of worked examples, from which suitable interpolations can be made if need be for cases which do not exactly fit the conditions chosen. Examples of applications of the tables of cable characteristics to the solution of problems are given in demonstration of their usefulness. Still remaining to be solved are the influences of transient perturbations imposed on the mooring systems by waves and fluctuating winds.

Those who have assisted in computations for this study include Mrs. Linda Lindsay and Mrs. Beth Porter. To Mr. Robert E. Kilmer belongs the considerable credit of programming and executing the intricate calculations of cable functions on the No. 704 and, latterly, No. 709 IBM electronic computers. Mrs. Maxine Polaski, assisted by Mr. Joe Graham, has been responsible for drafting of figures, while Mrs. Carolyn Williams has undertaken the considerable task of typing the manuscript. The writer is greatly appreciative of the fine contributions of all these persons.

Basil W. Wilson
Principal Investigator

March, 1961
College Station, Texas

CONTENTS

LIST OF FIGURES

LIST OF TABLES

ABSTRACT

This report examines the steady state configuration of a deep-sea mooring cable in realistic ocean currents in a nominal water depth of 12,000 ft. The earlier solutions of the problem of a cable in a uniform current are here adapted to variable distributions of velocity by the artifice of considering the ocean as a series of laminae within each of which the current can be regarded as uniform. The calculation procedure is developed for stepwise numerical integrations, and computations have been made for a wide range of sizes of steel-wire and nylon rope mooring lines under two conditions of severe ocean currents, involving 6 and 3 knot velocities at the surface. Influences of the current are taken to vanish at a depth below the surface of 1000 m (3280 ft). Justifications for the choice of design currents are given. Results of the calculations are available in a series of figures and tables (the latter in companion Report 204-3A). Several examples of the use of the tables are given in solution of mooring problems.

CHARACTERISTICS OF DEEP-SEA ANCHOR CABLES IN STRONG OCEAN CURRENTS

SUMMARY AND CONCLUSIONS

1. Re-statement of Relevant Formulae

In continuation of the work of Report 204-1 of this series, the problem here considered is that of determining the shape and tensions in a deep-sea mooring cable when the moored object and the cable are subject to a strong ocean current having a velocity distribution variable with the depth. A review is given of applicable equations developed in Report 204-1.

2. Analysis of the New Problem

Solution of the problem of a variable current is approached by artificially layering the ocean depth and supposing that within such layers the current flow has uniform velocity. For each segment of cable that passes through a layer it is then possible to apply the equations of Report 204-1. To obtain continuity of results it is necessary that segments of cable in adjacent layers should have the same slope and the same tension at the contiguous boundary.

It is shown that the lower portion of a deep-sea mooring cable can be considered to pass through still water so that for this portion the simpler equations of a catenary can be applied.

For purposes of evaluating cable characteristics the equations of 1, suitably modified for digital procedures are integrated from the bottom of the cable upwards towards the surface. The flow diagram for the numerical process is detailed in an appendix.

3. Selection of Deep-Ocean Design Currents

To arrive at suitably severe design conditions consideration is given to the magnitudes of the flow in the ocean currents of the world. The surface and abyssal circulations are both discussed. Wind, it seems, is the principal agent in generating the major ocean circulations, though the earth's rotation and the land masses have important deflecting influences, and complex adjustments are required to accomodate the thermal and salinity structure of the oceans. The Gulf Stream in the North Atlantic, the Kuroshio in the West Pacific, the East Astralian as well as the East African coastal currents usually exhibit the highest velocities of flow. It

is shown that the steady flow in the Gulf Stream can be influenced by the lunar phases and by barometric pressure changes over the Gulf of Mexico. Local storms too can be expected to add current velocity to the extent of about 1 knot from the influence of wind stress and wave transport if wind direction is favorable.

As surface currents two design distributions of velocity are adopted for calculation purposes, one with a surface velocity of 6 knots and the other 3 knots. Based on measurements and calculations, the velocities are taken to decline with depth to insignificant values at about 1000 m below the surface.

Available information in regard to currents below this depth is examined and the conclusion reached that they are unlikely to exceed about 0.35 knot. They are therefore neglected entirely in the two design currents.

4. Numerical Computation of Cable Parameters

The hydrodynamic constants applicable to each artificial layer of moving water are calculated and tabulated for the design currents. Computations of cable characteristics in a water depth of 12,000 ft have been undertaken for a range of sizes of steel wire and nylon rope cables using the facilities of No. 704 and 709 IBM electronic digital computers. Results are given in detail in a series of tables forming a companion report (No. 204-3A) to the present one. Main features of the cable configurations are illustrated in a series of figures, suitable for quick reference.

5. Examples of Cable Calculations

As examples of the manner of interpreting and applying the tables of Report 204-3A four problems are posed and the solutions given. These treat

(a) Mooring conditions of typical ships in the design currents
(b) Disposition of a taut-line submerged buoy in design current A
(c) Use of a ground line and clump in anchoring a ship in design current A
(d) Possible use of drogue-anchor systems for large ships in strong currents.

The conclusion is reached that it would generally be impractical to moor very large ships in such severe conditions as a 6 knot current with a following wind of gale force without the use of extremely heavy equipment or a duplication of anchor lines.

CHARACTERISTICS OF DEEP-SEA ANCHOR CABLES IN STRONG OCEAN CURRENTS

Basil W. Wilson

I. RE-STATEMENT OF RELEVANT FORMULAE

1. Introduction

The problem here posed is that of applying the methods of computation evolved in the first report of this series (No. 204-1 : Characteristics of Anchor Cables in Uniform Ocean Currents, April 1960) to the case of an anchor cable in deep water (nominally 12,000 feet in depth) in which the moored object and cable are subject to realisticly strong ocean currents. Such currents, of course, are normally non-uniform over the depth, as will be shown later from numerous sources of supporting evidence, and this variability therefore introduces a new complication into the problem treated in the earlier report.

The new problem otherwise retains the simple features of that solved in Report 204-1. Thus the cable is assumed to lie only in a vertical plane, the same as the variable current vectors throughout the water depth. The cable is considered to have uniform line density, though in point of fact this need not be a condition; it is also taken to be flexible enough not to require consideration of any moment transmission along its length. The current is assumed to flow horizontally only and the drag on the ship (or surface float) may be inclusive of the wind drag provided the latter is in the same direction as the stream flow of the water. The water is again assumed to be free of transient disturbances such as gravity waves or turbulence which could lead to temporary fluctuations in the strength of the current.

2. Review of Analysis for a Cable in a Uniform Current

It is appropriate here to review the equations that represent the equilibrium of a cable in a uniform ocean current as analysed in Report 204-1. These equations will have significant application to the more complex problem of the cable in a non-uniform current.

We revert for description to Fig. 1 which is reproduced from Report 204-1. In that report the configuration of the cable was conveniently represented by the radius of curvature R at any point (x', z'), in the length AB of the cable, referred to an origin B (the anchor) on the sea-bed. The magnitude of R could be calculated as a ratio of R_o the radius of curvature (or height above

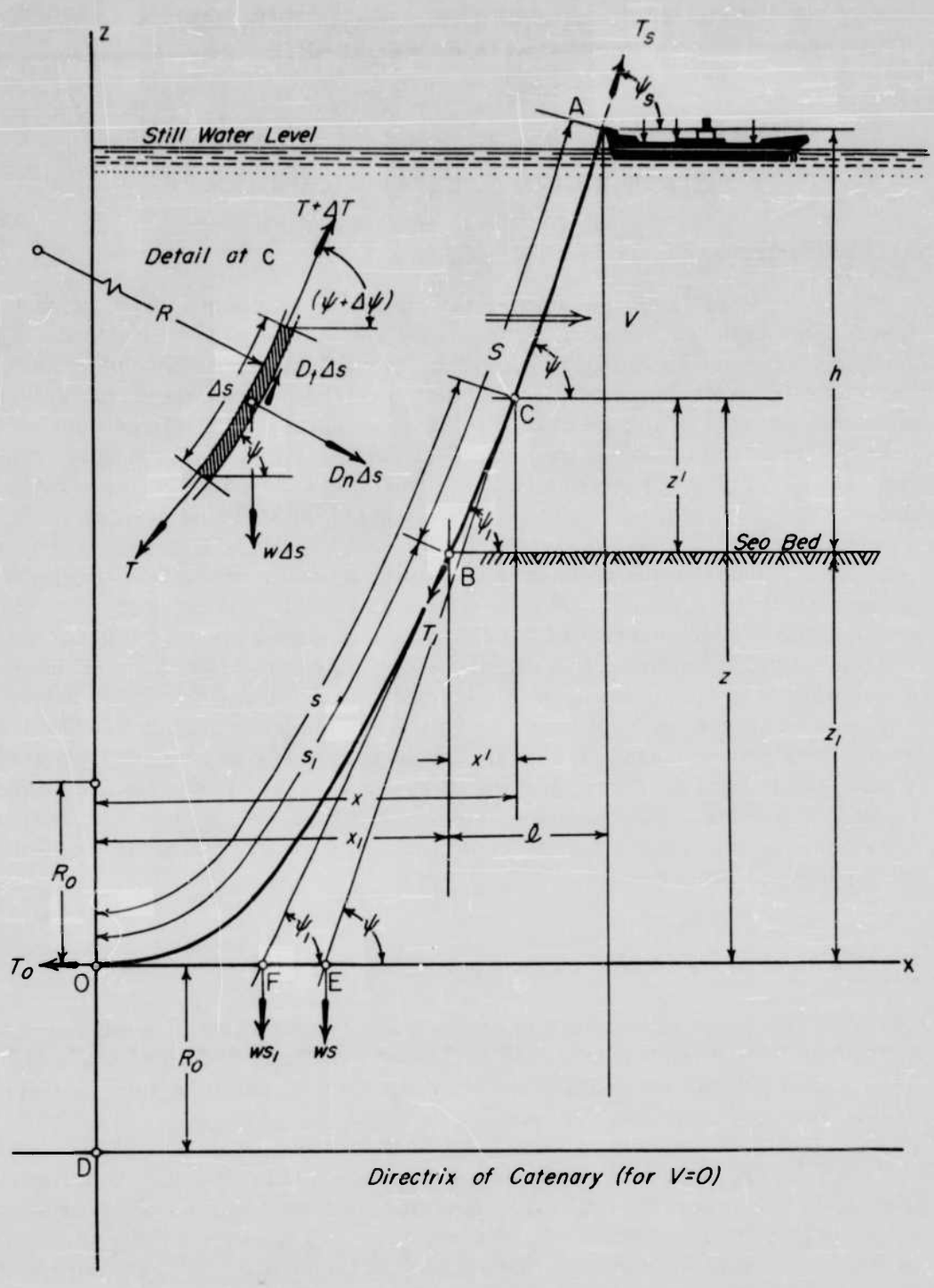

FIG 1: Schematic diagram showing geometry and equilibrium of a mooring cable.

the directrix) at the lowest point 0 of a hypothetical extension of the cable to the place where its tension would be wholly horizontal. This ratio at (x' , z') is defined by

$$\log \frac{R}{R_o} = a_1 \log \left| \frac{a_2 + b_1}{a_2 + b_1 \cos \psi} \right| + a_2 \log \left| \frac{a_1 - b_1}{a_1 - b_1 \cos \psi} \right|$$

$$+ \gamma[\psi - d_1 \tanh^{-1} (e_1 \tan \tfrac{\psi}{2}) - d_2 \tan^{-1} (e_2 \tan \tfrac{\psi}{2})]$$

_____ (1)

in which ψ is the angle of inclination of the cable to the horizontal and the coefficients $a_1 , a_2 , b_1 , c_1 , c_2 , d_1 , d_2 , e_1$, and e_2 are all functions of an angle α expressive of the hydrodynamic constant μ of the cable, while γ is a ratio of the tangential and normal drag coefficients for the current flow round the cable. Thus

$$\left.\begin{array}{ll} \text{(i)} & \alpha = \tan^{-1} (\frac{\mu}{2}) \\ \text{(ii)} & \mu = \dfrac{w}{C'_D d V^2} \\ \text{(iii)} & \gamma = \dfrac{C''_D}{C'_D} \end{array}\right\} \qquad (2)$$

where w is the weight of the cable per unit length in water, d the diameter of the cable, V the horizontal current velocity and C'_D , C''_D respectively the dimensional normal and tangential drag coefficients as used in the first report.

The coefficients a_1 , a_2 ...etc., are related to α by

$$\left.\begin{array}{lll} \text{(i)} & a_1 = 1 + \sin \alpha & \text{(vi)} \quad d_1 = a_2^2/c_1 \\ \text{(ii)} & a_2 = 1 - \sin \alpha & \text{(vii)} \quad d_2 = a_1^2/c_2 \\ \text{(iii)} & b_1 = \cos \alpha & \text{(viii)} \quad e_1 = \dfrac{c_1}{a_2 + b_1} \\ \text{(iv)} & c_1 = \sqrt{2a_2 \sin \alpha} & \\ \text{(v)} & c_2 = \sqrt{2a_1 \sin \alpha} & \text{(ix)} \quad e_2 = \dfrac{c_2}{a_1 - b_1} \end{array}\right\} \qquad (3)$$

The value of R_o in Eq. (1) is actually unknown, so that R can not be determined explicitly. However the ratio is used only as a means to an end in determining other quantities which specify the cable configuration, notably the total length S of the cable and its horizontal projection ℓ. Thus from Section 6 of Report 204-1, we find, in relation to the water depth h,

$$\frac{S}{h} = \int_{\psi_1}^{\psi_s} \frac{R}{R_o}\, d\psi \Bigg/ \int_{\psi_1}^{\psi_s} \frac{R}{R_o} \sin\psi\, d\psi \qquad (4)$$

$$\frac{\ell}{h} = \int_{\psi_1}^{\psi_s} \frac{R}{R_o} \cos\psi\, dx \Bigg/ \int_{\psi_1}^{\psi_s} \frac{R}{R_o} \sin\psi\, d\psi \qquad (5)$$

in which the limits of integration are the angles ψ_s and ψ_1 at which the cable is inclined to the horizontal at the surface and the sea bed respectively.

The cable tension at the anchor, T_1, and at the surface, T_s, are given by the equations: -

$$T_1 = \frac{wh\left[1 + \int_o^{\psi_1} \frac{R}{R_o} \sin\psi\, d\psi - \frac{\gamma}{\mu} \int_o^{\psi_1} \frac{R}{R_o} \cos^2\psi\, d\psi\right]}{\int_{\psi_1}^{\psi_s} \frac{R}{R_o} \sin\psi\, d\psi} \qquad (6)$$

and

$$\left.\begin{aligned} &(i) \quad T_s = wh + T_1 - \Delta T_s \\ &(ii) \quad \Delta T_s = \frac{wh\,\gamma \int_{\psi_1}^{\psi_s} \frac{R}{R_o} \cos^2\psi\, d\psi}{\mu \int_{\psi_1}^{\psi_s} \frac{R}{R_o} \sin\psi\, d\psi} \end{aligned}\right\} \qquad (7)$$

If the cable should happen to hang as a catenary in motionless water ($V = 0$), its properties are readily determined from another set of equations to

which Eqs. (4) to (7) reduce when $\mu = \infty$ and $\gamma = 0$ in Eqs. (2), as apply in this case. These simplified equations are: for the scope, S/h

$$\left.\begin{aligned} &\text{(i)} \quad S/h = \frac{b}{c} \\ &\text{(ii)} \quad b = \tan\psi_s - \tan\psi_1 \\ &\text{(iii)} \quad c = \sec\psi_s - \sec\psi_1 \end{aligned}\right\} \tag{8}$$

and for the stance, ℓ/h

$$\ell/h = \frac{1}{c}\left[\left\{12(b^2 - c^2) + 36\right\}^{\frac{1}{2}} - 6\right]^{\frac{1}{2}} \tag{9}$$

while the terminal tensions are given simply by

$$T_s = \frac{wh}{c}\sec\psi_s \tag{10}$$

and

$$T_1 = \frac{wh}{c}\sec\psi_1 \tag{11}$$

II. ANALYSIS OF THE NEW PROBLEM

3. Cable in a Current of Non-Uniform Vertical Distribution of Velocity

Though a uniform current of velocity V over the entire water depth may be approximated in rivers, estuaries and tideways where the water is reasonably shallow, it is certainly not typical of currents in the deeper ocean. The nature of real ocean currents in the deep sea will be discussed at some length in a later section of this report but for the present it is sufficient to recognize that, in general, horizontal velocity will vary with depth and may even become negative below a so-called layer of no-motion.

If our considerations embrace the deep sea we are concerned with the currents prevailing in the abyssal depths. Though there is normally some movement going on even in the deepest parts of the oceans it will be shown later that it can be considered to be virtually negligible as regards its hydrodynamic

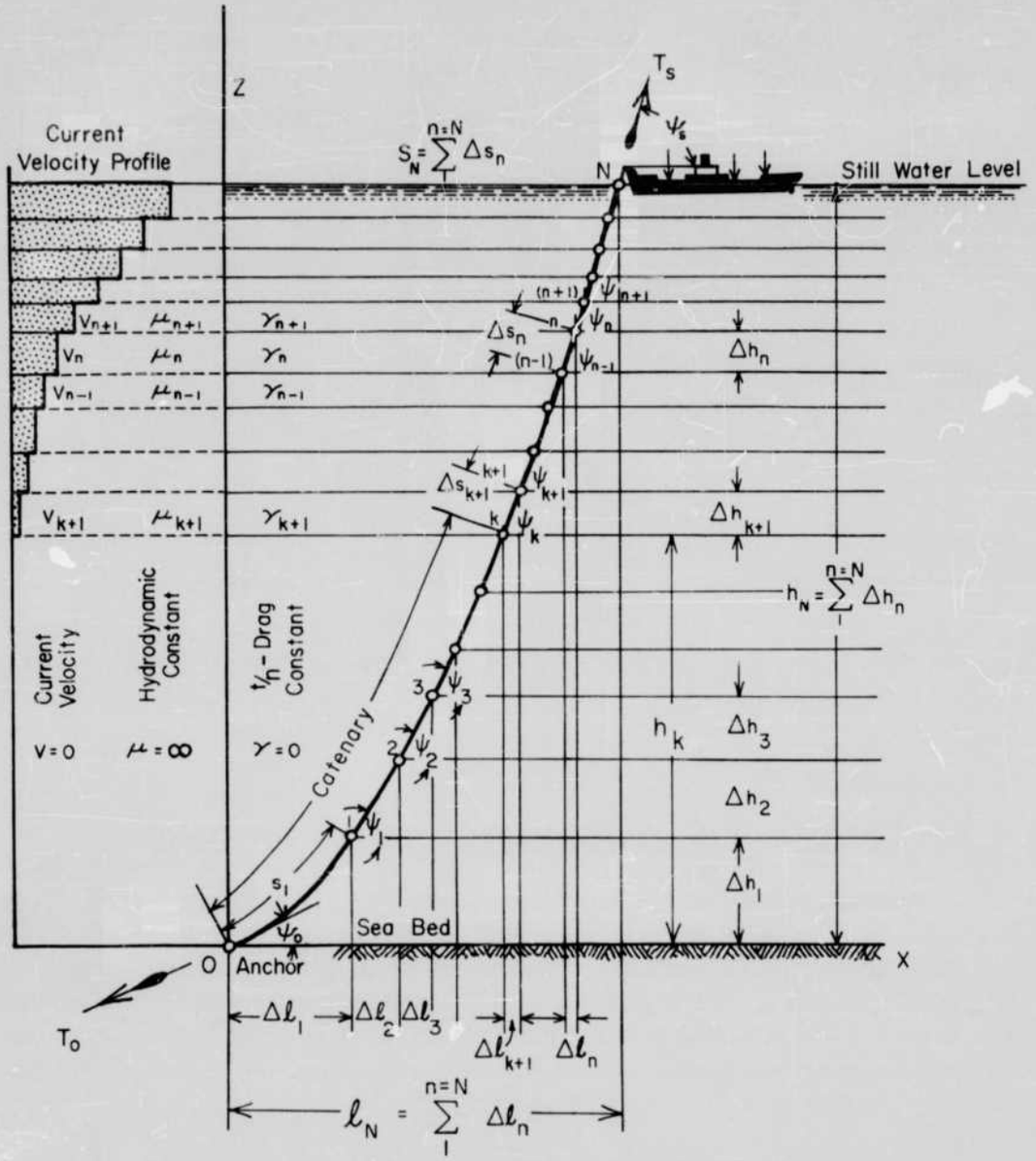

FIG 2: Schematic representation of step-wise composition of a deep-sea mooring cable.

effects, ostensibly over a height h_k above the bottom (Fig. 2). Thus the lower portion of a deep mooring cable, Ok in Fig. 2, will hang as a catenary and obey the stipulations of Eqs. (8) to (11).

Above the zone of no-motion the true variable nature of the current may be approximated by supposing that the depth of water to the surface is layered in fluid laminae of individual thickness Δh_n (a variable quantity) at any n-th lamina (Fig. 2), within which the velocity V_n may be considered constant. Values of V_n for different layers, however, will not be constant.

Within the assumption that the velocity vectors V_n all lie in the same vertical plane, it is seen then that a deep-ocean mooring-cable can be considered to consist of N segments of cable each of which individually obeys the equations of Section 2. From the anchor upwards the first k-th segments will each be catenaries, since $V = 0$ ($\mu = \infty$, $\gamma = 0$) in this zone of effective no-motion. From k to N (Fig. 2) each segment of cable can be treated separately as a cable in a uniform current and its terminal tensions T_n and T_{n-1} and terminal angles ψ_n and ψ_{n-1} evaluated along with its length Δs_n and horizontal projection $\Delta \ell_n$. Conditions of continuity however prescribe that for any two adjacent segments of cable the lower terminal tension and angle of the uppermost one must be identical with the upper terminal tension and angle respectively of the lowermost segment.

Accordingly it becomes possible to integrate the overall cable configuration and tensions over the entire water depth of variable currents by a stepwise procedure which artificially laminates the total water depth h_N .

4. Catenary Portion of the Deep-Sea Mooring Cable

Since simple equations may be used to evaluate the properties of catenaries it is convenient to treat the lower portion of the mooring cable in the zone of no-motion separately from the rest.

Any n-th segment (below k) in this region will subscribe to the following equations which are adapted from Eqs. (8) to (11).

$$\left.\begin{aligned} &\text{(i)}\quad s_n = \frac{b_n}{c_n} h_n \\ &\text{(ii)}\quad b_n = \tan\psi_n - \tan\psi_o \\ &\text{(iii)}\quad c_n = \sec\psi_n - \sec\psi_o \end{aligned}\right\} \qquad (12)$$

where s_n is here the length of the cable from 0 to $n (n < k)$, h_n the height of the point n above the sea bed, ψ_n the angle of inclination of the cable at n and ψ_o the corresponding angle at the anchor, 0 .

The horizontal projection of this length of cable will be ℓ_n as given by

$$\ell_n = \frac{h_n}{c_n}\left[\left\{12 b_n^2 - c_n^2) + 36\right\}^{\frac{1}{2}} - 6\right]^{\frac{1}{2}} \qquad (13)$$

and the tension T_n at n and T_o at the anchor will be respectively

$$T_n = \frac{wh_n}{c_n} \sec \psi_n \qquad (14)$$

and

$$T_o = \frac{wh_n}{c_n} \sec \psi_o \qquad (15)$$

It is convenient to specify any particular cable configuration in terms of the two angles of inclination ψ_k and ψ_o at the transition point k and the anchor 0 respectively. The tension T_o is then readily given by Eqs. (15) and (12iii) when $n = k$. Thus

$$T_o = wh_k \left(\frac{\sec \psi_o}{\sec \psi_k - \sec \psi_o}\right) \qquad (16)$$

The height h_k is, of course, a known quantity in this equation.

From Eqs. (15) and (12iii) the angle ψ_n at any point n in the catenary may then be obtained from

$$\left.\begin{aligned} &\text{(i)} \quad \psi_n = \tan^{-1}\left[\frac{(1 - a_n^2)^{\frac{1}{2}}}{a_n}\right] \\ &\text{(ii)} \quad a_n = \frac{T_o \cos \psi_o}{T_o + wh_n} \end{aligned}\right\} \qquad (17)$$

With the value of ψ_n now known, all the other characteristics of the catenary defined by Eqs. (12), (13) and (14) are specified at any n-th point ($n < k$).

5. Upper Portion of Deep-Sea Mooring Cable in Variable Current

In the zone of water movement above the point k in Fig. 2, it is necessary to start with the first [(k+1)th] segment of the cable in the artificial layer of water of thickness Δh_{k+1} within which the current velocity is V_{k+1} and for which the hydrodynamic constants specified by Eqs. (2) are μ_{k+1} and γ_{k+1}.

The known quantities with which to enter the Eqs. (4) to (7) are the lower terminal angle ψ_k and tension T_k and the lamina depth Δh_{k+1}. Since the investigation of any n-th layer ($n > k$) will be the same as that for the (k+1)-th layer, it is appropriate to pursue the study of integration along the cable on the basis that the lower terminal angle ψ_{n-1} and tension T_{n-1} are known from calculation of the preceding (n-1)-th layer. Since the process of calculation will be numerical integration, methods of finite differences will be employed to determine the upper terminal conditions which apply to the n-th segment of cable.

From Eqs. (2) we specify first of all that the values of the hydrodynamic constants prevailing for the n-th lamina are:

$$\left.\begin{aligned} &\text{(i)} \quad \alpha_n = \tan^{-1}\left(\frac{\mu_n}{2}\right) \\ &\text{(ii)} \quad \mu_n = \frac{w}{C'_D\, d\, V_n^2} \\ &\text{(iii)} \quad \gamma_n = \frac{C''_D}{C'_D} \end{aligned}\right\} \qquad (18)$$

It may be noted here that account could easily be taken of a change in diameter and weight along the cable length by assigning subscripts n to w and d. For present purposes, however, we shall assume constancy of these dimensions.

The coefficients of Eq. (3) which apply to the n-th lamina are now

$$
\left.
\begin{array}{lll}
\text{(i)} & a_1 = 1 + \sin\alpha_n & \text{(vi)} \quad d_1 = a_2^2/c_1 \\
\text{(ii)} & a_2 = 1 - \sin\alpha_n & \text{(vii)} \quad d_2 = a_1^2/c_2 \\
\text{(iii)} & b_1 = \cos\alpha_n & \text{(viii)} \quad e_1 = \dfrac{c_1}{a_2 + b_1} \\
\text{(iv)} & c_1 = \sqrt{2a_2 \sin\alpha_n} & \\
\text{(v)} & c = \sqrt{2a_1 \sin\alpha_n} & \text{(ix)} \quad e_2 = \dfrac{c_2}{a_1 - b_1}
\end{array}
\right\} \qquad (19)
$$

If at any point on the n-th segment of cable, the angle of inclination is ψ_i, then from Eq. (1) the corresponding value of the ratio $\frac{R}{R_o}$ will be

$$
\left(\frac{R}{R_o}\right)_i = \exp\left[a_1 \log\left|\frac{a_2 + b_1}{a_2 + b_1\cos\psi_i}\right| + a_2 \log\left|\frac{a_1 - b_1}{a_1 - b_1\cos\psi_i}\right|\right.
$$

$$
\left. + \gamma_n\left\{\psi_i - d_1 \tanh^{-1}\left(e_1 \tan\frac{\psi_i}{2}\right) - d_2 \tan^{-1}\left(e_2 \tan\frac{\psi_i}{2}\right)\right\}\right] \qquad (20)
$$

By selecting a suitably small interval of angle $\Delta\psi$ such that ψ_i is an integral multiple of $\Delta\psi$, $[\psi_i = \psi_{i-1} + \Delta\psi]$, the various functions of $\frac{R}{R_o}$ and ψ which appear in Eqs. (4), (5), (6) and (7) may be integrated as follows:

$$
\text{(i)} \quad \left(\Sigma\frac{R}{R_o}\Delta\psi\right)_i = \left(\Sigma\frac{R}{R_o}\Delta\psi\right)_{i-1} + \frac{\Delta\psi}{2}\left[\left(\frac{R}{R_o}\right)_i + \left(\frac{R}{R_o}\right)_{i-1}\right]
$$

$$
\text{(ii)} \quad \left(\Sigma\frac{R}{R_o}\sin\psi\,\Delta\psi\right)_i = \left(\Sigma\frac{R}{R_o}\sin\psi\,\Delta\psi\right)_{i-1} + \frac{\Delta\psi}{2}\left[\left(\frac{R}{R_o}\right)_i \sin\psi_i + \left(\frac{R}{R_o}\right)_{i-1}\sin\psi_{i-1}\right]
$$

$$
\text{(iii)} \quad \left(\Sigma\frac{R}{R_o}\cos\psi\,\Delta\psi\right)_i = \left(\Sigma\frac{R}{R_o}\cos\psi\,\Delta\psi\right)_{i-1} + \frac{\Delta\psi}{2}\left[\left(\frac{R}{R_o}\right)_i \cos\psi_i + \left(\frac{R}{R_o}\right)_{i-1}\cos\psi_{i-1}\right]
$$

$$
\text{(iv)} \quad \left(\Sigma\frac{R}{R_o}\cos^2\psi\,\Delta\psi\right)_i = \left(\Sigma\frac{R}{R_o}\cos^2\psi\,\Delta\psi\right)_{i-1} + \frac{\Delta\psi}{2}\left[\left(\frac{R}{R_o}\right)_i \cos^2\psi_i + \left(\frac{R}{R_o}\right)_{i-1}\cos^2\psi_{i-1}\right]
$$

(21)

The starting values that apply in these integrations for the case of $i = 0$ are

$$\left.\begin{aligned} &\text{(i)} && \left(\frac{R}{R_o}\right)_o = 1 \\ &\text{(ii)} && \left(\frac{R}{R_o}\right)_o \sin\psi_o = 0 \\ &\text{(iii)} && \left(\frac{R}{R_o}\right)_o \cos\psi_o = 1 \\ &\text{(iv)} && \left(\frac{R}{R_o}\right)_o \cos^2\psi_o = 1 \end{aligned}\right\} \qquad (22)$$

and

$$\left.\begin{aligned} &\text{(i)} && \left(\Sigma\frac{R}{R_o}\Delta\psi\right)_o = 0 \\ &\text{(ii)} && \left(\Sigma\frac{R}{R_o}\sin\psi\,\Delta\psi\right)_o = 0 \\ &\text{(iii)} && \left(\Sigma\frac{R}{R_o}\cos\psi\,\Delta\psi\right)_o = 0 \\ &\text{(iv)} && \left(\Sigma\frac{R}{R_o}\cos^2\psi\,\Delta\psi\right)_o = 0 \end{aligned}\right\} \qquad (23)$$

It must be noted here that the angle $\psi_{i=o}\ (= 0)$ in Eqs. (22) is not the same angle as ψ_o, the actual angle of inclination of the cable at the anchor as shown in Fig. 2. The integrations of eqs. (21) start at some imaginary lowest point of a hypothetical extension of the cable segment, as in Fig. 1, in which the cable length AB is equivalent to the cable segment between $(n - 1)$ and n in Fig. 2. The hypothetical extension would not be in agreement with the real cable below the point $(n - 1)$ in Fig. 2.

If $\Delta\psi$ is selected as some small constant value (say 0.01 radian), we are faced with the problem that ψ_i may never agree exactly with either ψ_{n-1} or ψ_n. The value of ψ_{n-1} is known, however, at the lowest terminal of the cable segment, so that the value of i can be found for which

$$\psi_{i-1} < \psi_{n-1} < \psi_i$$

If this value of i is p, then

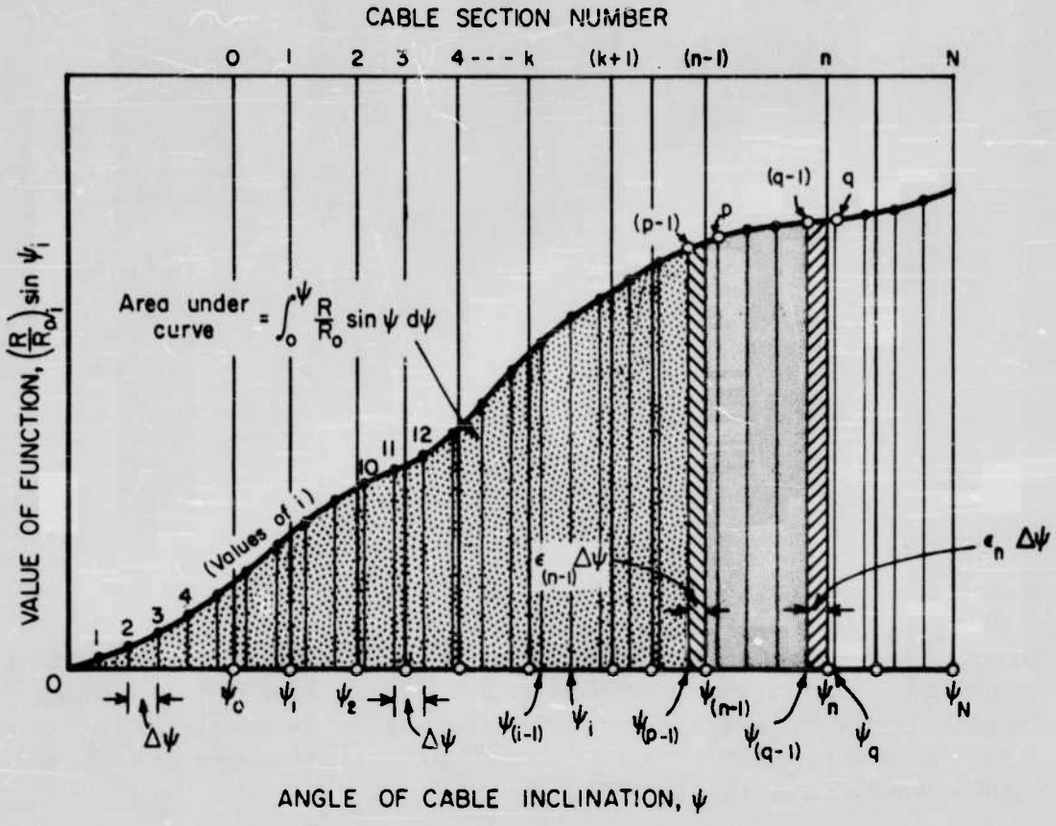

FIG 3: Schematic representation of numerical integration of a cable function.

$$(i)\quad \int_{o}^{\psi_{n-1}} \frac{R}{R_o}\, d\psi = \left(\Sigma \frac{R}{R_o}\,\Delta\psi\right)_{p-1} + \frac{\epsilon_{n-1}\,\Delta\psi}{2}\left[\left(\frac{R}{R_o}\right)_p + \left(\frac{R}{R_o}\right)_{p-1}\right]$$

$$(ii)\quad \int_{o}^{\psi_{n-1}} \frac{R}{R_o}\sin\psi\, d\psi = \left(\Sigma \frac{R}{R_o}\sin\psi\,\Delta\psi\right)_{p-1} + \frac{\epsilon_{n-1}\,\Delta\psi}{2}\left[\left(\frac{R}{R_o}\right)_p \sin\psi_p + \left(\frac{R}{R_o}\right)_{p-1}\sin\psi_{p-1}\right]$$

$$(iii)\quad \int_{o}^{\psi_{n-1}} \frac{R}{R_o}\cos\psi\, d\psi = \left(\Sigma \frac{R}{R_o}\cos\psi\,\Delta\psi\right)_{p-1} + \frac{\epsilon_{n-1}\,\Delta\psi}{2}\left[\left(\frac{R}{R_o}\right)_p \cos\psi_p + \left(\frac{R}{R_o}\right)_{p-1}\cos\psi_{p-1}\right]$$

$$(iv)\quad \int_{o}^{\psi_{n-1}} \frac{R}{R_o}\cos^2\psi\, d\psi = \left(\Sigma \frac{R}{R_o}\cos^2\psi\,\Delta\psi\right)_{p-1} + \frac{\epsilon_{n-1}\,\Delta\psi}{2}\left[\left(\frac{R}{R_o}\right)_p \cos^2\psi_p + \left(\frac{R}{R_o}\right)_{p-1}\cos^2\psi_{p-1}\right]$$

wherein (24)

$$\epsilon_{n-1}\,\Delta\psi = \psi_{n-1} - \psi_{p-1} \qquad (25)$$

A schematic representation of the integrations defined by Eqs. (21) and (24) is shown in Fig. 3, in which the integrals are the accumulated areas of the vertical strips of width $\Delta\psi$ under the curve of the function of R/R_o and ψ. The final strip of width ϵ_{n-1} is shown between ψ_{n-1} and ψ_{p-1}.

The continued integration of Eqs. (21) up to the limit ψ_n at the upper terminal n of the cable segment requires a knowledge of the angle ψ_n, which is unknown. However the integral

$$\int_{\psi_{n-1}}^{\psi_n} \left(\frac{R}{R_o}\right)\sin\psi\, d\psi$$

can be determined precisely in terms of known quantities by resorting to Eq. (6). Adapted to the present situation, this transforms to

$$\int_{\psi_{n-1}}^{\psi_n} \frac{R}{R_o}\sin\psi\, d\psi = \frac{w\Delta h_n}{T_{n-1}}\left[1 + \int_{o}^{\psi_{n-1}} \frac{R}{R_o}\sin\psi\, d\psi - \frac{\gamma_n}{\mu_n}\int_{o}^{\psi_{n-1}} \frac{R}{R_o}\cos^2\psi\, d\psi\right]$$

(26)

This may be written otherwise as

$$\left.\begin{aligned} &(i)\quad \int_{o}^{\psi_n} \frac{R}{R_o} \sin\psi \, d\psi = \beta \\ &(ii)\quad \beta = \frac{w\Delta h_n}{T_{n-1}} \left[1 + \int_{o}^{\psi_{n-1}} \frac{R}{R_o} \sin\psi \, d\psi - \frac{\gamma_n}{\mu_n} \int_{o}^{\psi_{n-1}} \frac{R}{R_o} \cos^2\psi \, d\psi\right] \\ &\qquad\qquad + \int_{o}^{\psi_{n-1}} \frac{R}{R_o} \sin\psi \, d\psi \end{aligned}\right\} (27)$$

In Eqs. (27) all of the integrals are known, as also is the lower terminal tension T_{n-1}. It is possible therefore to specify a value $i = q$ such that

$$\left(\Sigma \frac{R}{R_o} \sin\psi \Delta\psi\right)_{q-1} < \beta < \left(\Sigma \frac{R}{R_o} \sin\psi \Delta\psi\right)_{q}$$

Accordingly, if

$$\psi_n = \psi_{q-1} + \epsilon_n \Delta\psi \ , \qquad (28)$$

the unknown angle ψ_n can be determined from Eq. (28) in which the fraction ϵ_n is known from

$$\epsilon_n = \frac{\beta - \left(\Sigma \frac{R}{R_o} \sin\psi \Delta\psi\right)_{q-1}}{\left(\Sigma \frac{R}{R_o} \sin\psi \Delta\psi\right)_{q} - \left(\Sigma \frac{R}{R_o} \sin\psi \Delta\psi\right)_{q-1}} \qquad (29)$$

In this way the integrals of Eqs. (21) can be extended to the precise upper limit of ψ_n, yielding

$$\text{(i)}\quad \int_o^{\psi_n} \frac{R}{R_o}\, d\psi = \left(\Sigma \frac{R}{R_o}\Delta\psi\right)_{q-1} + \epsilon_n\left[\left(\Sigma \frac{R}{R_o}\Delta\psi\right)_q - \left(\Sigma \frac{R}{R_o}\Delta\psi\right)_{q-1}\right]$$

$$\text{(ii)}\quad \int_o^{\psi_n} \frac{R}{R_o}\sin\psi\, d\psi = \beta$$

$$\text{(iii)}\quad \int_o^{\psi_n} \frac{R}{R_o}\cos\psi\, d\psi = \left(\Sigma \frac{R}{R_o}\cos\psi\, d\psi\right)_{q-1} + \epsilon_n\left[\left(\Sigma \frac{R}{R_o}\cos\psi\Delta\psi\right)_q - \left(\Sigma \frac{R}{R_o}\cos\psi\Delta\psi\right)_{q-1}\right]$$

$$\text{(iv)}\quad \int_o^{\psi_n} \frac{R}{R_o}\cos^2\psi\, d\psi = \left(\Sigma \frac{R}{R_o}\cos^2\psi\, d\psi\right)_{q-1} + \epsilon_n\left[\left(\Sigma \frac{R}{R_o}\cos^2\psi\Delta\psi\right)_q - \left(\Sigma \frac{R}{R_o}\cos^2\psi\Delta\psi\right)_{q-1}\right] \qquad \text{(30)}$$

The final calculation of the cable segment characteristics now follows readily from Eqs. (4), (5) and (7) which are adapted here to the form

$$\left.\begin{aligned}
\text{(i)}\quad \Delta s_n &= \frac{\Delta h_n\left[\int_o^{\psi_n} \frac{R}{R_o}\, d\psi - \int_o^{\psi_{n-1}} \frac{R}{R_o}\, d\psi\right]}{\int_o^{\psi_n} \frac{R}{R_o}\sin\psi\, d\psi - \int_o^{\psi_{n-1}} \frac{R}{R_o}\sin\psi\, d\psi} \\
\text{(ii)}\quad \Delta \ell_n &= \frac{\Delta h_n\left[\int_o^{\psi_n} \frac{R}{R_o}\cos\psi\, d\psi - \int_o^{\psi_{n-1}} \frac{R}{R_o}\cos\psi\, d\psi\right]}{\int_o^{\psi_n} \frac{R}{R_o}\sin\psi\, d\psi - \int_o^{\psi_{n-1}} \frac{R}{R_o}\sin\psi\, d\psi} \\
\text{(iii)}\quad \Delta T_n &= \frac{w\gamma_n \Delta h_n\left[\int_o^{\psi_n} \frac{R}{R_o}\cos\psi\, d\psi - \int_o^{\psi_{n-1}} \frac{R}{R_o}\cos\psi\, d\psi\right]}{\mu_n\left[\int_o^{\psi_n} \frac{R}{R_o}\sin\psi\, d\psi - \int_o^{\psi_{n-1}} \frac{R}{R_o}\sin\psi\, d\psi\right]}
\end{aligned}\right\} \text{(31)}$$

The cumulative cable length s_n and horizontal projection ℓ_n from the anchor to the point n ($n > k$) are given at once by

$$\left.\begin{aligned} &\text{(i)} \quad s_n = s_{n-1} + \Delta s_n \\ &\text{(ii)} \quad \ell_n = \ell_{n-1} + \Delta \ell_n \end{aligned}\right\} \tag{32}$$

and the upper terminal tension of the n-th cable segment by

$$T_n = T_{n-1} + w\Delta h_n - \Delta T_n \tag{33}$$

6. Components of Cable Tensions at the Anchor and Sea Surface

The step-wise calculations of the last section may be pursued until $n = N$ (Fig. 2) which marks the upper limit of the complete cable. Since the basic premises on which the calculation depends are that the inclinations of the cable at the anchor and the level of no-motion at height h_k above the sea-bed are respectively ψ_o and ψ_k it behoves us to check that the final computed angle ψ_N at $n = N$ does not exceed 90°. Any value greater than 90° would be impossible since it would imply that the horizontal component of the cable tension at the surface $(T_s)_x$ would be negative and the moored ship could not therefore be in equilibrium under the cable tension and the drag from the surface current. Any selected combinations of ψ_o and ψ_k that result in $\psi_N > 90°$ must therefore be considered impossible and rejected.

The horizontal and vertical components of cable tension at the surface respectively $(T_s)_x$ and $(T_s)_z$ are given by

$$\left.\begin{aligned} &\text{(i)} \quad (T_s)_x = T_N \cos \psi_N \\ &\text{(ii)} \quad (T_s)_z = T_N \sin \psi_N \end{aligned}\right\} \tag{34}$$

The corresponding components $(T_o)_x$ and $(T_o)_z$ at the anchor are

$$\left.\begin{aligned} &\text{(i)} \quad (T_o)_x = T_o \cos \psi_o \\ &\text{(ii)} \quad (T_o)_z = T_o \sin \psi_o \end{aligned}\right\} \tag{35}$$

For equilibrium of the moored object it is necessary that $(T_s)_x$ be equal to the current drag (and wind drag, if in the same direction,) acting upon

it. The vertical component $(T_s)_z$ of surface cable tension must also be balanced by the increase of buoyancy from sinking of the bow or stern of the ship into the water under the downward pull of the cable.

If W_a be the negative buoyancy or weight of the anchor in sea water, it is necessary for equilibrium of the anchor that

$$W_a > (T_o)_z \quad . \tag{36}$$

Finally if H be the holding power of the anchor in the horizontal direction the condition must obtain that

$$H > (T_o)_x \tag{37}$$

if the anchor is not to be pulled along the sea bed.

III. SELECTION OF DEEP-OCEAN DESIGN CURRENTS

7. Requirements of a Design Current

For purposes of numerical evaluation of the tensions in, and configuration of, specific types of mooring cables in the deep sea (nominal depth 12,000 ft), it is necessary to decide on the vertical distribution of velocity in typically strong ocean currents, representative of what might be encountered in areas of well-defined oceanic circulation.

The nature of the surface circulation over the oceans of the world is portrayed in Fig. 4, which is based on information assembled from a variety of sources [Goodall and Darby, 1940; Carson, 1951; U.S. Hydrographic Office, 1944, 1947; Dietrich, 1957; Stommel, 1958]. The approximate magnitudes of the surface velocities are there indicated for the principal current patterns over the world as existing in July. At other times the current system does not sensibly depart from the circulations shown, taking a gross point of view, though there are undoubtedly numerous local deviations and diversions which are seasonal or secular, such as occur particularly in the Arabian Sea and the North Indian Ocean. As Munk [1955] points out, moreover, the fine structure of the currents which overlies the gross features is itself quite variable, as result of large-scale meanders, eddies and pertubations, and this may impose continual localized changes on the steady circulations.

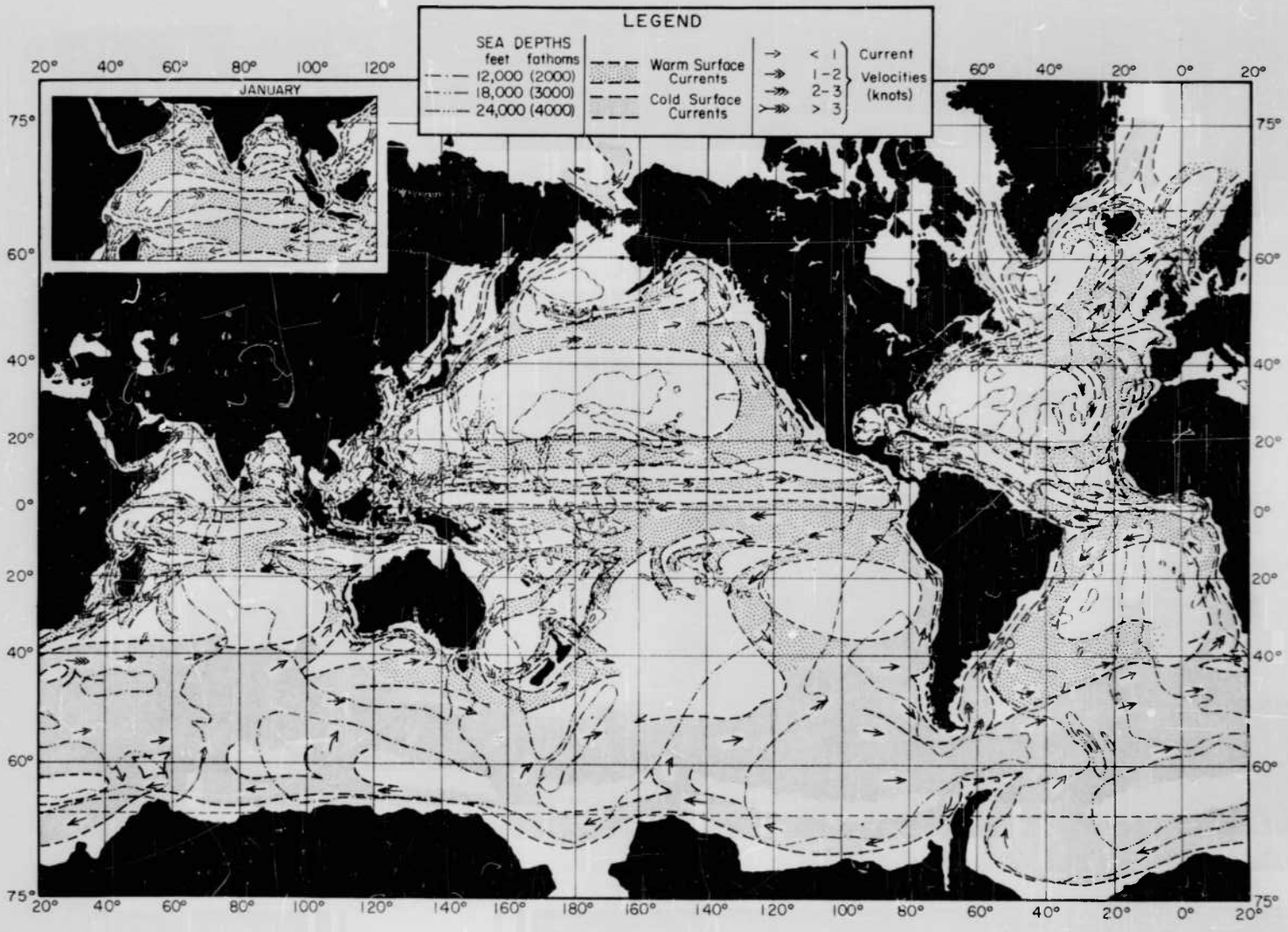

FIG 4: Surface currents and velocities in the oceans of the world for July. Inset, currents in the Indian Ocean in January. (Adapted from Goodall and Darby, Dietrich, U. S. Navy Hydrographic Office and others).

Normally the strongest currents (in excess of 3 knots) are encountered in the swift flowing Gulf Stream off the Eastern seaboard of the United States and in the somewhat comparable Kuroshio or Japan Current in the North-western Pacific. These are therefore areas of ocean where one might logically look for currents of design magnitudes.

The major ocean gyres of circulation shown in Fig. 4 can be ascribed to the cumulative effect of large-scale wind systems acting on the water surface, taken in conjunction with the deflecting influences of the earth's rotation and of the obstructions formed by the land masses. The displacement of enormous masses of surface water by these means inevitably sets in motion counter currents at deeper levels which, through upwellings in certain areas, help to restore the intricate balances required by wind, tide, pressure and density in conformity with the thermal and salinity structure of the oceans. These deep currents are not well understood at present but are believed to conform to some such pattern as illustrated in Fig. 5, which is adapted from the concepts of Stommel [1958]. Available evidence, which will be considered later, suggests that these deep currents are extremely weak though their overall motions are ponderously great in respect of the volumes of water transported.

Though the surface currents are now considered to be primarily wind-driven through the mechanism of skin friction or drag from the shear stress of wind over water, it can be shown that a local wind of itself is incapable of accounting for such high water velocities as are encountered in the swiftest part of the Gulf Stream and in many other parts of the world. Thus, if the surface shear stress τ_a of wind (air) over open land be defined as

$$\tau_a = \tfrac{1}{2}[C_D]_a \rho_a U^2 \quad , \tag{38}$$

in which $[C_D]_a$ is a dimensionless drag coefficient, ρ_a the mass density of air and U the wind velocity near the surface, while the surface shear stress τ_w of water flowing over a rough plate is

$$\tau_w = \tfrac{1}{2}[C_D]_w \rho_w u_1^2 \tag{39}$$

in which $[C_D]_w$ is a dimensionless drag coefficient, ρ_w the mass density of water and u_1 the velocity of the water, we may employ the artifice of Chatley [1950] to regard the interaction of wind over water as a combination of flows above and below an artificial "solid interface". For equilibrium of the drags on this interface

$$[C_D]_a \rho_a (U - u_1)^2 = [C_D]_w \rho_w u_1^2 \quad . \tag{40}$$

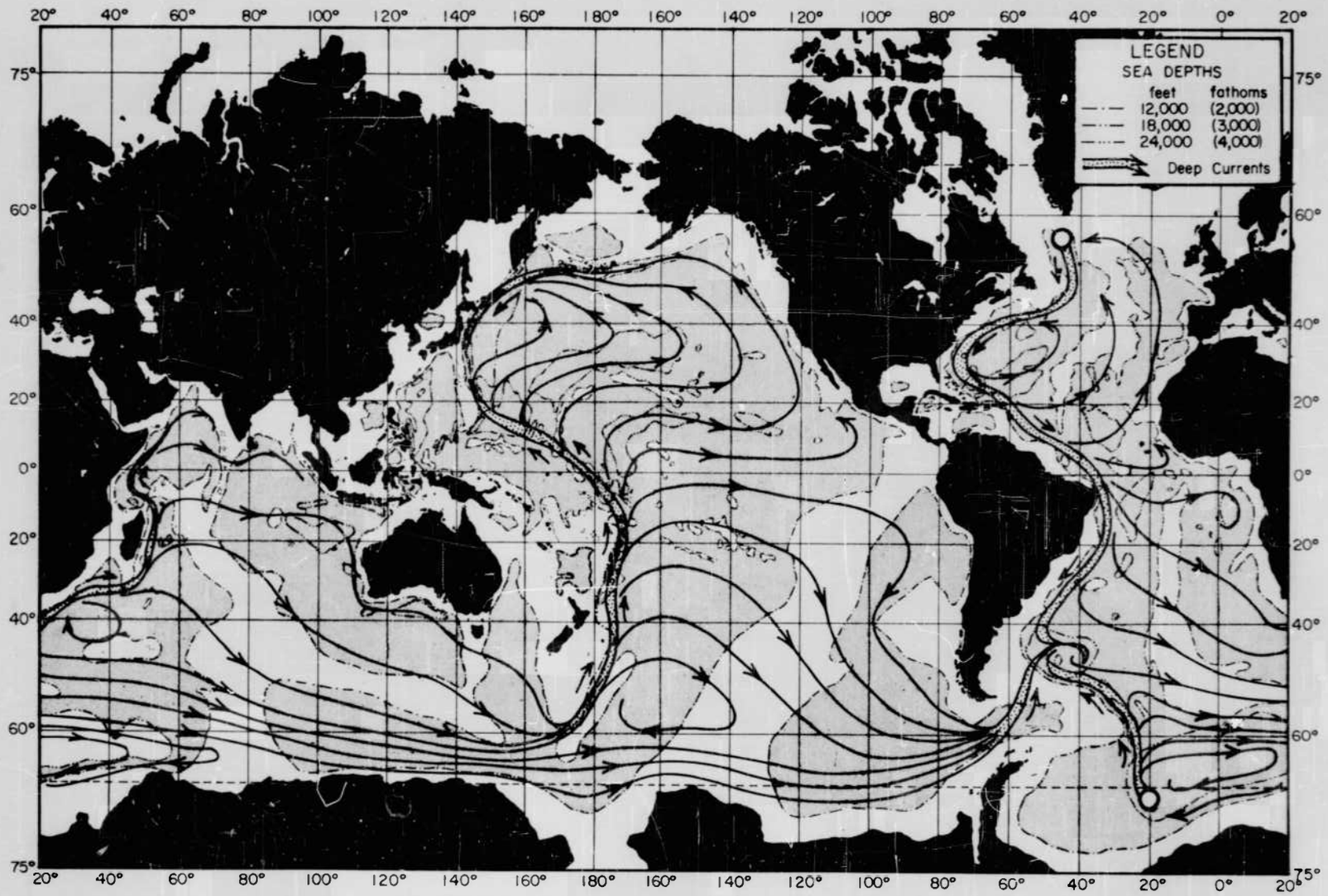

FIG 5: Probable trends of the circulation of deep water in the oceans of the world (adapted from Stommel, 1958).

The water velocity u_1 resulting from the wind velocity U will normally be negligible in comparison with U, so that Eq. (40) readily yields

$$\frac{u_1}{U} = \left[\frac{[C_D]_a}{[C_D]_w}\,\frac{\rho_a}{\rho_w}\right]^{\frac{1}{2}} . \qquad (41)$$

Taylor [1916] shows that $[C_D]_a$ tends to have a value of about 0.005 while an extensive literature of experimentation indicates that a suitable value for $[C_D]_w$ would appear to be about the same, as one might even expect from dimensional analysis considerations. Hence, with $\rho_a/\rho_w \simeq 1.24 \times 10^{-3}$, Eq. (41) yields

$$u_1/U \simeq 1/30 \text{ or } 3.5\% . \qquad (42)$$

Though this rough-and-ready estimate has many shortcomings it serves to indicate an upper limit of value, which suggests that the wind-induced current u_1 will normally be less than 1 knot in an average wind of $U = 30$ knots. Transient gusts up to $\pm$ 50% or more of this would be unlikely to affect this picture owing to the great inertia of the water in response to rapid change.

More accurately than the above, Ekman [cf. Sverdrup et al, 1943] used the observations of Mohn and Nansen to derive an empirical relationship for the ratio u_1/U, namely

$$u_1/U = 0.0127\,[\sin\phi]^{-\frac{1}{2}} \qquad (43)$$

in which ϕ is the angle of latitude of the place of observation. For values of ϕ from 60° to 30°, this equation gives values of u_1/U of only 1.4 to 1.8%, which are considerably lower than Eq. (42).

The relatively high surface velocities found in some of the ocean currents must then be ascribed to the constrictions and funnelling effects of islands, land-masses and of Coriolis force all of which tend to squeeze the broad flows set in motion by the semi-permanent trade and anti-trade wind systems. Also as Pillsbury [1890] points out, notably in respect of the Gulf Stream, both the tidal regime and the pumping effects of atmospheric pressure on filling basins such as the Gulf of Mexico, can inject spasmodic pulses of significant magnitude on the general stream-flow.

From a design point of view it must be supposed that it is entirely possible for a normal maximum current velocity in fine weather (say in the Gulf Stream) to be increased locally at the surface by as much as about 1/2 knot under the influence of severe local wind arising from an intrusion, say, of a tropical or

extratropical storm. The theoretical work of Ekman and numerous supporting observations [cf. Sverdrup et al, 1943; Bowden, 1954] indicate that if this increment is to be additive in the direction of the main current, the wind direction would in most cases have to be inclined about 30° thereto, to the left in the northern hemisphere and to the right in the southern. If the water tends to be shallow, however, the drift current and wind will be very nearly aligned.

Additional to the drift current from wind drag will be a mass transport set in motion by the wind-generated waves, which according to Lamb [1932 Edn.] can result in a surface current whose velocity u_2 will approximate

$$u_2 \simeq \frac{2H^2}{T^3} \text{ ft/sec} \qquad (44)$$

for waves of period T (secs) and height H (ft). For 30 ft waves of 12 secs period, u_2 would thus be about 1 ft/sec or a little over 1/2 knot. Both the wave current u_2 and the drag current u_1 decline exponentially with depth and may be considered to evanesce at depths of about 500 ft below the ocean surface.

The strongest ocean current known to exist occurs apparently to the south of the island of Socotra off the east coast of Africa in the northern Indian Ocean. Here during the southwest monsoon when the easterly set attains an average of 3 to 5 knots, the current has been known to flow at 7 knots [Frankcom and Barlow, 1954]. It seems probable that the combined effects of local wind drift and mass transport from waves are at work here in augmenting the normal circulation.

From all these considerations then it seems reasonable to increase the maximum surface current velocity selected for design purposes by an amount of 1 knot to allow for any superimposed storm effects which may be aligned with the stream flow.

8. Strong Surface Currents of the Oceans

According to Francom and Barlow [1954] there is probably no part of the ocean where currents do not at times attain at least 1 knot. Currents of 2 to 3 knots, as shown in Fig. 4, are to be found in the equatorial and warm currents on the western sides of the oceans, notably in the Gulf Stream, Kuroshio, Agulhas (East African) coastal current and the East Australian coastal current. The Brazil current is a notable exception.

The observations which Pillsbury [1890] made of the Gulf Stream are a classical example of thoroughness. Most of his work was confined to the Yucatan channel and the Florida Straits, in the latter of which areas he found velocity

distributions with depth in accord with the profile given in Fig. 6. Pillsbury discovered distinct changes in the stream traceable to the moon's declination and therefore presumably an influence of the lunar fortnightly and monthly tidal constituents, an effect which has been confirmed by Griswold [1952]. In addition to this Pillsbury showed that typical semi-diurnal variations of $\pm 1/3$ knot about the mean velocity revealed the superposition of the daily astronomical tides.

His discussion of pressure effects is discerning. In the open ocean he acknowledges that atmospheric pressure changes are likely to have quite insignificant effects in promoting ocean currents, but in partially confined bodies of water such as the Gulf of Mexico their effect may be quite different and important. Thus a low pressure over the Gulf would necessitate an inflow of water from the Caribbean Sea which would both divert the Stream supply from the Yucatan channel and hinder the Stream outflow through the Florida straits. With restoration of pressure over the Gulf as might happen after a few days the impounded water would be pumped out, resulting in a strong pulse of current that could presumably permeate the Gulf Stream far out into the Atlantic.

Since Pillsbury's time a great deal of attention has been focussed on the Gulf Stream by such investigators as Iselin, Stommel, Fuglister, von Arx and many others. From the observations of some of these we select samplings of velocity distributions with depth, (either measured or calculated), which are considered representative of some of the maximum currents to be found in the Stream (Fig. 6). Thus two velocity profiles off Cape Hatteras [Stommel, 1958] reveal strong surface flows between $4\frac{1}{2}$ and 5 knots, declining almost exponentially to insignificant proportions at depths of 1000 m. (3280 ft). Griswold [1952], reporting the results of a Loran survey of 1950-1951 in which nine oil-tankers participated, records maximum surface currents between 4.3 and 4.8 knots. Several cases of similar velocities between 3 and 5.8 knots have been reported by von Arx, et al [1955] for the region of Cape Fear, south of Cape Hatteras, in the offing of Onslow Bay.

Calculated velocity profiles in the Gulf Stream between Montauk and Bermuda, based on dynamical computations, have been made by Haurwitz and Panofsky [1950] and by Neumann [1956], using temperature and salinity measurements. These suggest that velocities decline almost linearly with depth to the 1000 m. level (Fig. 6), where they tend to become insignificant.

As examples of current velocity profiles in other parts of the world, Fig. 6 includes two versions of the recently discovered Cromwell current, which underruns the Equatorial Current from west to east in the Pacific Ocean [Knauss, 1959;1960] and one profile of the Kuroshio, east of Japan, according to Masuzawa [1955] . The Kuroshio exhibits an exponential decline of velocity with depth from

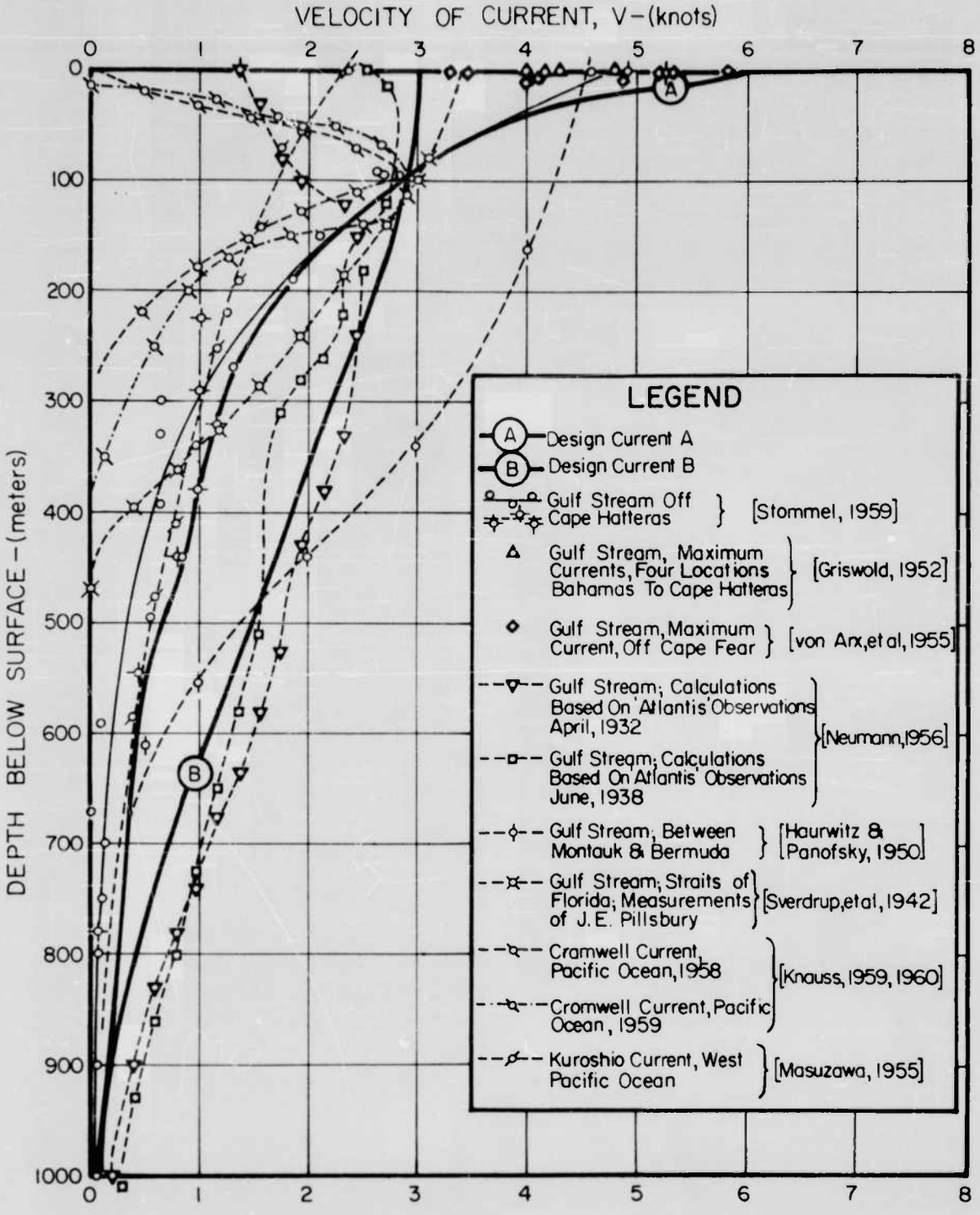

FIG 6: Vertical velocity profiles in the Gulf Stream and other ocean currents showing the adopted design distributions.

a maximum of between 2 and 3 knots at the surface to insignificant proportions at 1000 m depth. The Cromwell current, on the other hand, is unique in being a comparatively narrow filament of flow with its maximum velocity at about 100 m below the ocean surface.

Having regard to what has been said already in the last section regarding the possibility that a fortuitous infusion of severe weather and waves could augment the maximum stream flow in a current by about 1 knot and the possibility also (in the case of the Gulf Stream) that tidal currents and pressure pulsations from the Gulf of Mexico could be additive, we feel disposed to adopt for design purposes a maximum surface current of 6 knots. Design current A shown by the profile in Fig. 6 is thus somewhat arbitrarily designated to contain the observations of Stommel, Griswold and von Arx. Alternative design current B on the other hand, assumes less surface effect and stronger flow at lower depths in nearer accord with the calculations of Neumann. Both current profiles A and B would seem to be possible of realization in particular areas of the strongest ocean currents.

9. Deep Currents of the Oceans

The tendency noted in Fig. 6 for the surface circulations of the oceans to decline to inappreciable values at about 1000 m (3280 ft) below the surface raises the question as to the magnitudes of the deep currents below this level, already mentioned in Section 7 and Fig. 5.

The earliest available information derives from such pioneering expeditions as those of the Blake (USA, 1885-1890), Armauer-Hansen (Norway, 1913), Meteor (Germany, 1924), Altair (Germany, 1938) and is summarised conveniently in the table below , , which is adapted from Bowden [1954].

The velocities measured at the different levels are in all cases weak (less than 0.5 knot) and are apparently predominantly inclusive of a tidal constituent of semi-diurnal character which is normally invariable with depth but changeable of direction cum sole. Most of the stations occupied were in regions outside of zones of strong surface circulation. Table I shows that such velocities as were measured at depths below 1500 m ($\simeq$5000 ft) were generally less than 0.25 knot. The nature of the deep flow in the Atlantic Oceans at levels between 2000 and 3000 m was shown by Wüst (1936) and Defant (1941) to follow the main trends of circulation illustrated in Fig. 5 [cf. Dietrich, 1957]. According to a chart due to Defant the maximum velocities are found off Cape Recife on the east coast of Brazil and amount to some 12 to 18 cms/sec (0.26 to 0.35 knot) in a southerly

TABLE I : Sub-Surface Currents in the Atlantic Oceans

Location			Total Current Velocity (cms/sec)			Mean semi-diurnal tidal current cms/sec	Source*
Area of Atlantic	Long.	Lat.	Upper Layer (100-500 m)	Inter-mediate (500-1500 m)	Deep Layer (1500-3000 m)		
North	74.0W	35.0N				13.2	B
North	77.0W	28.0N				12.0	B
North	60.0W	13.0N				16.0	B
North	39.0W	44.5N	18	8	-	8.3	A
North	10.0W	38.0N	16	25	12	-	A-H
North	8.0W	34.0N	15	-	-	-	A-H
North	13.0W	30.0N	11	8	8	10.4	A-H
North	43.8W	30.0N	10	7	-	-	M
North	46.3W	16.8N	10	12	-	7.4	M
North	47.6W	12.6N	10	10	6	8.7	M
Equatorial	26.0W	03.5N	12	-	-	10.4	M
Equatorial	01.0W	04.0N	11	21	-	5.8	M
Equatorial	10.9E	09.0S	-	10	-	6.4	M
Equatorial	01.1E	03.8S	7	-	-	7.3	M
Equatorial	34.9W	02.5S	-	-	10	5.9	M
South	00.1W	15.0S	nil	-	nil	9.9	M
South	11.7W	21.5S	6	6	-	8.8	M
South	19.3W	28.1S	22	-	nil	10.6	M

*Name of Ship; B = Blake; A-H = Armauer-Hansen; M = Meteor; A = Altair

set. In the Pacific Ocean the drift of bottom water proceeds apparently at a still more leisurely pace [Dietrich, 1957]. According to information obtained from bathyscaphe descents by the French and Japanese to depths of 3000 m (10,000 ft) off the island of Honshu, the deep flow in the Kuroshio is extremely weak, being only about 0.04 knot. [Lumby, 1959]

These observations are generally borne out by more recent measurements that have been made using neutral buoyancy floats at deep levels. Thus Swallow [1955] found deep currents in the eastern North Atlantic at levels between 800 to 1500 m (2500 to 5000 ft) of the order of 9 to 12 cm/sec (0.2 to 0.4 knot) of which, however, only about 2 to 3 cm/sec was steady drift, the major part being a semi-diurnal tidal oscillation, and a small residue an inertial oscillation for the latitude of measurement. Later observations of Swallow and co-workers (see Table II opposite) confirm that the deep currents are extremely sluggish. Measurements in the Gulf Stream area have revealed a rather deep level of no-motion at about 1500-2000 m (5000-6600 ft) below the surface, under which a counter current courses southwards, somewhat as indicated in Fig. 5, at a maximum velocity of about 18 cm/sec (0.35 knot).

All this evidence suggests that the velocities of flow encountered at levels below 1000 m (3280 ft) are generally less than 0.35 knot and therefore of an order of magnitude likely to be hydrodynamically insignificant as regards the force such currents could exert on deep-sea mooring cables. In this study therefore the deep currents are neglected entirely.

10. Adoption of Design Currents

In Section 8 and Fig. 6 two design currents A and B were defined as being representative of strong current conditions down to a depth of 1000 m. below the surface. Over the balance of the nominal water depth of 3660 m. (12,000 ft) being considered, the design currents are assumed to be effectively zero, in accordance with the previous discussion.

For purposes then of applying the equations elaborated in Part II of this report it is necessary to approximate the vertical distributions of velocity of the design currents A and B of Fig. 6 as a step-wise series of velocities which are uniform over intervals of depth. This is accomplished in Fig. 7 by suitably defining intervals of depth Δh_n over which each velocity V_n is constant, to accord with the schematic representation given in Fig. 2. The criterion observed in performing this is that the departure in velocity from the accepted profile at any depth

TABLE II: Deep Ocean Currents in the North Atlantic

Location	Date	Depth (m)	Velocity (cm/sec)	Authority
Gulf of Cadiz	1955	1200	9.5	Swallow [1957]
(600 n. mi from		1900	2.4	
Gibraltar		1900	1.6	
100 to 300 n. mi	1956	840	10-16	Swallow [1957]
N & NE of				
British Isles		2900	0.7-0.9	
Gulf Stream off	1957	1500-2000	no motion	Swallow and
Cape Romain		2580	2.6-9.5	Worthington [1957,
S. Carolina		2840	9.7-17.4	1959]
($75\frac{1}{2}$°-76°W, 33°N)		3200 (bed)	5	
250 n. mi West	1958	1560	4.1	Swallow and
of Portugal		2120	4.7	Hamon [1959]
($14\frac{1}{2}$°W, $41\frac{1}{2}$°N)		2940	1.2	
		3680	2.6	
		4240	1.9	
250 n. mi West	1958	2210	3.0	Swallow and
of Portugal		2600	0.9-1.2	Hamon [1960]
		2590	4.9	
North Atlantic		1710	(16)	Laughton [1959 (i)
(sea mounts)		3000	(16)	& (ii)]

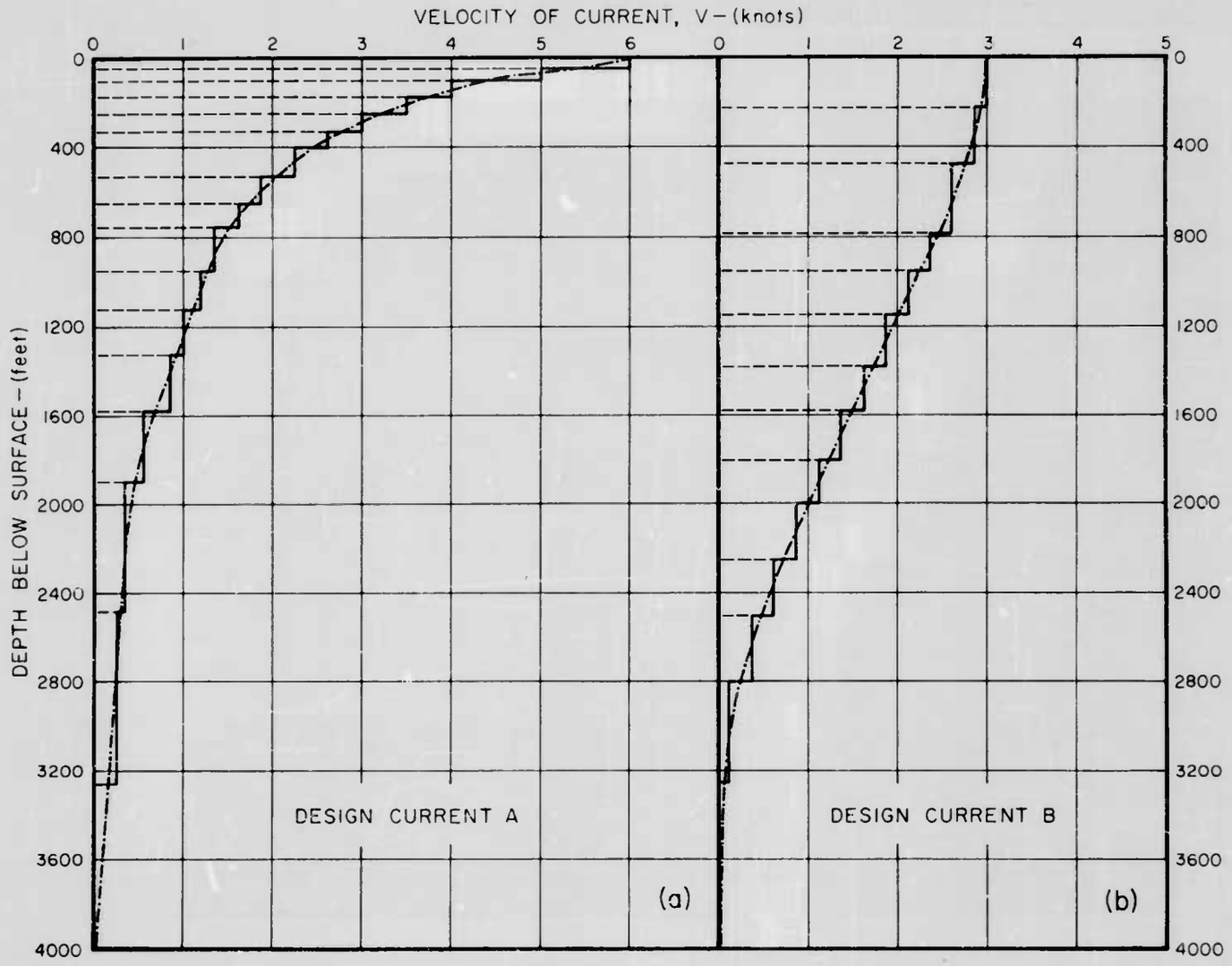

FIG 7: Adaptation of the design current velocity profiles to discontinuous velocities constant over increments of depth.

TABLE III : Increments of Height Δh_n and Velocities V_n for Design Currents

Lamina No. n	Design Current A			Design Current B			
	Δh_n (ft)	h_n (ft)	V_n (knots)	Δh_n (ft)	h_n (ft)	V_n (knots)	
1	500	500	0	500	500	0	dead water
2	500	1000	0	500	1000	0	
3	700	1700	0	700	1700	0	
4	1000	2700	0	1000	2700	0	
5	1500	4200	0	1500	4200	0	
6	2000	6200	0	2000	6200	0	
7	1500	7700	0	1500	7700	0	
8	1000	8700	0	1000	8700	0	
9	825	9525	0.250	450	9150	0.125	moving water
10	575	10,100	0.350	300	9450	0.375	
11	325	10,425	0.550	250	9700	0.625	
12	250	10,675	0.850	250	9950	0.875	
13	200	10,875	1.000	200	10,150	1.125	
14	175	11,050	1.200	225	10,375	1.375	
15	175	11,225	1.350	200	10,575	1.625	
16	125	11,350	1.625	225	10,800	1.875	
17	125	11,475	1.875	200	11,000	2.125	
18	125	11,600	2.250	175	11,175	2.375	
19	75	11,675	2.625	300	11,475	2.625	
20	75	11,750	3.000	275	11,750	2.875	
21	75	11,825	3.500	250	12,000	3.000	
22	75	11,900	4.000	-	-	-	
23	50	11,950	5.000	-	-	-	
24	50	12,000	6.000	-	-	-	

shall not exceed ± 0.20 knot, or about the actual magnitude of the current neglected in the depths below 1000 m.

In the total depth of 12,000 ft the bottom layer of effective dead-water may be taken as 8700 ft deep. In accordance with Fig. 2 it is convenient to divide this zone into k intervals and take $k = 8$. The values of the increments of height Δh_1, $\Delta h_2 \ldots \Delta h_8$ are selected somewhat arbitrarily to facilitate the plotting of the mooring cable configuration from location of the points 1, 2, 3...$k = 8$. The fact that the increments Δh in this zone are generally large, has no reflection on the accuracy of the calculations of cable configuration, as will be apparent from Section 4, which deals with the catenary portion of the cable.

In the upper layer of moving water, which is 3300 ft deep, the number of increments of height, Δh_n, is 16 for design current A and 13 for design current B, in accordance with Fig. 7. The specific values of Δh over the total water depth of 12,000 ft are given collectively in Table III, opposite.

IV. NUMERICAL COMPUTATION OF CABLE PARAMETERS

11. Values of Hydrodynamic Constants

The calculation procedure evolved in Eqs. (12) to (33) requires a knowledge of the values of the hydrodynamic constants μ_n and γ_n [Eqs. (18)] applicable to each of the N fluid laminae between sea bed and surface. The dimensional drag coefficients C'_D and C''_D occurring in Eqs. (18) are conveniently specified as to value by the considerations of Report 204-1 [Wilson, 1960 (i)]. There C'_D was inferred as having a constant value of 1.4 in the ft-lb-sec system of units. Though γ was susceptible of some variation a suitable quasi-constant value would seem to be 0.025.

In the dead-water zone, for which $V_n = 0$ ($n = 1, 2 \ldots 8$), the value of μ is infinity and the corresponding value of γ zero. While Eq. (18ii) ensures that successive values of μ_n for decreasing V_n, will show a reasonably gradual transition from small values to large, (that is, approaching infinity for $V_n \to 0$), no control regulates the value of γ, which must change from 0.025 to zero. An arbitrary control was therefore adopted as follows

$$\left.\begin{array}{ll} \text{(i)} & \gamma = 0.025 \quad \text{for } \mu < 1.0 \\ \text{(ii)} & \gamma = 0.010 \quad \text{for } 1.0 < \mu < 1.5 \\ \text{(iii)} & \gamma = 0 \quad\quad \text{for } \mu > 1.5 \end{array}\right\} \qquad (45)$$

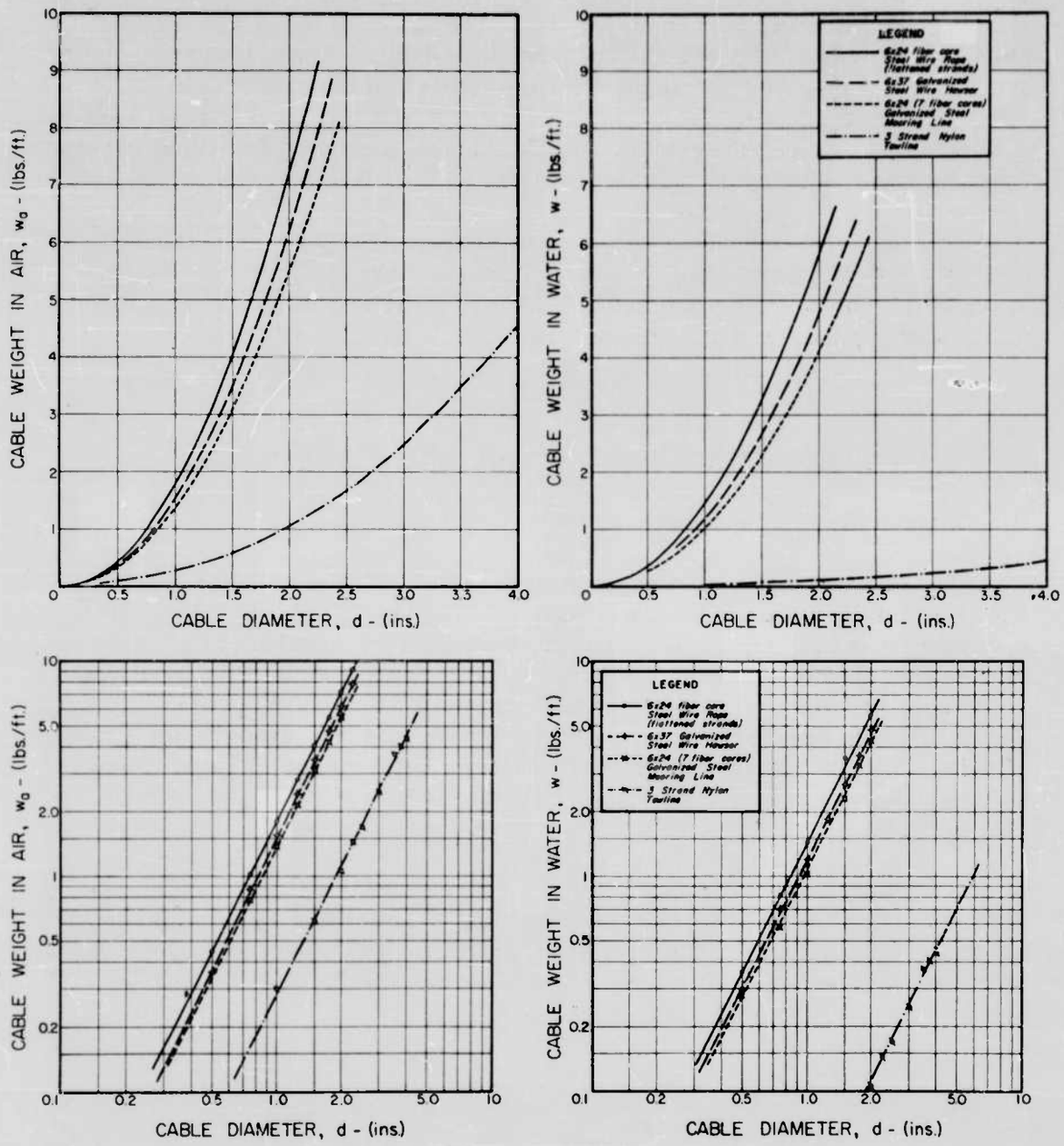

FIG 8: Relationships of cable weights in air and water to cable diameter.

this being based to some extent on the experience of calculations made for Report 204-1.

Eq. (18ii) shows that the hydrodynamic constant μ also involves the ratio w/d. From Fig. 8, which presents the weights per unit length in air (w_a) and water (w) of typical steel wire and nylon mooring ropes, as obtained from manufacturers, it is found that w is related to d very satisfactorily by a square-power law of the form

$$w = C_1 d^2 \tag{46}$$

Thus μ_n in Eq. (18ii) can be written as

$$\mu_n = \frac{C_1 d}{C_D' V_n^2} \tag{47}$$

Upon inserting $C_D' = 1.4$, the value of μ_n is given by

$$\mu_n = (3.007\, C_1)\, \frac{d}{V_n^2} \tag{48}$$

for d in ins, V_n in knots and C_1 in lbs/ft/sq in. Suitable values of C_1, obtained from Fig. 8, are

$$\begin{aligned} &\text{(i)} \quad C_1 = 1.233 \text{ lbs/ft/sq in for steel wire cables.} \\ &\text{(ii)} \quad C_1 = 0.028 \text{ lbs/ft/sq in for nylon ropes.} \end{aligned} \tag{49}$$

For purposes of evaluating the tensions and configurations of typical mooring cables in the design currents, it seems appropriate to choose a range of rope diameters, d, which might cover any eventuality of mooring condition. Thus we take

(i) $d = 1/8$, $1/4$, $1/2$, $3/4$, 1 , $1\frac{1}{4}$, $1\frac{1}{2}$, 2 , $2\frac{1}{2}$, 3 ins. for steel mooring lines

(ii) $d = \frac{1}{2}$, 1 , $1\frac{1}{2}$, 2 , $2\frac{1}{2}$, 3 ins for nylon mooring lines

The applicable values of the hydrodynamic constant μ_n, calculated from Eqs. (48) and (49), are then given by Tables IV and V. The corresponding values of γ_n are specified readily in terms of Eqs. (45). In Tables IV and V, γ_n is everywhere 0.025 below the horizontal full line in each column of figures and zero above the horizontal dash line. Between these lines the value of γ_n has been taken as 0.010.

TABLE IV : Hydrodynamic Constants μ_n for Design Current A

Fluid Lamina No n	Value of μ_n for STEEL Ropes										Value of μ_n for NYLON Ropes					
	d = 1/8	1/4	1/2	3/4	1	1¼	1½	2	2½	3	1/2	1	1½	2	2½	3 ins
1 thro' 8	∞	∞	∞	∞	∞	∞	∞	∞	∞	∞	∞	∞	∞	∞	∞	∞
9	7.9	15.8	31.6	47.4	63.2	79.0	94.8	126.4	158.0	189.6	0.693	1.38	3.12	5.54	8.65	12.47
10	3.9	7.9	15.8	23.7	31.6	39.5	47.4	63.2	79.0	94.8	0.346	0.693	1.56	2.77	4.33	6.24
11	1.6	3.2	6.3	9.5	12.6	15.8	19.0	25.3	31.6	37.9	0.138	0.277	0.623	1.11	1.73	2.49
12	0.66	1.3	2.6	3.9	5.3	6.6	7.9	10.5	13.2	15.8	0.058	0.115	0.260	0.462	0.722	1.04
13	0.47	0.95	1.9	2.8	3.8	4.7	5.7	7.6	9.5	11.4	0.042	0.083	0.181	0.332	0.520	0.748
14	0.33	0.66	1.3	2.0	2.6	3.3	3.9	5.3	6.6	7.9	0.029	0.058	0.130	0.231	0.361	0.520
15	0.26	0.52	1.0	1.6	2.1	2.6	3.1	4.2	5.2	6.3	0.023	0.046	0.103	0.183	0.285	0.411
16	0.18	0.36	0.72	1.1	1.4	1.8	2.2	2.9	3.6	4.3	0.016	0.032	0.071	0.126	0.197	0.283
17	0.14	0.27	0.54	0.81	1.1	1.3	1.6	2.2	2.7	3.2	0.012	0.024	0.053	0.095	0.148	0.213
18	0.09	0.19	0.38	0.56	0.75	0.94	1.1	1.5	1.9	2.2	0.008	0.016	0.037	0.066	0.103	0.148
19	0.07	0.14	0.27	0.41	0.55	0.69	0.83	1.1	1.4	1.7	0.006	0.012	0.027	0.048	0.075	0.109
20	0.05	0.11	0.21	0.31	0.42	0.53	0.63	0.84	1.1	1.3	0.005	0.009	0.021	0.037	0.058	0.083
21	0.04	0.08	0.16	0.23	0.31	0.39	0.46	0.62	0.77	0.93	0.003	0.007	0.015	0.027	0.042	0.061
22	0.03	0.06	0.12	0.18	0.23	0.30	0.36	0.47	0.59	0.71	0.003	0.005	0.012	0.021	0.033	0.047
23	0.02	0.04	0.08	0.11	0.15	0.19	0.23	0.30	0.38	0.46	0.002	0.003	0.007	0.013	0.021	0.030
24	0.01	0.03	0.05	0.08	0.10	0.13	0.16	0.21	0.26	0.31	0.001	0.002	0.005	0.009	0.014	0.021

TABLE V : Hydrodynamic Constants μ_n for Design Current B

Fluid Lamina No n	Value of μ_n for STEEL Ropes										Value of μ_n for NYLON Ropes				
	d = 1/8	1/4	1/2	3/4	1	1¼	1½	2	2½	3	1	1½	2	2½	3
1 thro' 8	∞	∞	∞	∞	∞	∞	∞	∞	∞	∞	∞	∞	∞	∞	∞
9	47.4	59.3	118.5	177.8	237.1	266.7	355.6	474.1	592.6	711.2	5.20	11.69	20.78	32.47	46.76
10	3.4	6.7	13.4	20.2	26.9	30.3	40.4	53.8	67.2	80.7	0.590	1.33	2.36	3.69	5.31
11	1.2	2.4	4.8	7.3	9.7	10.9	14.5	19.4	24.3	28.1	0.213	0.478	0.850	1.33	1.91
12	0.62	1.2	2.5	3.7	4.9	5.6	7.4	9.9	12.4	14.8	0.108	0.244	0.434	0.678	0.977
13	0.38	0.75	1.5	2.2	3.0	3.4	4.5	6.0	7.5	9.0	0.065	0.148	0.263	0.410	0.591
14	0.25	0.50	1.0	1.5	2.0	2.3	3.0	4.0	5.0	6.0	0.044	0.099	0.176	0.275	0.396
15	0.18	0.36	0.72	1.1	1.4	1.6	2.2	2.9	3.6	4.3	0.031	0.071	0.126	0.197	0.283
16	0.14	0.27	0.54	0.81	1.1	1.2	1.6	2.2	2.7	3.2	0.024	0.053	0.095	0.148	0.213
17	0.11	0.21	0.42	0.63	0.84	0.94	1.3	1.7	2.1	2.5	0.018	0.041	0.074	0.115	0.166
18	0.08	0.17	0.34	0.50	0.69	0.75	1.0	1.3	1.7	2.0	0.015	0.033	0.059	0.092	0.133
19	0.07	0.14	0.27	0.41	0.55	0.62	0.83	1.2	1.4	1.6	0.012	0.027	0.048	0.075	0.104
20	0.06	0.11	0.23	0.34	0.46	0.52	0.69	0.92	1.1	1.4	0.010	0.023	0.040	0.063	0.091
21	0.05	0.11	0.21	0.31	0.42	0.47	0.63	0.84	1.0	1.3	0.009	0.021	0.037	0.056	0.083

12. Ultimate Strengths of Mooring Cables

In Fig. 9 are presented manufacturers' data for the breaking strengths, T_u, of various sizes of steel and fiber mooring ropes. By and large, the ultimate strength, as a function of rope diameter d, conforms closely to a law of the type

$$T_u = C_2 d^2 \tag{50}$$

as will be noted from the distribution of the plotted points in relation to the diagonal lines which represent contours of the constant C_2. For steel, nylon, manila and coir ropes the square-power law is a very good approximation to the test results; only in the cases of dacron and polypropylene (prolene) ropes is there serious departure.

Next to steel, nylon ropes have the greatest strength for their size and would therefore be of great value for deep-sea mooring, particularly on account of their low weight. Dacron, prolene and manila ropes might be of value in certain instances where less elasticity is required than in nylon ropes. In this study consideration will be given only to steel and nylon ropes for which suitable values of C_2, obtained from Fig. 9, are

$$\left.\begin{array}{ll} \text{(i)} & C_2 = 70{,}000 \text{ lbs/sq in for steel ropes} \\ \text{(ii)} & \left.\begin{array}{l} C_2 = 25{,}000 \text{ lbs/sq in (dry)} \\ C_2 = 21{,}000 \text{ lbs/sq in (wet)} \end{array}\right\} \text{for nylon ropes} \end{array}\right\} \tag{51}$$

for T_u in lbs and d in ins. in Eq. (50).

For a tension T at any point in a mooring cable the safety factor, θ, against failure will be given by

$$\theta = \frac{T_u}{T} \tag{52}$$

This should normally not be less than 3 according to common usage and recommendations of rope manufacturers.

13. Numerical Evaluation of Cable Configurations and Tensions

With the necessary information now assembled for conducting numerical integrations of cable configurations and tensions the only remaining

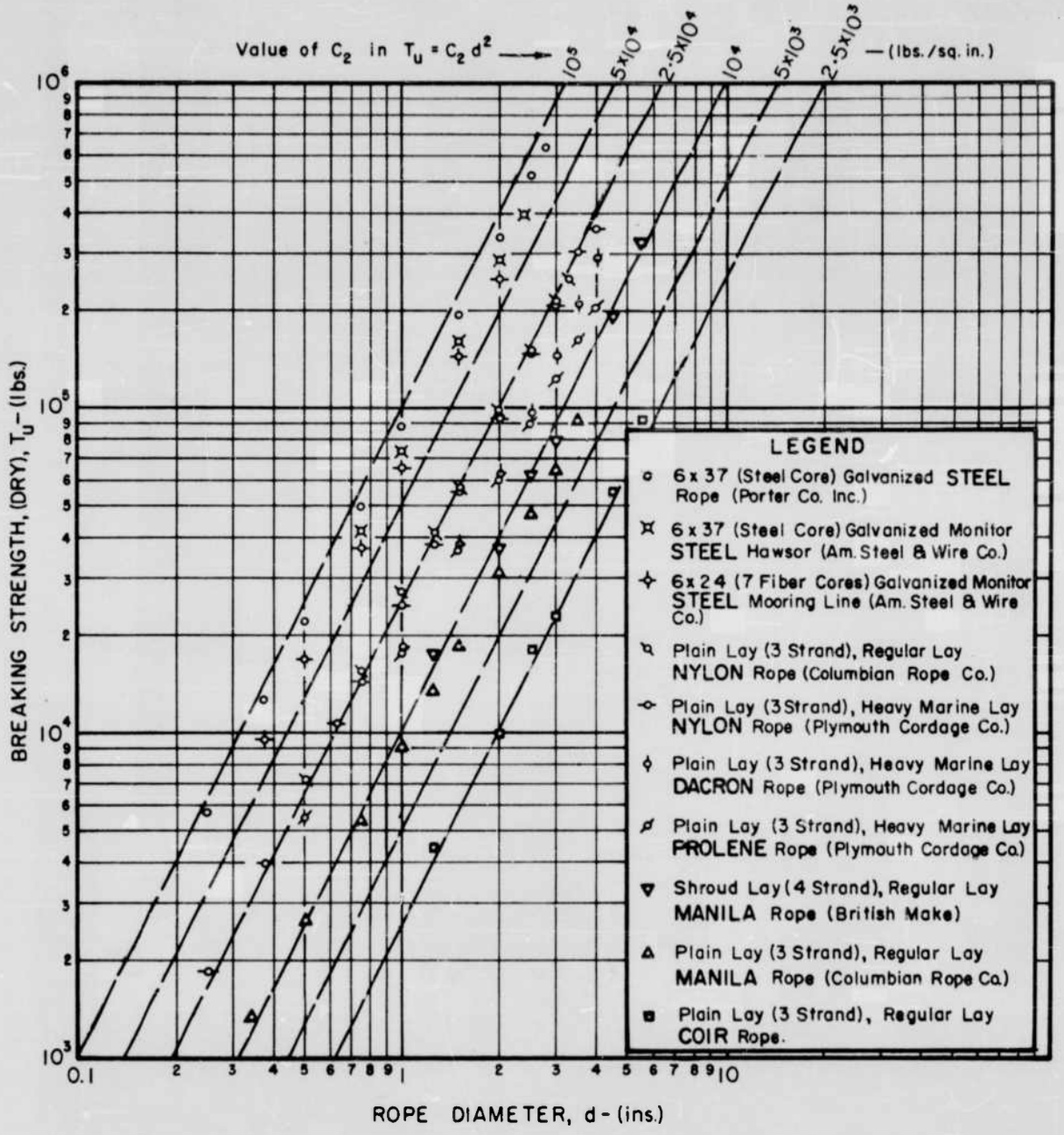

FIG 9: Relationships of breaking strength to rope diameter for steel and fiber mooring cables.

requirement for putting into effect the procedure detailed in Part II of this report concerns the specification of the terminal angles ψ_0 and ψ_k for the catenary portion of a cable in the layer of dead water below the surface current.

The selection of coupled values of ψ_0 and ψ_k for different sizes of steel and nylon ropes was made initially by trial and error, until the pattern of behaviour of the computed results could be assessed. One condition binding on the choice or retention of a pair of values of ψ_0 and ψ_k was that the safety factor θ should at no stage give a result less than unity or a value in excess of about 15. A second condition, already mentioned, was that ψ_N at the surface should not be permitted to exceed 90°. A third condition concerned the computed total length S_N of the mooring cable which was restricted to 30,000 ft (or $2\frac{1}{2}$ times the total water depth) for steel cables and 48,000 ft (or 4 times the depth) for nylon cables.

Calculations were undertaken using the facilities of No. 704 and 709 IBM high speed digital computers in accordance with the flow diagram given in Appendix A. The systemmatic use of the equations of this report in repetitive procedures is there indicated. Results of computations were stored on magnetic tapes and printed out finally in tabulated form, of which Table VI is an example. The table records basic information in respect of rope type, diameter, unit weight and strength and the type of current (A or B) in which the cable is suspended. The main body of the table defines the pertinent values of Δh_n, V_n, μ_n, γ_n, ψ_n, T_n, h_n, ℓ_n, s_n, s_n/h_n, ℓ_n/h_n and θ_n as applying to the different points n along the length of the cable. At the foot of the table are given components of tension in accordance with Eqs. (34) and (35) together with the overall scope (S_N/h_N) and stance (ℓ_N/h_N) of the cable.

The calculations made in this way for various sizes of mooring cables are collected in a series of tables (similar to Table VI) in Report No. 204-3A, which is companion to this report. The only difference to be noted in these tables is that column headings use descriptive symbolic notation owing to the inability of the IBM printer to reproduce Greek, script or lower case letters.

In the succeeding part of this report specific examples are given of the application of these tables to the solution of mooring problems. Some of the tables of Report 204-3A, it may be noted, are incomplete and contain no footing data. This is because the calculation could not proceed beyond the largest value of n tabulated, owing to the condition that ψ_n be less than 90°. These cases have been retained when the value of n was within close range of N (at the surface), as they could still apply to objects moored below the surface of the sea.

The configurations adopted by the cables in the design currents are shown in Figs. 10 to 21 of which Figs. 20 and 21 refer to nylon ropes and the balance to steel cables. The effects of the small negative buoyancy of nylon ropes in sea water, as compared with steel ropes, will be immediately apparent from comparison of Figs. 20 and 21 with the remaining figures; the nylon ropes show much less sag than the steel, as would be expected.

TABLE VI : Sample of Output Data for Typical Cable Calculation

CABLE CONFIGURATION AND TENSIONS IN VARIABLE OCEAN CURRENT

NYLON ROPE DIAMETER = 2.000 INCHES — DESIGN CURRENT TYPE B

WEIGHT PER FOOT RUN IN WATER = 0.111 LBS. — ULTIMATE STRENGTH OF CABLE = 94000. LBS.

ψ_o = 20. DEGREES — ψ (CATENARY) = ... ψ_8 = 25. DEGREES

SEA BOTTOM (n = 0)

n	Δh_n FEET	V_n KNOTS	μ_n	γ_n	ψ_n DEG.	T_n LBS.	h_n FEET	ℓ_n FEET	S_n FEET	S_n/h_n	ℓ_n/h_n	θ FACT
0	0.	0.	0.	0.	20.00	26169.	0.	0.	0.	0.	0.	0.
1	500.	0.	0.1000E 11	0.	20.33	26224.	500.	1361.	1450.	2.9	2.7	3.6
2	500.	0.	0.1000E 11	0.	20.65	26280.	1000.	2699.	2879.	2.9	2.7	3.6
3	700.	0.	0.1000E 11	0.	21.10	26357.	1700.	4535.	4843.	2.8	2.7	3.6
4	1000.	0.	0.1000E 11	0.	21.71	26468.	2700.	7086.	7583.	2.8	2.6	3.6
5	1500.	0.	0.1000E 11	0.	22.59	26634.	4200.	10771.	11562.	2.8	2.6	3.5
6	2000.	0.	0.1000E 11	0.	23.70	26856.	6200.	15449.	16650.	2.7	2.5	3.5
7	1500.	0.	0.1000E 11	0.	24.49	27022.	7700.	18803.	20324.	2.6	2.4	3.5
8	1000.	0.	0.1000E 11	0.	25.00	27133.	8700.	20972.	22713.	2.6	2.4	3.5
9	450.	0.125	0.2078E 02	0.	25.22	27183.	9150.	21925.	23766.	2.6	2.4	3.5
10	300.	0.375	0.2358E 01	0.010	25.38	27216.	9450.	22554.	24463.	2.6	2.4	3.5
11	250.	0.625	0.8500E 00	0.025	25.53	27242.	9700.	23074.	25040.	2.6	2.4	3.5
12	250.	0.875	0.4340E-00	0.025	25.71	27267.	9950.	23590.	25614.	2.6	2.4	3.4
13	200.	1.125	0.2630E-00	0.025	25.89	27285.	10150.	24000.	26070.	2.6	2.4	3.4
14	225.	1.375	0.1760E-00	0.025	26.12	27303.	10375.	24458.	26580.	2.6	2.4	3.4
15	200.	1.625	0.1260E-00	0.025	26.38	27318.	10575.	24861.	27030.	2.6	2.4	3.4
16	225.	1.875	0.9460E-01	0.025	26.73	27331.	10800.	25309.	27531.	2.5	2.3	3.4
17	200.	2.125	0.7360E-01	0.025	27.11	27340.	11000.	25701.	27972.	2.5	2.3	3.4
18	175.	2.375	0.5890E-01	0.025	27.51	27345.	11175.	26039.	28352.	2.5	2.3	3.4
19	300.	2.625	0.4820E-01	0.025	28.32	27350.	11475.	26605.	28992.	2.5	2.3	3.4
20	250.	2.875	0.4020E-01	0.025	29.12	27350.	11725.	27060.	29512.	2.5	2.3	3.4
21	225.	3.000	0.3690E-01	0.025	29.91	27349.	11950.	27457.	29968.	2.5	2.3	3.4

SEA SURFACE (n = N = 24)

HORIZONTAL COMPONENT OF CABLE TENSION AT ANCHOR = ... $T_o \cos \psi_o$ = 24591. LBS.

VERTICAL COMPONENT OF CABLE TENSION AT ANCHOR = ... $T_o \sin \psi_o$ = 8950. LBS.

HORIZONTAL COMPONENT OF CABLE TENSION AT SURFACE = ... $T_N \cos \psi_N$ = 23707. LBS.

VERTICAL COMPONENT OF CABLE TENSION AT SURFACE = ... $T_N \sin \psi_N$ = 13636. LBS.

SCOPE OF CABLE = ... S_N/h_N = 2.51

STANCE OF CABLE = ... ℓ_N/h_N = 2.30

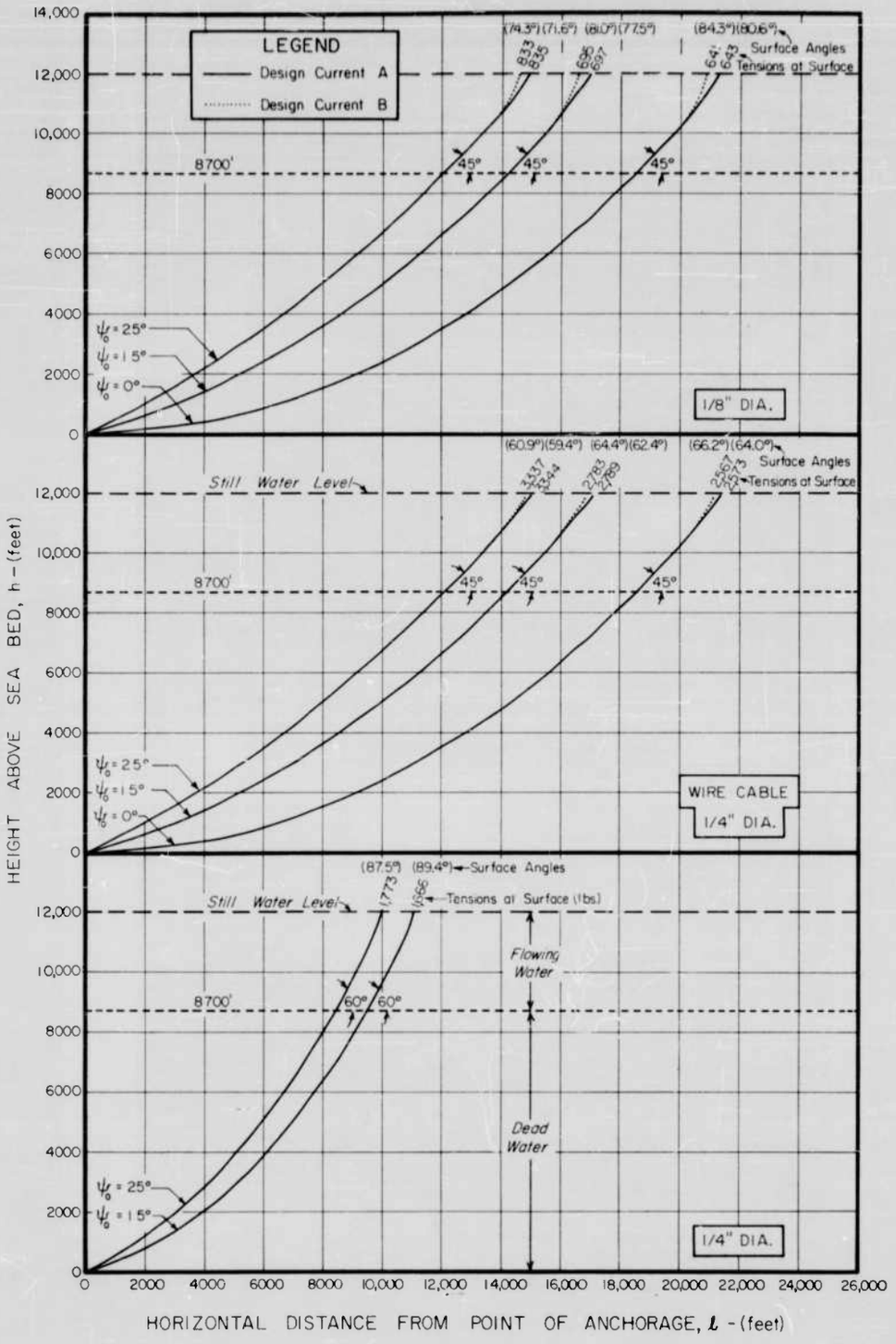

FIG 10: Configurations assumed by STEEL-wire mooring cables of 1/8 and 1/4-in diameter in design currents A nd B.

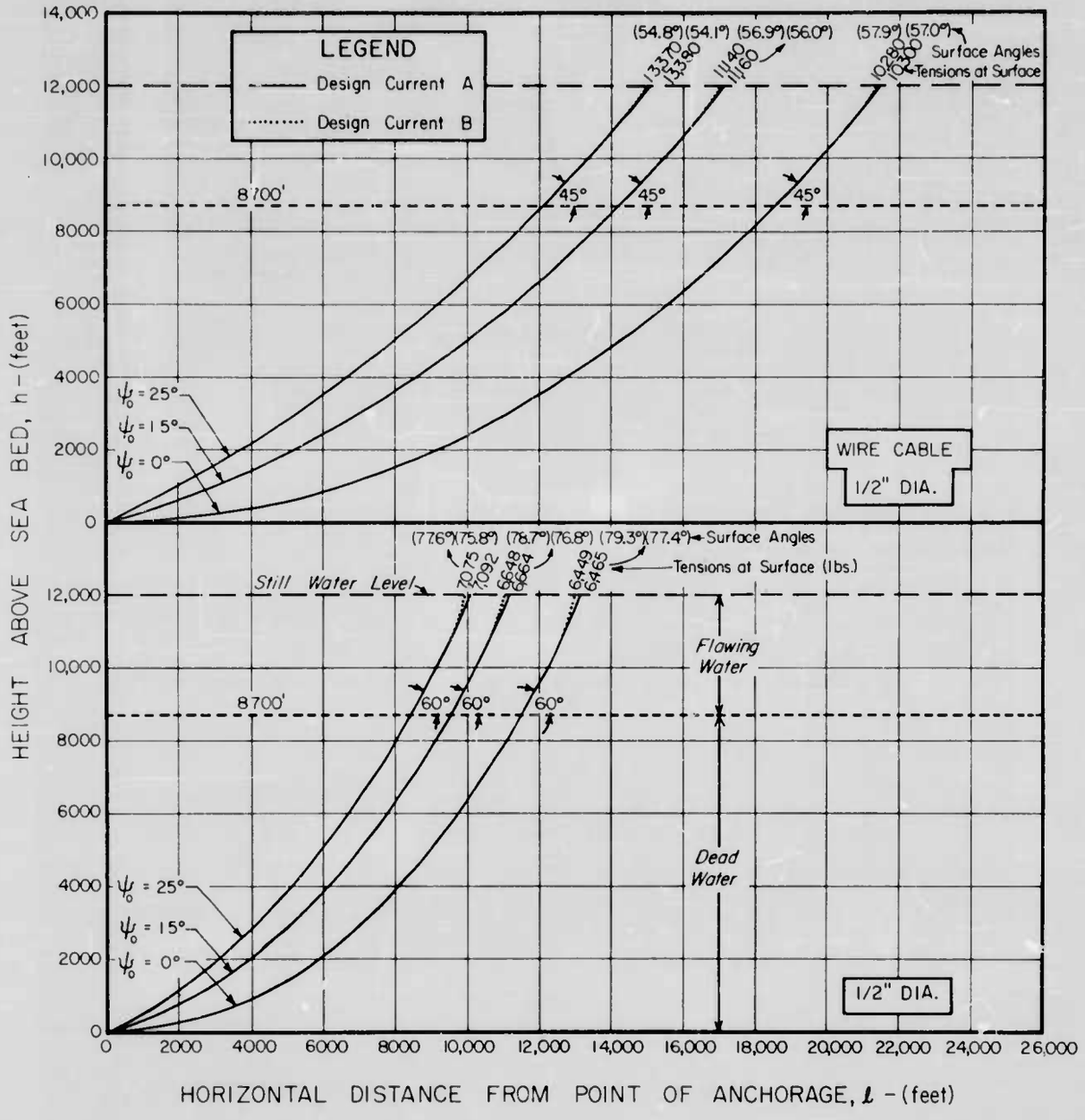

FIG 11: Configurations assumed by STEEL-wire mooring cables of 1/2-in diameter in design currents A and B.

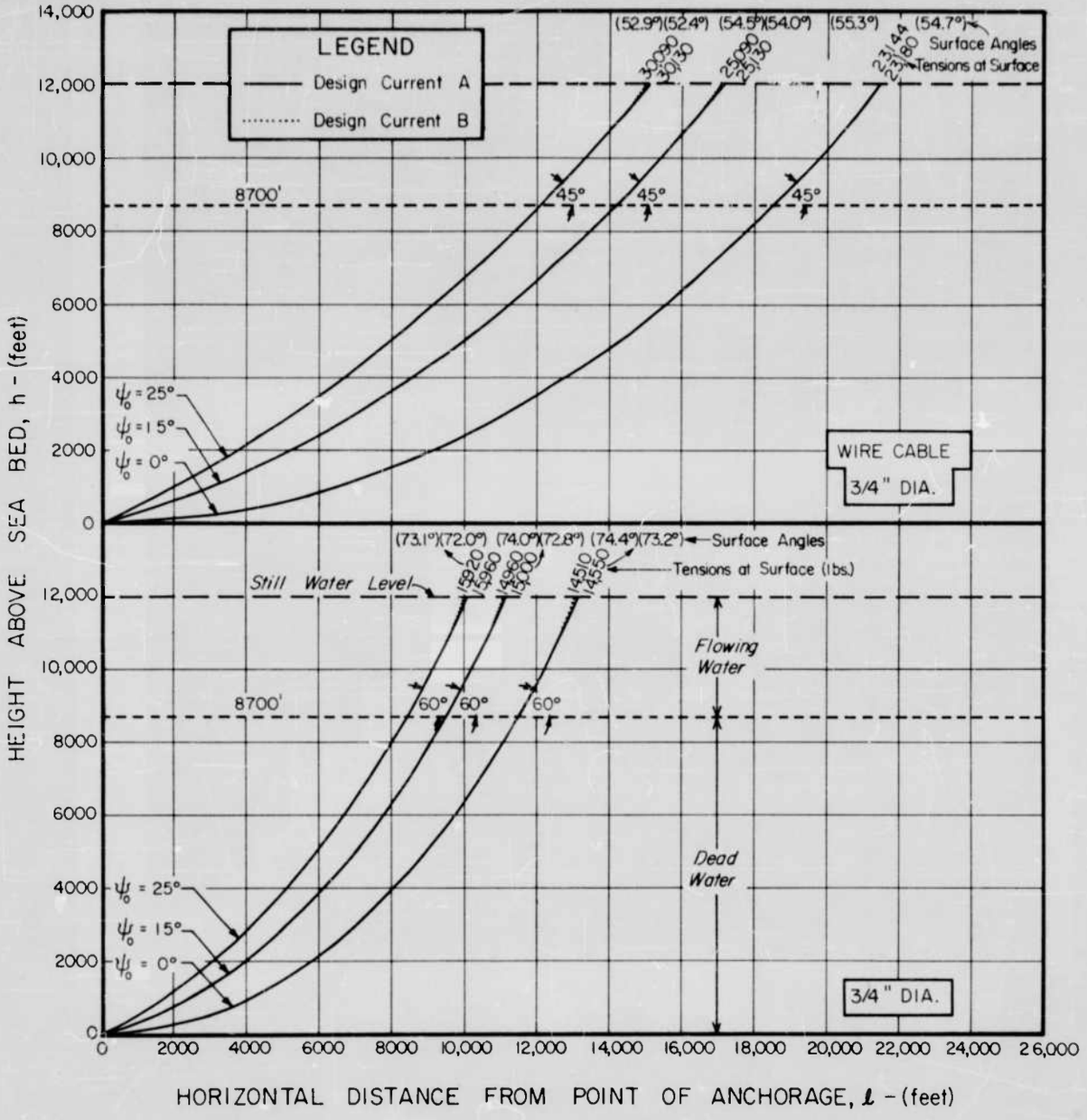

FIG 12: Configurations assumed by STEEL-wire mooring cables of 3/4-in diameter in design currents A and B.

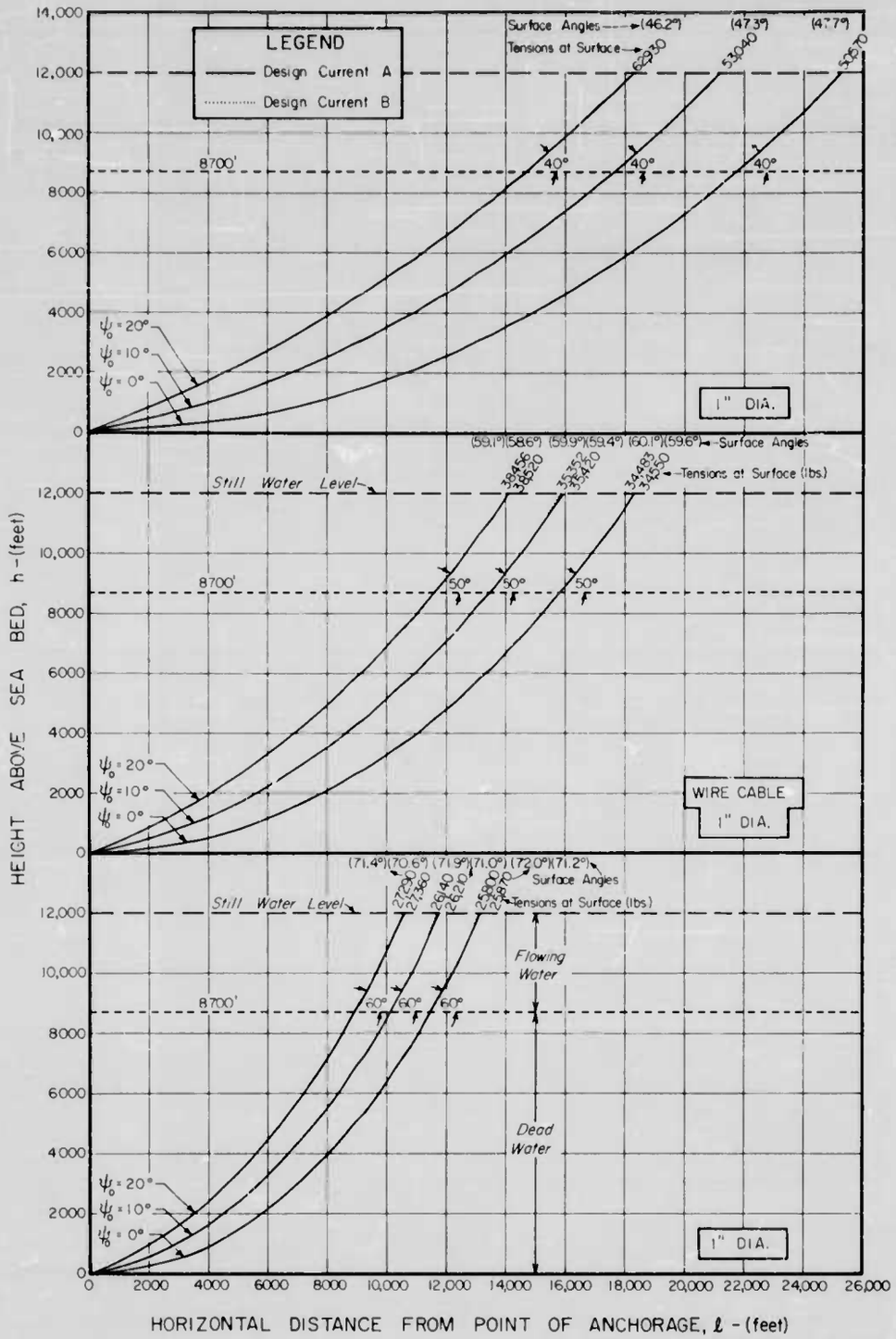

FIG 13: Configurations assumed by STEEL-wire mooring cables of 1-in diameter in design currents A and B.

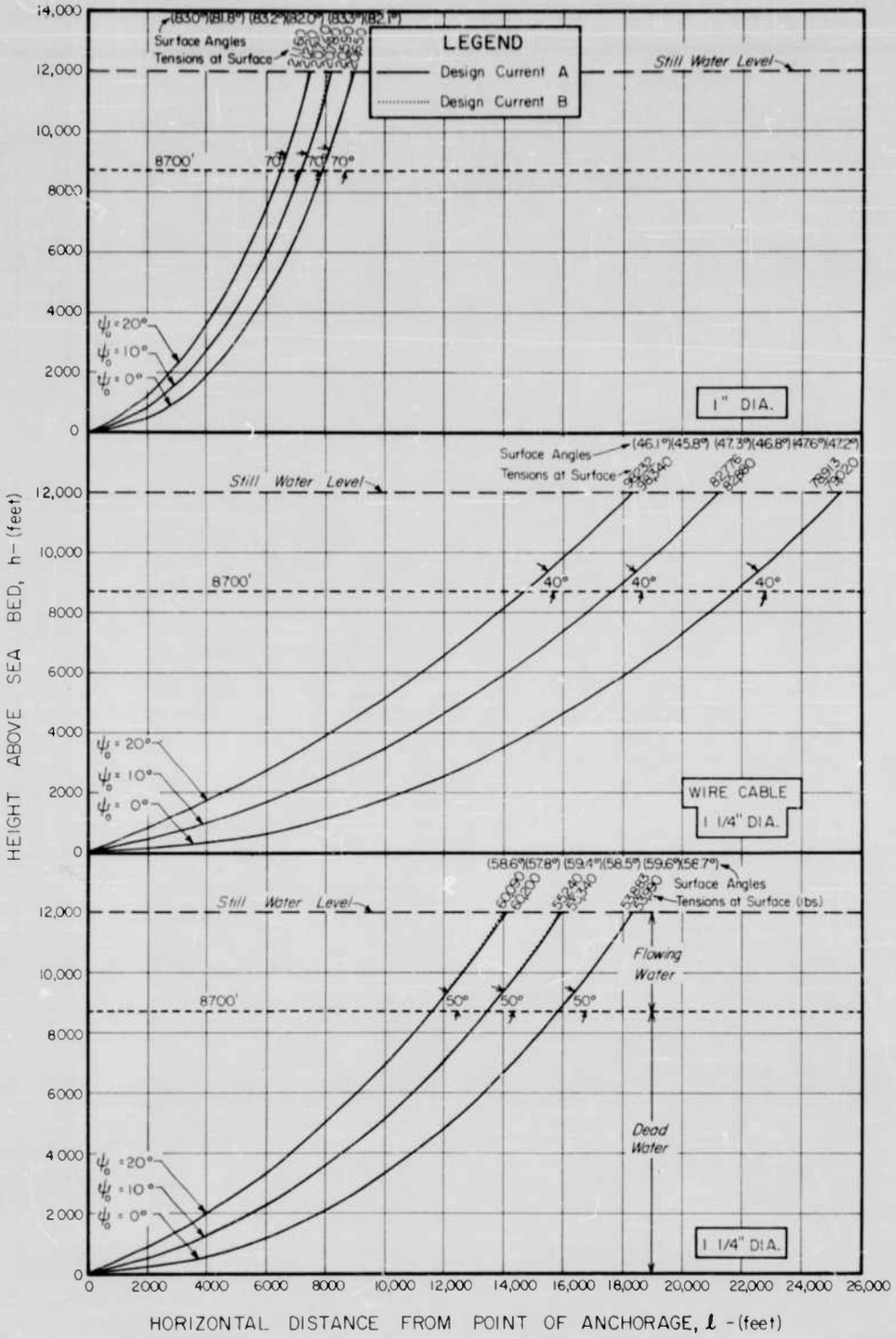

FIG 14: Configurations assumed by STEEL-wire mooring cables of 1 and $1\frac{1}{4}$-in diameter in design currents A and B.

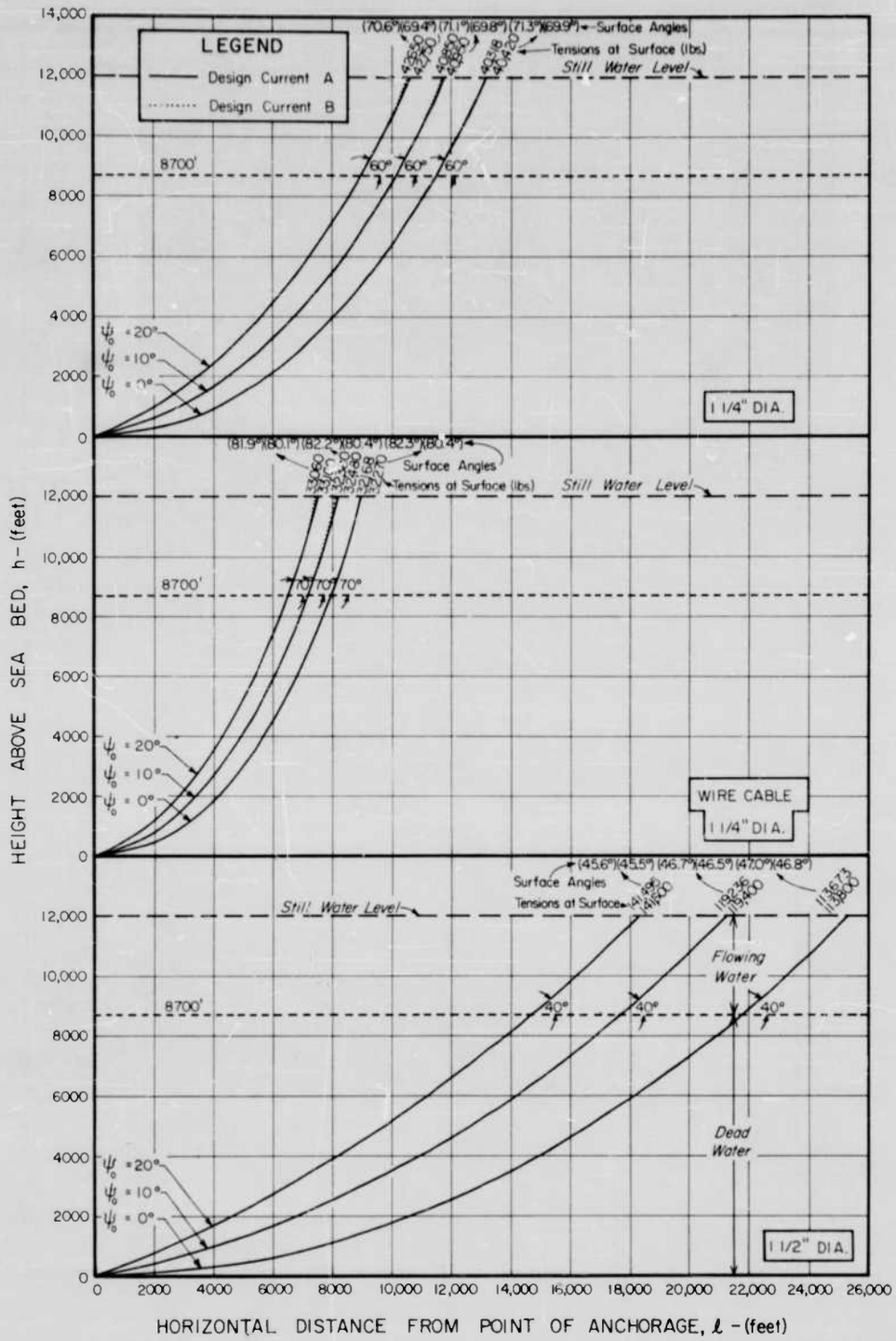

FIG 15: Configurations assumed by STEEL-wire mooring cables of $1\frac{1}{4}$ and $1\frac{1}{2}$-in diameter in design currents A and B.

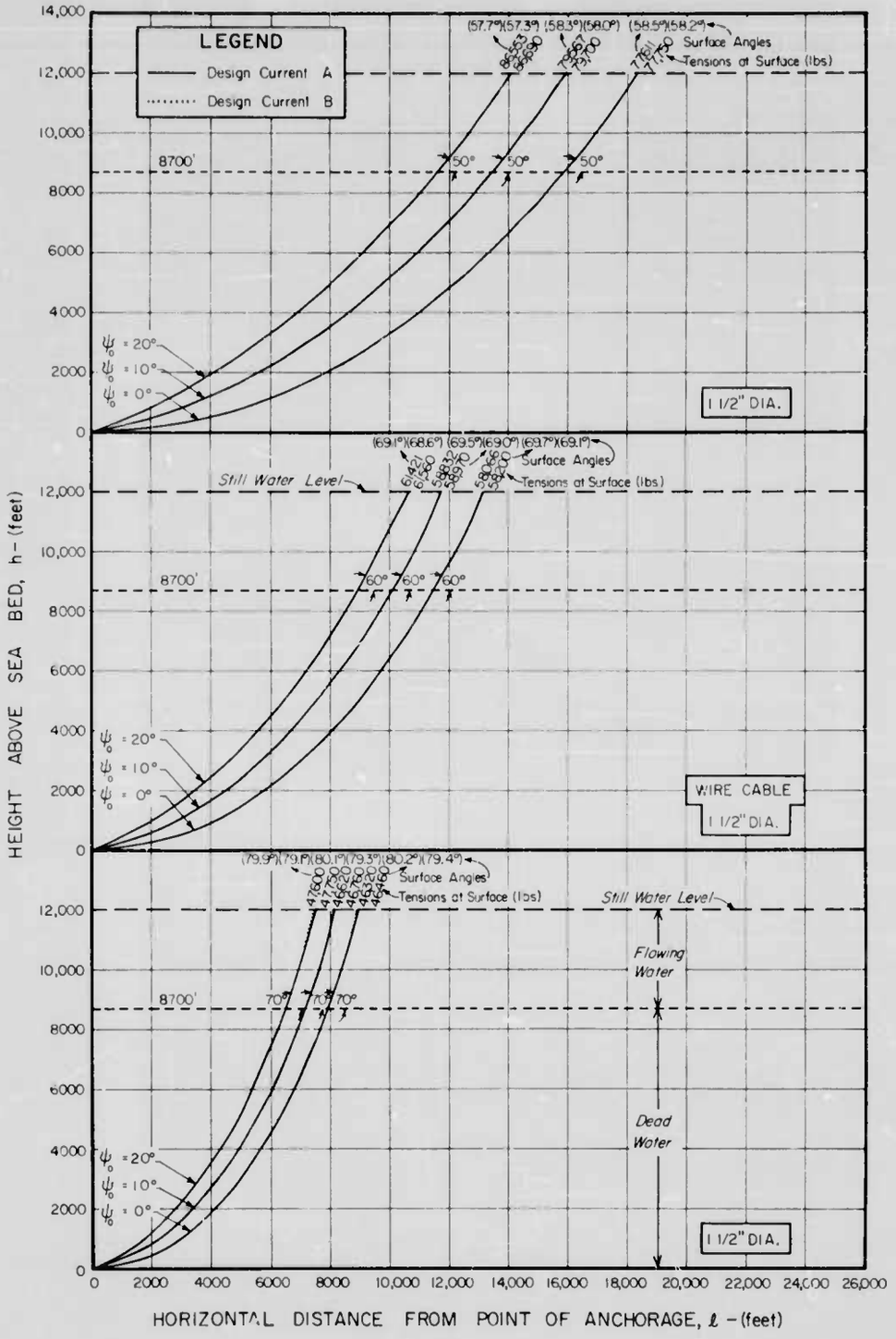

FIG 16: Configurations assumed by STEEL-wire mooring cables of $1\frac{1}{2}$-in diameter in design currents A and B.

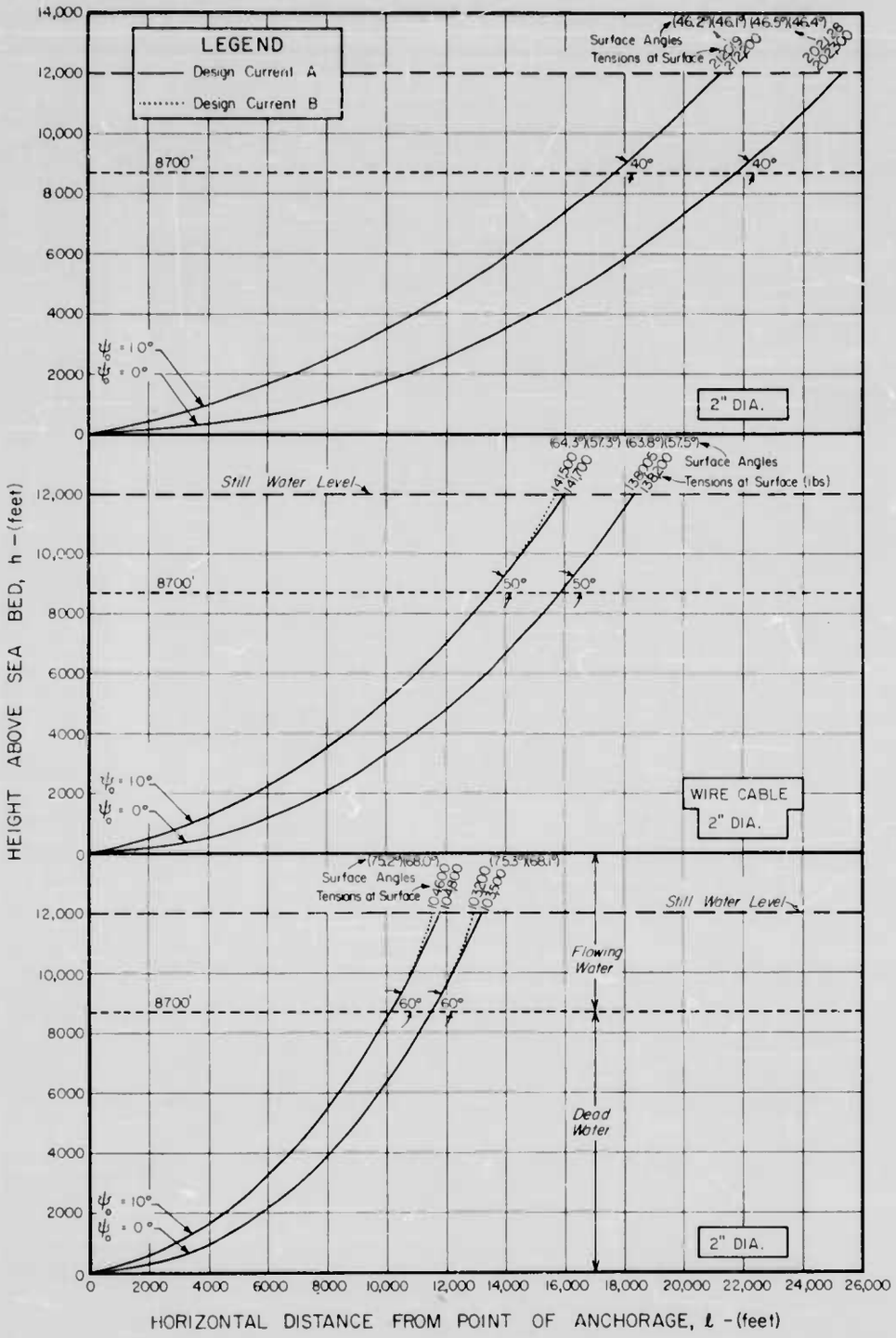

FIG 17: Configurations assumed by STEEL-wire mooring cables of 2-in diameter in design currents A and B.

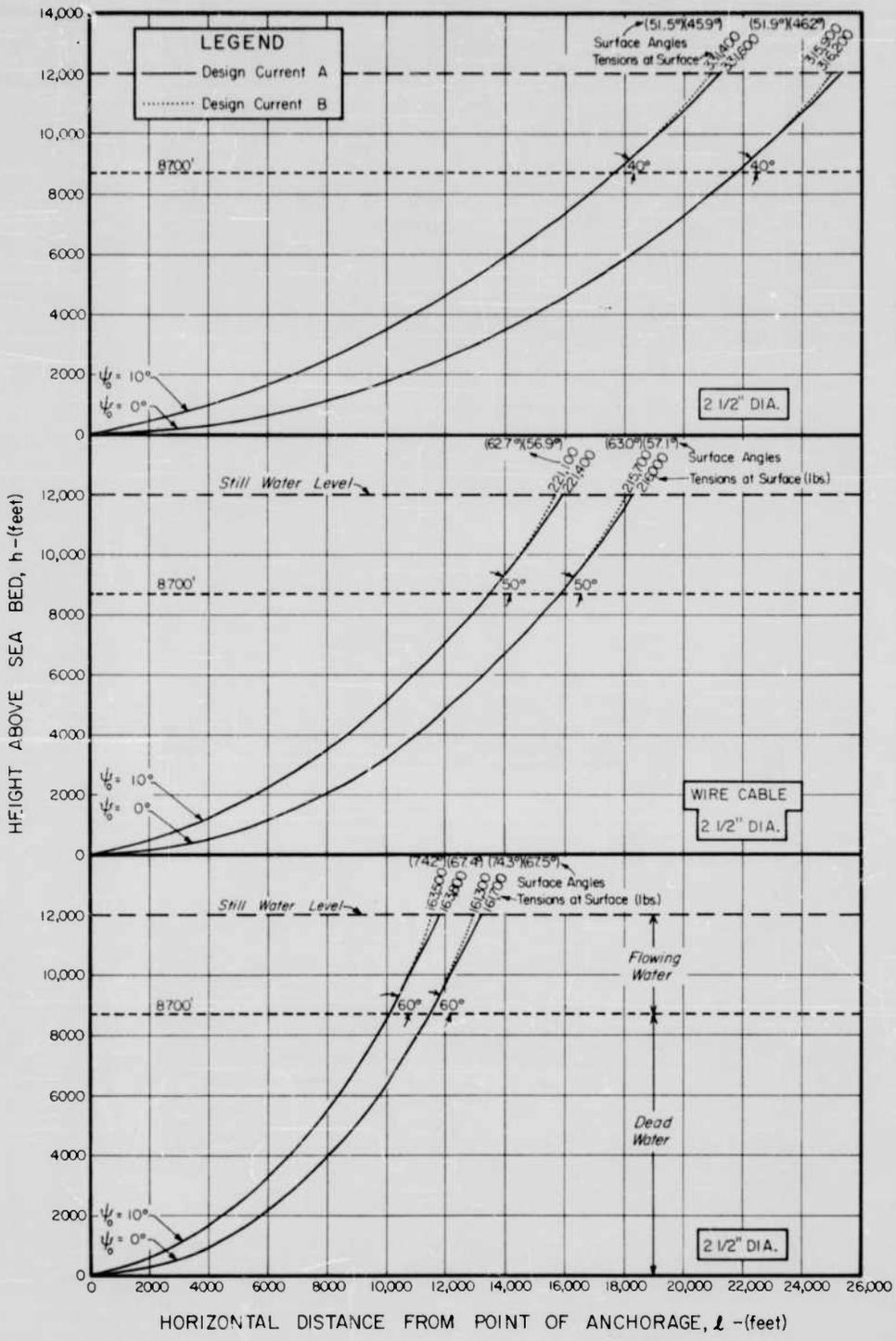

FIG 18: Configurations assumed by STEEL-wire mooring cables of $2\frac{1}{2}$-in diameter in design currents A and B.

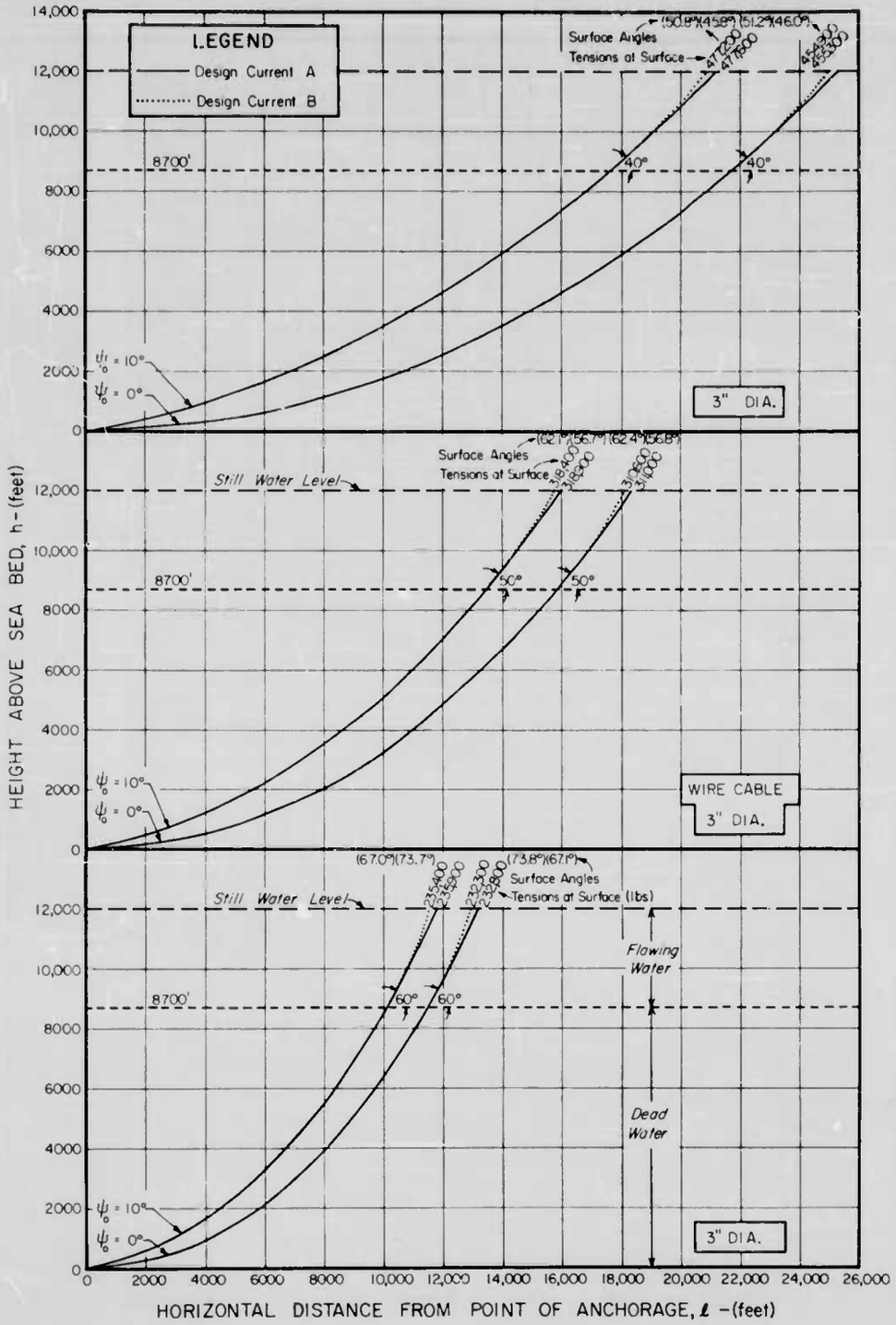

FIG 19: Configurations assumed by STEEL-wire mooring cables of 3-in diameter in design currents A and B.

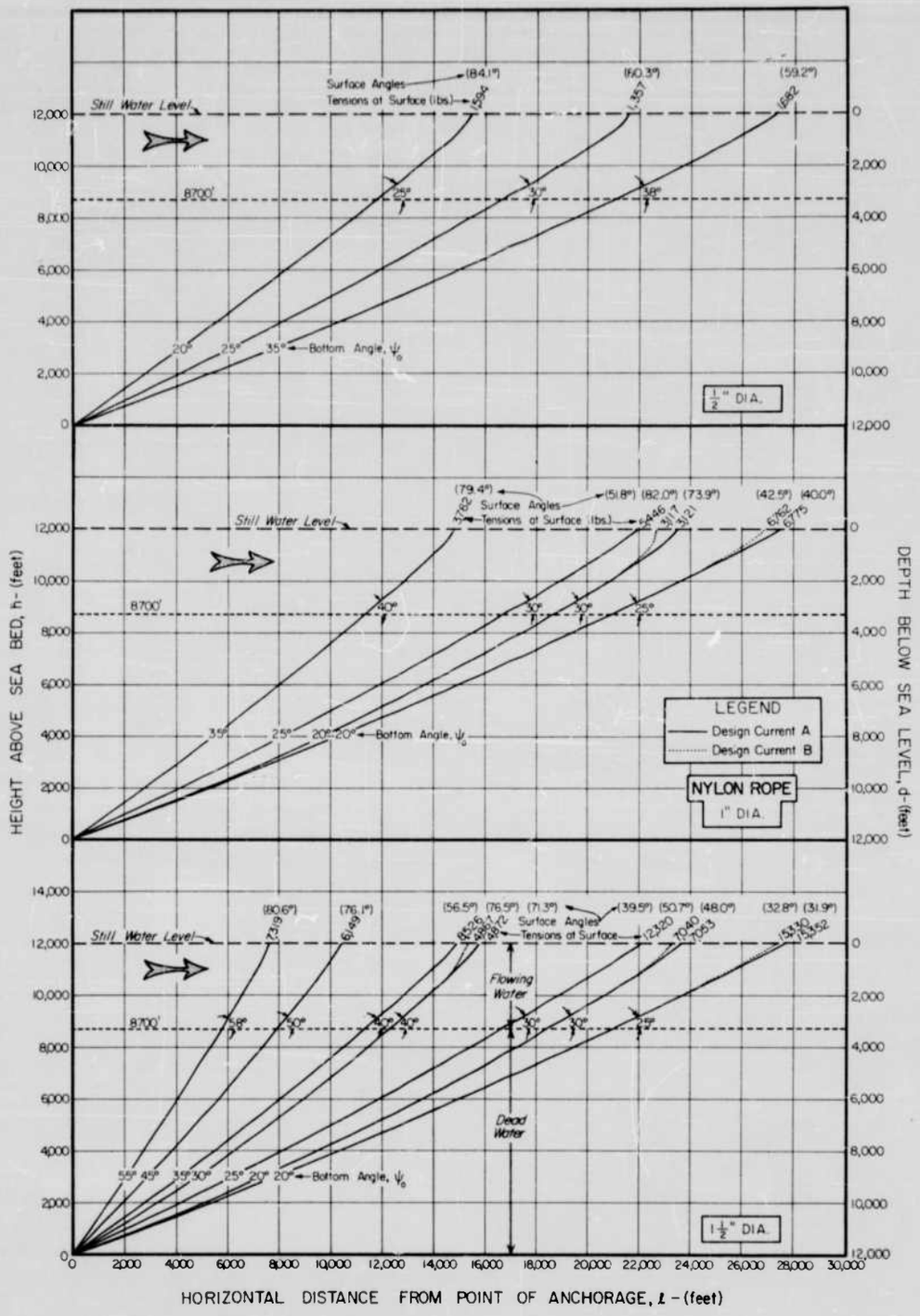

FIG 20: Configurations assumed by NYLON-rope mooring cables of ½ , 1 and 1½- in. diameter in design currents A and B.

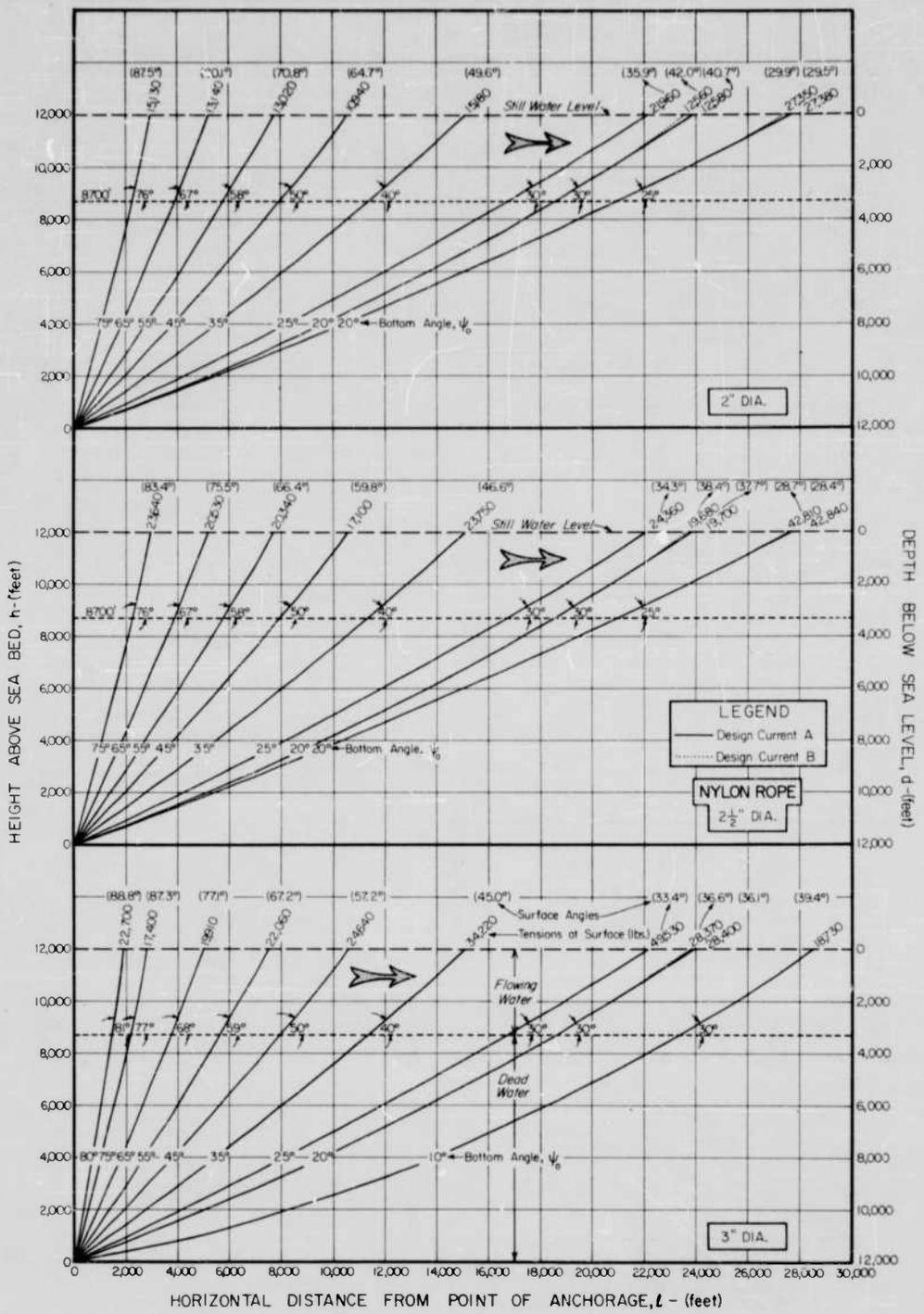

FIG 21: Configurations assumed by NYLON-rope mooring cables of 2, $2\frac{1}{2}$ and 3-in diameter in design currents A and B.

There is no great difference at first sight between the shapes assumed by the cables in the two design currents A and B. The dotted curves for design current B largely overly the full-line curves for design current A and deviate only near the surface. Congruence, however, is more apparent than real, for it must be remembered that the surface angle defines what proportion of the tension resists the current drag on the moored object. For a given object the drags from currents A and B would not normally both agree with the horizontal components of the surface tensions shown by an overlapping pair of dotted and full line curves. This difference will become apparent in the examples of the next part.

V. EXAMPLES OF CABLE CALCULATIONS

14. Tensions in a Deep-Sea Mooring Cable Holding a Ship in a Current

By way of illustrating the application of the tables of Report 204-3A and Figs. 10 to 21 of this report, the first problem posed will be that of anchoring typical ships in a water depth of 12,000 ft in a region such as the Gulf Stream where the surface currents may be strong. The problem may be framed as follows

Problem No. 1 :

Determine the size and scope (S/h) of a single anchor cable needed to anchor typical ships of the following sizes:

(i) a cargo vessel of 15,000 tons displacement
(ii) a passenger liner of 45,000 tons displacement
(iii) a super-tanker of 80,000 tons displacemtn in deep water of 12,000 ft depth in
  (a) design current A (surface velocity 6 knots) with a collinear surface wind of 40 knots (waves neglected)
  (b) design current B (surface velocity 3 knots) with calm atmosphere

assuming no drag of the anchor and a minimum safety factor of 2 for the mooring cable for (a) and of 3 for (b).

Solution:

The principal dimensions of the three ships as adapted from Wilson [1958, 1959] are listed below in Table VII: -

TABLE VII : Dimensions of Typical Ships

Type of Vessel	Displacement Tonnage W (Sht. tons)	Length between perpendiculars L (ft)	Beam B (ft)	Loaded Draft D (ft)	Area of Wetted Surface A_w $(ft)^2$	Area of Midship (Wetted) Section A_m $(ft)^2$	Transverse Projected Area of Ship above Water A_p $(ft)^2$
					$(x\ 10^4)$	$(x\ 10^3)$	$(x\ 10^3)$
Cargo	15,000	450	59.5	28.5	4.52	1.61	2.16
Liner	45,000	775	92.5	33.5	9.68	2.78	7.85
Tanker	80,000	930	110.0	37.5	14.45	3.91	8.75

The drag of the current and of the wind on these ships will constitute the horizontal component $(T_s)_x$ of the cable tension, T_s, at the surface. The drag from the current, F_c, may be computed from the formula [Landweber, 1947]

$$F_c = 0.12\ V^2\ \sqrt{LW}\ \text{lbs} \qquad (53)$$

where V is the current velocity in knots, L the length of the ship in feet and W its displacement tonnage. An alternative formula of Taylor [Thorpe and Farrell, 1947] is

$$F_c = A_w [0.0042\ V + 0.00657\ V^2] \qquad (54)$$

in which A_w is the area of the wetted surface in square feet and V is the current velocity in knots.

As in Report 204-1 [Wilson, 1960] the mean value of F_c as computed from Eqs. (53) and (54) will be increased by a factor ζ to allow for the effects of locked propellors after a 20% addition has been made for fouling, appendages and form factor.

The drag, F_w, from a wind of velocity U along the longitudinal axis of the ship may be estimated from

$$F_w = C_D \frac{\rho_a}{2} A_p U^2 \qquad (55)$$

where C_D is a dimensionless drag coefficient, ρ_a the mass density of the air and A_p the projected area of the ship above water opposing the wind. Suitable values of C_D for the three types of ships may be taken [cf. Gawn, 1948] as

$$\begin{aligned} &\text{(i)} \quad C_D = 0.90 \text{ for the freighter} \\ &\text{(ii)} \quad C_D = 0.70 \text{ for the liner} \\ &\text{(iii)} \quad C_D = 0.80 \text{ for the tanker} \end{aligned} \tag{56}$$

For the specified values of velocities, namely,

$$\begin{aligned} &\text{(a)} \quad V = 6 \text{ knots} \; ; \; U = 40 \text{ knots}, \\ &\text{(b)} \quad V = 3 \text{ knots} \; ; \; U = 0 \, , \end{aligned}$$

the total drag on a ship is

$$(T_s)_x = F_c + F_w \tag{57}$$

and is evaluated for the three ships in Table VIII: -

TABLE VIII : Wind and Current Drag on Ships

Type of Vessel	Current Drag, F_c					Wind Drag; F_w		Total Drag $(T_s)_x$ (lbs)
	Eq. (53) F_c (lbs)	Eq. (54) F_c (lbs)	Mean 20% (lbs)	Factor ζ	Final F_c (lbs)	C_D	Eq. (55) F_w (lbs)	
Case (a) V = 6 knots, U = 40 knots								
	($\times 10^4$)	($\times 10^4$)	($\times 10^4$)		($\times 10^4$)		($\times 10^4$)	($\times 10^4$)
Cargo	1.12	1.18	1.38	2.5	3.45	0.90	1.10	4.55
Liner	2.55	2.51	3.03	3.0	0.09	0.70	3.12	12.21
Tanker	3.72	3.78	4.50	3.0	13.50	0.80	3.97	17.47
Case (b) V = 3 knots, U = 0								
	($\times 10^3$)	($\times 10^3$)	($\times 10^3$)		($\times 10^4$)			($\times 10^4$)
Cargo	2.81	3.24	3.62	2.5	0.91	0.90	0	0.91
Liner	6.36	6.95	7.98	3.0	2.39	0.70	0	2.39
Tanker	9.28	10.36	11.77	3.0	3.53	0.80	0	3.53

TABLE IX : Cable Sizes and Scopes for Deep-Sea Mooring of Typical Ships

Ocean Current and Wind Condition	Type of Vessel	Surface Drag of Ship $(T_s)_x$ (lbs)	Required Safety Factor θ	Page No. Applicable Table [Rept.No. 204-3A]	Properties of the Most Suitable Single Mooring Line										Minimum Requirements of the Anchor	
					Diam. d (ins)	Material	Holding Power $(T_s)_x$ (lbs)	Factor of Safety θ	Surface Angle ψ_s (dig)	Cable Paid Out S (ft)	Scope S/h	Stance ℓ/h	Weight in Water w (lbs/ft)	Total Negative Buoyancy Sw (lbs)	Holding Power H (lbs)	Weight in Water W_a (lbs)
		(x 10^3)					(x 10^3)			(x 10^3)				(x 10^3)	(x 10^3)	(x 10^3)
Design Current A Wind 40 knots	Cargo	45.5	2.0	60	1.50	steel	42.2	2.0	58.0	20.5	1.71	1.33	2.81	57.6	45.3	8.0
				61	1.50	steel	46.8	1.8	57.3	18.8	1.57	1.17	2.81	52.8	49.8	18.1
	Liner	122.1	2.0	76	2.50	steel	117.2	2.0	57.1	22.8	1.90	1.53	7.81	178.1	122.3	0
	Tanker	174.7	2.0	82	3.00	steel	170.1	2.0	56.8	22.8	1.90	1.53	11.25	256.5	176.1	0
Design Current B Calm	Cargo	9.1	3.0	243	1.50	nylon	12.9	3.4	32.8	29.8	2.50	2.29	0.06	1.8	13.8	5.0
				198	1.25	steel	12.9	2.7	71.2	18.7	1.56	1.09	1.95	36.5	17.0	0
				215	1.50	steel	8.3	3.3	79.9	14.5	1.22	0.62	2.81	40.7	13.1	4.8
	Liner	23.9	3.0	250	2.00	nylon	23.7	3.4	29.9	30.0	2.51	2.30	0.11	3.3	24.6	8.9
				221	2.00	steel	38.6	2.7	68.3	17.4	1.45	0.98	5.00	87.0	44.2	7.8
	Tanker	35.3	3.0	256	2.50	nylon	37.6	3.4	28.7	30.0	2.51	2.30	0.17	5.1	38.4	14.0
				221	2.00	steel	38.6	2.7	68.3	17.4	1.45	0.98	5.00	87.0	44.2	7.8

We may now resort to the tables of Report 204-3A and without difficulty arrive at the solutions of the problem. The latter are suitably contained in Table IX. As an example of solution, say in respect of the cargo vessel moored in design current A with a head wind of 40 knots, (for which we seek a mooring line of such size, scope and stance as will give a value of $(T_S)_X$ at the surface of about 45,500 lbs with a factor of safety θ of 2.0), we find on page 60 of Report 204-3A that a $1\frac{1}{2}$ - in diameter steel cable, 20,500 ft long (scope 1.71, stance 1.33), will provide a restraining force of 42,250 lbs with a factor of safety of 2.0. This is not quite adequate, but on page 61 it is found that by slightly reducing the scope to 1.57 (stance 1.17) the restraining force can be increased to about 46,800 lbs with an increase of anchor weight and a slight loss of safety factor to 1.8. It may be inferred therefore that the cargo ship could be satisfactorily moored in these rather extreme conditions with a $1\frac{1}{2}$ - in diam. ($4\,3/4$ - in circumference) steel line paid out to about 20,000 ft in the water depth of 12,000 ft.

No single nylon cable can be found capable of holding the freighter under the above conditions, though the table on p. 149 of Report 204-3A suggests that a 3-in diameter nylon rope on a heavy anchor, paid out to 25,200 ft, could come close to the required performance. Certainly the larger ships could only be held on steel lines. The super-tanker would require a very heavy line indeed, weighing $11\frac{1}{4}$ lbs/ft in water, or some 14 lbs/ft in air, which might be extremely difficult to handle, let alone to store in any great length. On this account it would probably be desirable not to attempt to anchor so large a ship in such conditions, or otherwise to use the anchor as a drogue on a lighter line and permit the ship some drift as will be discussed in a later example.

15. Tensions in a Taut-line Mooring Cable Holding a Submerged Buoy.

The tables of Report 204-3A lend themselves readily to solution of problems of deep-sea mooring of submerged buoys, where, let us say, it is desirable that the mooring line should be as nearly vertical as possible in the ocean current. As an example the following problem is posed:

Problem No. 2

Determine the position assumed by a cylindrical buoy 5 ft in diameter and 10 ft long, made of 1/4" steel plate, suitably reinforced, when dropped with a 5 ton anchor on a 12,000 ft length of (a) $1\frac{1}{2}$", (b) 3", diameter nylon mooring line in design current A in a water depth of 12,000 ft.

Solution:

For the size of buoy given, the volume of plate steel is 4.083 cu ft which at 490 lbs/cu ft would weigh 2000 lbs in air. Allowing 25% for reinforcements to withstand external pressure the total weight may be assumed to be 2500 lbs. The buoy displaces 195.4 cu ft of sea water weighing 12,500 lbs and has a buoyancy, therefore of 10,000 lbs. Since the weights in water of $1\frac{1}{2}$-in and 3-in diameter nylon mooring lines are respectively 0.062 and 0.249 lbs/ft, the total weights suspended from the buoy will be 744 and 3000 lbs for the cable lengths of 12,000 ft. The net buoyancy B of the cylinder, neglecting the downward drag on the cable from the current, will thus be

$$\left.\begin{array}{ll} \text{(i)} & B = 9260 \text{ lbs for } d = 1\frac{1}{2} \text{ ins} \\ \text{(ii)} & B = 7000 \text{ lbs for } d = 3 \text{ ins} \end{array}\right\} \qquad (58)$$

If the buoy is pulled below the water surface by the current to some equilibrium position at a depth where the current velocity is V_n, the drag of the current, F_c, on the buoy, taken transverse to the cylinder, may be calculated from the equation

$$F_c = \tfrac{1}{2} C_D \rho_w A_b V_n^2 \qquad (59)$$

where C_D is a dimensionless drag coefficient, ρ_w the mass density of sea water and A_b the projected area of the buoy in the vertical plane incorporating its longitudinal axis. Since A_b can be expressed conveniently in terms of the buoy diameter D_b as

$$A_b = 2D_b^2 , \qquad (60)$$

Eq. (59) may be adapted to the form

$$\left.\begin{array}{ll} \text{(i)} & F_c = C_D \rho_w \nu^2 [R]_n^2 \\ \text{(ii)} & [R]_n = \dfrac{D_b V_n}{\nu} \end{array}\right\} \qquad (61)$$

in which ν is the kinematic viscosity of sea water and $[R]_n$ the Reynolds Number applicable to the flow round the cylinder. The value of C_D is itself here a function of $[R]_n$.

The tension, T_N, in the mooring line at its point of fixture to the buoy will be the resultant of the buoyancy B and the horizontal drag F_c. Thus

$$T_N = [B^2 + F_c^2]^{\frac{1}{2}} \qquad (62)$$

The slope of the cable at this point, making the angle ψ_N to the horizontal, will be defined by

$$\tan \psi_N = \frac{B}{F_c} \qquad (63)$$

In Table X, then, values of T_N and ψ_N are calculated from Eqs. (61) and (62) by taking different values of V_n corresponding to values of n applicable to the design current A . Appropriate values of Reynolds Number are adopted from the now-standard C_D - [R] relationship for flow transverse to an infinitely long cylinder [cf. Eisner, 1930; Rouse, 1946, etc.], modified by a factor of 0.57 to allow for the finite cylinder length (length/diameter ratio of 2) [cf. Goldstein, 1938].

TABLE X : Terminal Cable Tensions and Angles for Moored Buoy in Design Current A

Step No. n	Depth below Surface (ft)	Veloc. V_n (knots)	Reynolds No. $[R]_n$	Drag Coefft. C_D	Current Drag F_c (lbs)	Terminal Tension, T_N (lbs)		Terminal Angle ψ_N (deg)	
						(a) d = 1	(b) d = 3	(a) d = 1	(b) d = 3
			($\times 10^6$)			($\times 10^3$)	($\times 10^3$)		
24	50	6.000	5.07	0.177	945	9.30	7.06	84.2	82.3
23	100	5.000	4.22	0.296	1054	9.32	7.08	83.5	81.4
22	175	4.000	3.37	0.484	1100	9.32	7.09	83.2	81.1
21	250	3.500	2.96	0.547	957	9.31	7.07	84.1	82.2
20	325	3.000	2.53	0.598	764	9.29	7.04	85.4	81.9
19	400	2.625	2.22	0.627	618	9.28	7.03	86.1	85.0

It is apparent at once from Table X that the current drag would be greatest on the buoy at a depth of about 175 ft below the surface. The implication, therefore, is that the buoy, once submerged, would be slowly sucked down to about this level, at which it would finally stabilize.

Three conditions have to be met at the terminal position at which the buoy establishes itself. Two of these are specified in Table X by the tension T_N and the cable angle ψ_N . The third condition is that the total cable length must comprise the specified pay-out of 12,000 ft plus the elongation of the rope under the average tension along its length. If the average tension, T_{av} , be taken as T_N less one-half the cable weight in water, then

$$\left.\begin{aligned} &(a)\quad T_{av} \simeq 8950 \text{ lbs for } d = 1\tfrac{1}{2}" \\ &(b)\quad T_{av} \simeq 5590 \text{ lbs for } d = 3" \end{aligned}\right\} \qquad (64)$$

Rope manufacturers' data suggest that the cable extension for case (a) of (64) would be about 23% for wet rope and about 12% for case (b) . The cable lengths S_N involved, therefore, are

$$\left.\begin{aligned} &(a)\quad S_N \simeq 14{,}760 \text{ ft for } d = 1\tfrac{1}{2}" \\ &(b)\quad S_N \simeq 13{,}440 \text{ ft for } d = 3" \end{aligned}\right\} \qquad (65)$$

Quick reference to Figs. 20 and 21 indicates that the configuration assumed by nylon mooring ropes is in most cases virtually straight. To a first approximation therefore the location of the submerged buoy can be established from the simple trigonometry that the bottom angle ψ_o should conform to

$$\sin \psi_o \simeq \frac{h - 175}{S_N} \qquad (66)$$

(where h is the total water depth of 12,000 ft) and the horizontal projection ℓ_N of the cable to

$$\ell_N \simeq S_N \cos \psi_o \qquad (67)$$

Inserting (65) in (66) and (67), values of ψ_o and ℓ_N are found to be

$$\begin{aligned} &(a)\quad \psi_o \simeq 53.2° ; \ell_N \simeq 8850 \text{ ft for } d = 1\tfrac{1}{2} \\ &(b)\quad \psi_o \simeq 61.5° ; \ell_N \simeq 6410 \text{ ft for } d = 3 \text{ ins} \end{aligned} \qquad (68)$$

With this information it is now possible to consult Report 204-3A and confirm from page 118 for case (a) that the solutions given by (68) are of the right order of magnitude and yield values of T_N , ψ_N and S_N in reasonable accord with Table X and Eq. (65) for $N = n = 22$. Exact correspondence cannot be expected because the table is based on $\psi_o = 55°$ and $\psi_8 = 58°$. To obtain a complete solution to part (a) of the problem it would be necessary to compute a table or tables with $\psi_o = 5° \pm 0.5$ and $\psi_8 = 55° \pm 1.0$, say, and interpolate between them until the prescribed conditions were met.

Case (b) is similarly confirmed as to orders of magnitude by the table of p. 153, and the same remarks apply in respect of seeking a precise solution.

It would appear then in the light of the approximate solutions given by (68) that on a $1\frac{1}{2}$-in diameter nylon mooring line the buoy would be submerged 175 feet below the surface, 8850 ft downstream of the anchor, while on a 3-in diameter nylon line it would be about 6410 ft downstream of the anchor, in design current A.

16. Deep-Sea Mooring with Wire Cable, Ground-Line and Clump

In Fig. 22 (a) a ship is shown anchored in an ocean current with a combination 2-part anchor line and clump. The clump serves the purpose of ensuring that the cable angle ψ_o at the anchor will be small and the holding power of the anchor thus as great as possible, thereby also permitting a smaller scope for the major portion of the anchor line. It serves in addition as a useful shock-absorber for cushioning any transient disturbances capable of penetrating down the line, but this aspect is not of present concern. As an example of a situation in which a clump is utilised in deep-sea mooring, the following problem is posed:

Problem No. 3

Determine the weight of clump and the length and size of chain cable to be used for the ground line between clump and anchor in order that the cargo ship of problem No. 1 may be anchored in a 40 knot wind in design current A with 18,000 ft of $1\frac{1}{2}$ - in diameter steel wire cable and an anchor of 3 tons weight in water.

Solution.

If the general conditions are the same as for problem No. 1, the cargo vessel will be subject to a horizontal surface drag of 45,000 lbs which can be resisted, as we have seen, by the $1\frac{1}{2}$ - in diameter wire cable so as to yield a factor of safety of 2 against failure of the line. The inference from pages 60 and 61 of Report 204-3A, which apply to this case, is that the cable configuration would have to conform very largely to that of the table on page 60 or to the center curve of the three uppermost curves shown in Fig. 16. From the table referred to it is seen that the total length of cable would be about 20,500 ft, of which about 2100 ft would be below a height of 500 ft from the sea-bed. It may be assumed therefore that the specified 18,000 ft length of $1\frac{1}{2}$ - in diameter wire cable would necessitate that the clump be suspended at or near the point $n = 1$ at 500 ft from the bottom.

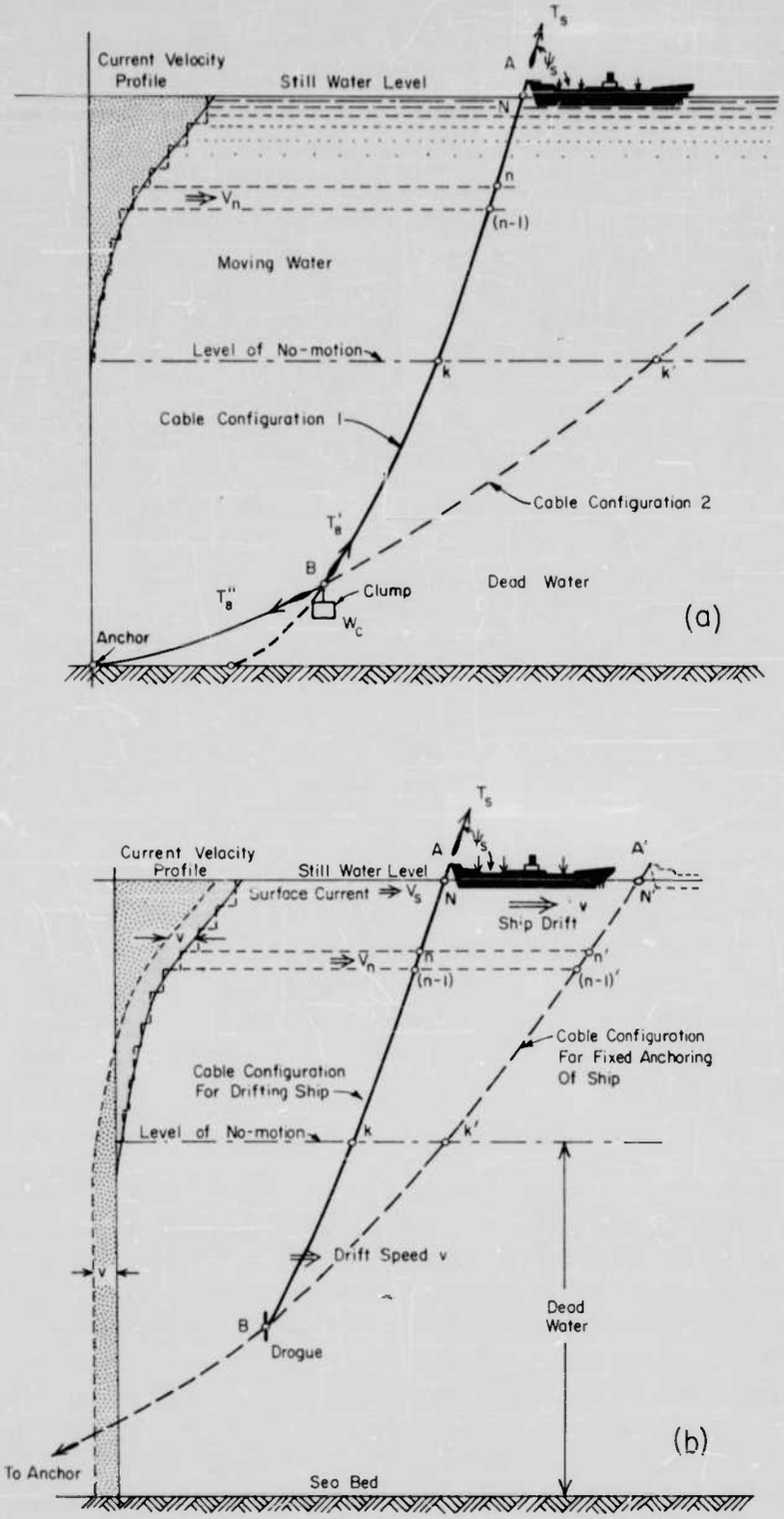

FIG 22: Schematic diagrams of deep-sea mooring systems. (a) Composite anchor, groundline and clump (b) Drogue-anchor permitting drift of the ship.

Allowing for a slight degree of interpolation between the tables on pages 60 and 61 of Report 204-3A, it may be assumed that the cable tension T_n and angle ψ_n at $n = 1$ will be

$$\left.\begin{aligned} &(i) \quad T_1 = 49{,}000 \text{ lbs} \\ &(ii) \quad \psi_1 = 19.0° \end{aligned}\right\} \qquad (69)$$

Fig. 22(a) which shows the anchoring system for this problem makes it clear that equilibrium of the junction point B of the chain cable, wire cable and clump requires that

$$\left.\begin{aligned} &(i) \quad T'_B \cos \psi'_B = T''_B \cos \psi''_B \\ &(ii) \quad T'_B \sin \psi'_B = W_c + T''_B \sin \psi''_B \end{aligned}\right\} \qquad (70)$$

where T'_B and T''_B are the tensions and ψ'_B and ψ''_B the angles of elevation of the wire cable and chain cable respectively at the point B, and W_c is the weight in water of the clump.

It is obvious that

$$T'_B = T_1 = 49{,}000 \text{ lbs}$$

$$\psi'_B = \psi_1 = 19° ,$$

so that Eqs. (70) yield

$$\left.\begin{aligned} &(i) \quad T''_B \cos \psi''_B = 46{,}350 \text{ lbs} \\ &(ii) \quad T''_B \sin \psi''_B + W_c = 15{,}950 \text{ lbs} \end{aligned}\right\} \qquad (71)$$

Now the portion of chain cable lying between the clump and the anchor will hang as a catenary in the sensibly dead water close to the ocean bottom, so that Eqs. (10) and (11) of Part I may be applied directly. If ψ_o at the anchor is chosen as zero, to ensure good holding for the light anchor Eqs. (11) and (12) (with suitable changes of notation), give

$$\left.\begin{aligned} &\text{(i)} \quad \frac{T_o}{w_1 h_1} = \frac{1}{\sec \psi''_B - 1} \\ &\text{(ii)} \quad \frac{T''_B}{w_1 h_1} = \frac{\sec \psi''_B}{\sec \psi''_B - 1} \end{aligned}\right\} \qquad (72)$$

in which h_1 is the height $h_n (n = 1)$ of the point B above the sea-bed and w_1 is the weight per unit length in water $w_n (n = 1)$ of the chain cable between anchor and clump. For $\psi_o = 0$

$$T_o = T''_B \cos \psi''_B = 46{,}350 \text{ lbs} \qquad (73)$$

and Eqs. (72) thus resolve to

$$w_1 h_1 = 46{,}350 (\sec \psi''_B - 1)$$

or, for $h_1 = 500$ ft,

$$w_1 = 92.6 (\sec \psi''_B - 1) \text{ lbs/ft} \qquad (74)$$

It is convenient now to choose the unit weight of chain cable as, say, 4 lbs per ft in water and hence find

$$\psi''_B = 16.6° \qquad (75)$$

From Eqs. (71), then,

$$\left.\begin{aligned} &\text{(i)} \quad T''_B = 48{,}350 \text{ lbs.} \\ &\text{(ii)} \quad W_c = 2140 \text{ lbs} \end{aligned}\right\} \qquad (76)$$

The length s_1 of chain cable required may be found quite readily from Fig. 2 of Report No. 204-1 from which, for $\psi''_B = 16.6°$ and $\psi_o = 0$,

$$s_1 / h_1 = 7.0 ,$$

whence, for $h_1 = 500$ ft

$$s_1 \simeq 3500 \text{ ft} \qquad (77)$$

It seems then that the cargo ship could be satisfactorily moored in the 40 knot wind and 6 knot surface current by introducing about 600 fathoms of 4 lbs/ft (in water) chain cable and a clump weighing about 1 ton in water, as groundline between the 3 ton anchor and the 18,000 ft of regular $4\frac{3}{4}$-in circumference steel mooring wire. The advantage of doing this will be apparent from Table IX which shows, in the last column, that the minimum weight of the anchor in water would otherwise have to be 5 tons or more, merely to offset the lifting tendency of the cable. In that case even a 10-ton anchor might be incapable of developing the requisite holding power to prevent dragging of the anchor.

17. Deep-Sea Anchoring by Cable Weight and Drogue

In the example of Problem No. 1 it was found (in Table X) that the holding powers required of the anchors for mooring the liner and the supertanker in strong wind and current were of very high order. In the circumstances, rather than risk the loss of the anchor or anchors as result of serious anchor dragging, it might be more satisfactory to use some form of drogue-anchor which would remain clear of the sea-bed and would mobilize the weight of the mooring line and the drogue and the resistance of the latter to an acceptable slow drift of the ship and the line in the direction of the wind and current. This situation, illustrated schematically in Fig. 22(b), is posed in the final problem

Problem No. 4

> Determine the size and weight of the drogue-anchor, suspended from $2\frac{1}{2}$-in diameter steel-wire mooring line, needed to restrain the motion of an 80,000 ton tanker to a drift of 1 knot in design current A and a wind of 40 knots, bearing in the same direction.

Solution.

Owing to the drift of the ship, the current and wind drags on the ship will both be reduced somewhat in comparison with their values shown in Table VIII. Thus the current drag computed on the basis of Eqs. (53) and (54), has a mean value here of $F_c = 9.48 \times 10^4$ lbs and the wind drag $F_w = 3.78 \times 10^4$ lbs, giving a total drag of $(T_s)_x = 13.26 \times 10^4$ lbs.

If the weight of the drogue-anchor in water is W_d and its projected area in the vertical plane perpendicular to the direction of drift, A_d, the tension in the cable at the lower end will be composite of vertical and horizontal

components W_d and F_d respectively, where the latter defines the drag on the drogue-anchor from its motion through still water at the drift velocity v of 1 knot, namely

$$F_d = \tfrac{1}{2} C_D \rho_w A_d v^2 \tag{78}$$

The lower terminal tension T_B in the mooring line will thus be

$$T_B = [W_d^2 + F_d^2]^{\frac{1}{2}} \tag{79}$$

and the angle of inclination ψ_B will be defined by

$$\tan \psi_B = \frac{W_d}{F_d} \tag{80}$$

The effect of the drift on the mooring system is indicated in Fig. 22(b) by the adjusted velocity profile over the water depth. The velocity of the water relative to the system gives a negative flow in deep water and is such that the level of no-motion has in effect been elevated and the surface current reduced from V_s to $(V_s - v)$. To make a completely satisfactory analysis of this situation it would really be necessary to evaluate applicable values of hydrodynamic constant μ along this new velocity profile and thence make special computations using the equations of this report, to arrive at the shape of the suspended anchor line. At the risk of some loss in accuracy we can avoid this complicated procedure by assuming that the effect of the negative current v will be relatively minor insofar as the hydrodynamic forces on the cable are concerned and that the major influence on cable configuration will derive from the terminal tensions and the cable weight.

Thus on the basis that the imposition of a negative velocity v on the system renders the ship and its mooring motionless for which condition the surface drag on the ship is 132,600 lbs, Report No. 204-3A may be consulted for such a value of $(T_s)_x$. On page 74 we find $(T_s)_x$ = 218,832 lbs for $\psi_8 = 40°$ and $\psi_o = 0$ and on page 76 $(T_s)_x$ = 117,291 lbs for $\psi_8 = 50°$ and $\psi_o = 0$. By linear interpolation we should expect $(T_s)_x$ = 132,600 lbs for $\psi_8 = 48.5°$ and $\psi_o = 0$.

If the level of the drogue-anchor be taken at n = 8 (the level of no-motion) the interpolated tension T_B and cable inclination ψ_B from the tables would be

$$\left.\begin{array}{ll} \text{(i)} & T_B = 205{,}300 \text{ lbs} \\ \text{(ii)} & \psi_B = 48.5° \end{array}\right\} \qquad (81)$$

Since the horizontal component of the tension T_B must balance the drag F_d given by Eq. (78), the necessary area of the drogue-anchor required for retarding the ship's drift in the current will be

$$A_d = \frac{2T_B \cos \psi_B}{C_D \rho_w v^2} \qquad (82)$$

For $v = 1$ knot and $C_D \simeq 1.5$, the area is found to be $A_d = 31{,}800$ sq. ft. The weight of the drogue-anchor would have to be

$$W_d = T_B \sin \psi_B \ , \qquad (83)$$

which would have a value of 153,800 lbs. Very clearly these values are outside the bounds of practicality and the inference must be that no simple drogue-anchor system could slow the drift of the ship under the combined wind and current action to just 1 knot.

If the allowable ship drift were increased to $v = 3$ knots the current drag on the ship would be $F_c = 3.53 \times 10^4$ lbs, and the wind drag $F_w = 3.40 \times 10^4$ lbs making the total drag $(T_s)_x = 6.93 \times 10^4$ lbs. In this circumstance the tables for design current B would be better approximations to the cable configuration when there is imposed on the system a negative velocity $v = -3$ knots to make the ship and cable motionless. The table on p. 227 of Report 204-3A shows $(T_s)_x = 62{,}009$ lbs and is thus a reasonable match. At $n = 8$, we then find

$$\left.\begin{array}{ll} \text{(i)} & T_B = 138{,}067 \text{ lbs} \\ \text{(ii)} & \psi_B = 60° \end{array}\right\} \qquad (84)$$

from which are readily found $A_d \simeq 1800$ sq ft and $W_d = 119{,}500$ lbs. As this would still require a drogue-anchor of very great weight and size it would not seem to be a practical proposition in general to attempt any arresting action by this means under such severe conditions.

REFERENCES

Bowden, K. F. [1954]; The Direct Measurement of Subsurface Currents in the Oceans; Deep-Sea Research, v. 2, 1954, pp. 33-47.

Carson, R. [1951]; The sea around us; (Staples Press Ltd.) London, 1951.

Chatley, H. [1950]; Water Currents due to Wind; Engineering (London), v. 169, Jan. 1950, p. 19.

Dietrich, G. [1957]; Allgemeine Meereskunde, (Gerbruder Borntraeger), Berlin, 1957.

Eisner [1930]; Das Widerstands Problem; 3rd Internatl. Congr. Appld. Mechs., Stockholm, 1930.

Frankcom, C. E. N. and Barlow, E. W. [1954]; Surface Currents of the Ocean and Their Effects on Navigation, Journl. Inst. Navig., v. 7(1), Jan. 1954, pp. 343-361.

Gawn, R. W. L. [1948]; Discussion on Thorpe and Farrel; Trans. Inst. Nav. Arch., v. 90, 1948, p. 150.

Griswold, W. [1952]; Loran Survey of the Gulf Stream; Internatl. Hydrographic Rev., v. 29(2), Nov. 1952, pp. 93-104.

Goldstein, S. [1938]; Modern Developments in Fluid Dynamics; v. II (Oxford Univ. Press), 1938.

Goodall and Darby [1941]; The University Atlas; (George Philip and Son Ltd.) London, 1940.

Haurwitz, B. and Panofsky, H. A. [1950]; Stability and Meandering of the Gulf Stream; Trans. Am. Geophys. Union, v. 31(5), Oct. 1950, pp. 723.

Hydrographic Office, U. S. Navy [1944]; Atlas of Surface Currents, Indian Ocean, Pub. No. 566, 1944.

Hydrographic Office, U. S. Navy [1944]; Atlas of Current Charts, Southwestern Pacific Ocean, Pub. No. 568, 1944.

Hydrographic Office, U. S. Navy [1944]; Atlas of Surface Currents, Northwestern Pacific Ocean, Pub. No. 569, 1944.

Hydrographic Office, U. S. Navy [1944]; Atlas of Surface Currents, Northeast Pacific Ocean, Pub. No. 570, 1947.

Hydrographic Office, U. S. Navy [1947]; Atlas of Surface Currents, North Atlantic Ocean, Pub. No. 571, 1947.

Knauss, J. A. [1959]; Direct Current Measurements at the Equator - The Cromwell Current; Proc. Internatl. Oceanographic Congr., New York, Sept. 1959, pp. 515-517.

Knauss, J. A. [1960]; Measurements of the Cromwell Current, Deep-Sea Research, v. 6, 1960, pp. 265-286.

Lamb, H. [1932]; Hydrodynamics; (Dovers Public Inc.), New York, 1932, 6th Edition.

Landweber, L. [1947]; Hydrodynamic Forces on an Anchor Cable, Tech. Report R-317, David Taylor Model Basin, U. S. Navy, Nov. 1947, 13 pp.

Laughton, A. S. [1959]; Disturbance of the Sediment Surface in the Deep Sea as Observed by Underwater Photography; Proc. Internatl. Oceanographic Congr., New York, Sept. 1959, p. 466.

Laughton, A. S. [1959]; Photography of the Ocean Floor; Endeavour, v. 18(72), Oct. 1959, pp. 178-185.

Lumby, J. R. [1959]; The IGY World Data Centers for Oceanography, Texas Journ. Sci., v. 11(3), Sept. 1959, pp. 259-269.

Masuzawa, J. [1955]; Preliminary Report on the Kuroshio in the Eastern Sea of Japan (Currents and Water Masses of the Kuroshio System III), Records of Oceanographic Works in Japan, v. 2(1), Mar. 1955, pp. 132-140.

Munk, W. [1955]; The Circulation of the Oceans; Scientific American, v. 193(3), Sept. 1955, pp. 96-104.

Neumann, G. [1956]; Zun Problem der "Dynamischen Bezugsflache" insbesondere im Golfstroom gebiet; Deutsche Hydrograph. Zeits. v. 9(2), 1956, pp. 66-78.

Pillsbury, J. E. [1890]; The Gulf Stream; Report of Superintendent, U. S. Coast and Geod. Survey, June, 1890, pp. 461-620.

Rouse, H. [1946]; Elementary Mechanics of Fluids (J. Wiley and Sons), New York, 1946.

Stommel, H. [1958]; The abyssal circulation; Deep-Sea Research, v. 5(1), May 1958, pp. 80-82.

Sverdrup, H. V., Johnson, M. W. and Fleming, R. H. [1942]; The Oceans (Prentice Hall, Inc.), New York, 1942.

Swallow, J. C. [1955]; A Neutral Buoyancy Float for Measuring Deep Currents; Deep-Sea Research, v. 3, 1955, pp. 74-81.

Swallow, J. C. [1957]; Some Further Deep Current Measurements using Neutrally-Buoyant Floats; Deep-Sea Research, v. 4, 1957, pp. 93-104.

Swallow, J. C. and Worthington, L. V. [1957]; Measurements of Deep Currents in the Western North Atlantic; Nature, v. 179, June 1957, pp. 1183-1184.

Swallow, J. C. and Worthington, L. V. [1959]; The Deep Counter Current of the Gulf Stream off South Carolina; Proc. Internatl. Oceanographic Congr., New York, Sept. 1959, pp. 443-444.

Swallow, J. C. and Hamon, B. V. [1959]; Some Measurements of Deep Currents in the Eastern North Atlantic; Proc. Internatl. Oceanographic Congr., New York, Sept. 1959, pp. 442-443.

Taylor, G. I. [1916]; Skin Friction of the Wind on The Earth's Surface; Proc. Roy. Soc. (London), v. 92(A), 1916, pp. 196-199.

Thorpe, T. and Farrell, K. P. [1947]; Permanent Moorings; Trans. Inst. Nav. Arch. (London), v. 90, 1948, pp. 111-153.

von Arx, W. S., Bumbus, D. F. and Richardson, W. S. [1955]; On the Fine-Structure of the Gulf Stream Front; Deep-Sea Research, v. 3, 1955.

Wilson, B. W. [1958, 1959]; The Energy Problem in the Mooring of Ships Exposed to Waves, Proc. Princeton Univ. Conf. on Berthing and Cargo Handling in in Exposed Places; Princeton, Oct. 1958, pp. 1-67; Bulln. No. 50, Permanent Internatl. Assoc. Navig. Congr., 1959, pp. 1-65.

Wilson, B. W. [1960(i)]; Characteristics of Anchor Cables in Uniform Ocean Currents; Tech. Report No. 204-1 (Ref. 60-5T), Texas A & M Research Foundation, April 1960, 157 pp.

Wilson, B. W. [1960 (ii)]; Mooring of Ships Exposed to Waves; Tech. Report No. 204-2 (Ref 60-21T), Texas A & M Research Foundation, Nov. 1960, 65 pp.

APPENDIX A

FLOW DIAGRAM FOR DIGITAL CABLE COMPUTATION

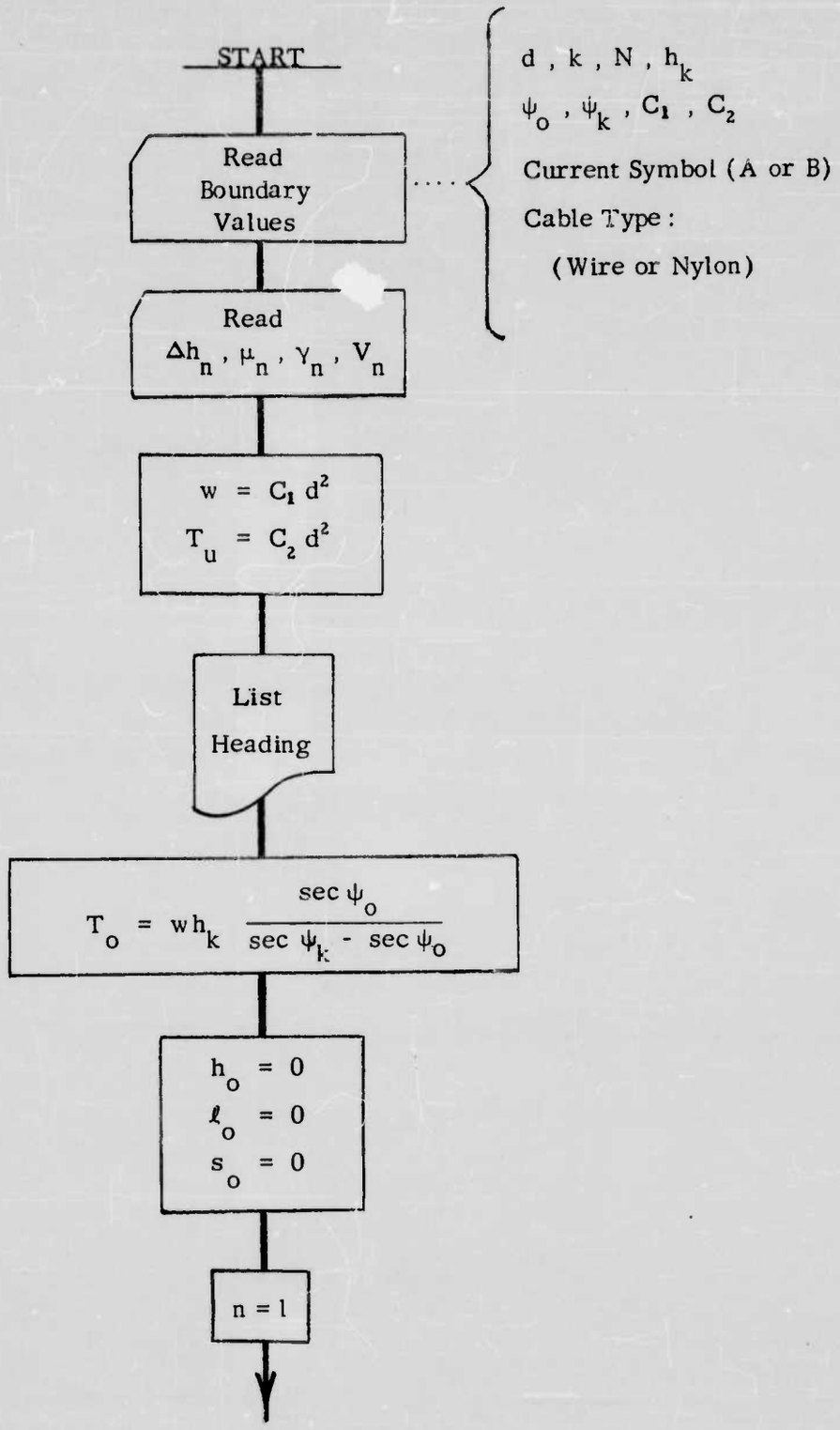

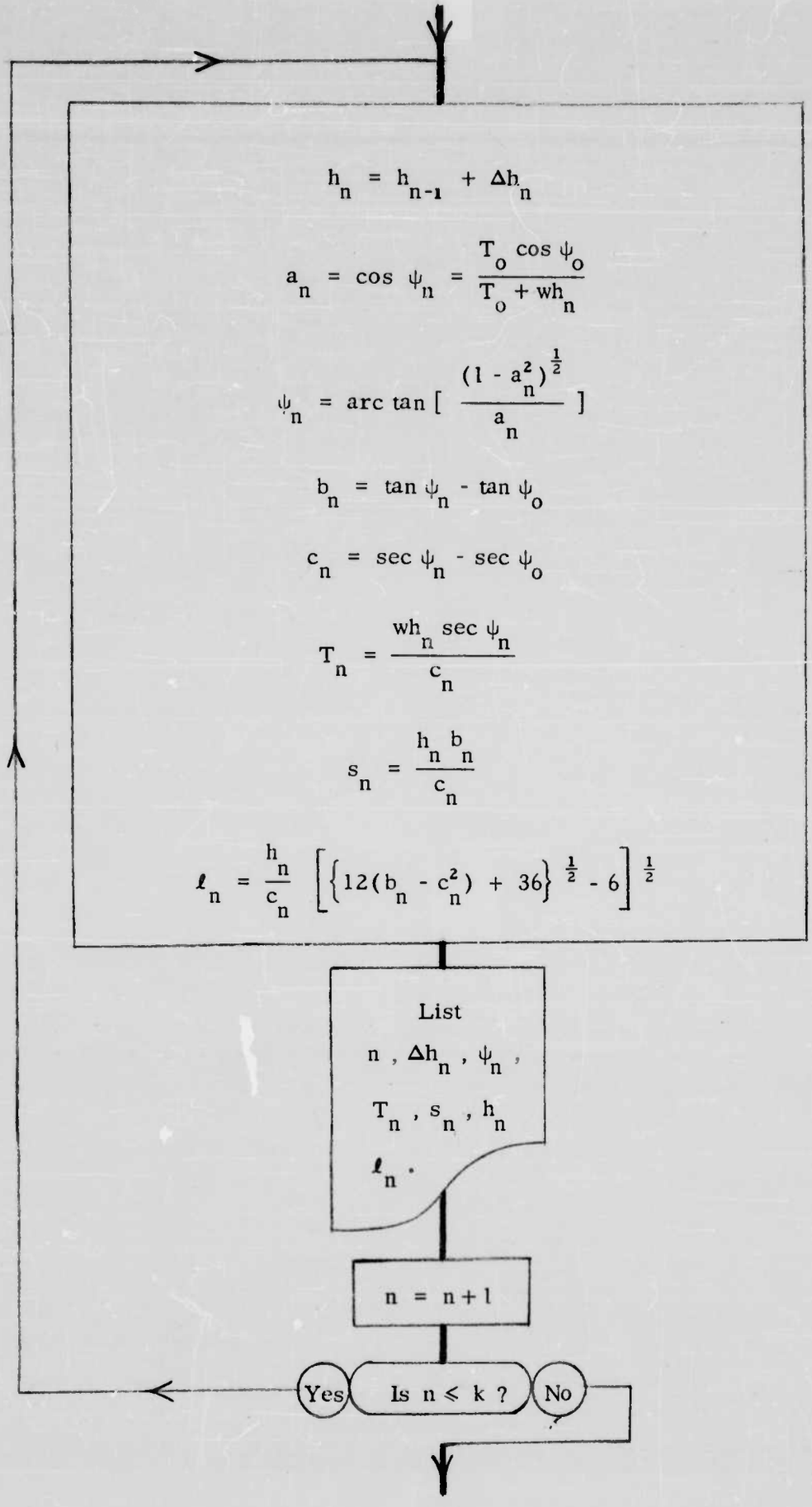
$h_n = h_{n-1} + \Delta h_n$
$a_n = \cos \psi_n = \frac{T_o \cos \psi_o}{T_o + wh_n}$
$\psi_n = \arctan \left[\frac{(1 - a_n^2)^{\frac{1}{2}}}{a_n} \right]$
$b_n = \tan \psi_n - \tan \psi_o$
$c_n = \sec \psi_n - \sec \psi_o$
$T_n = \frac{wh_n \sec \psi_n}{c_n}$
$s_n = \frac{h_n b_n}{c_n}$
$\ell_n = \frac{h_n}{c_n} \left[\left\{ 12(b_n - c_n^2) + 36 \right\}^{\frac{1}{2}} - 6 \right]^{\frac{1}{2}}$
List
n , Δh_n , ψ_n ,
T_n , s_n , h_n
ℓ_n .
$n = n+1$
Yes
Is $n \leq k$?
No

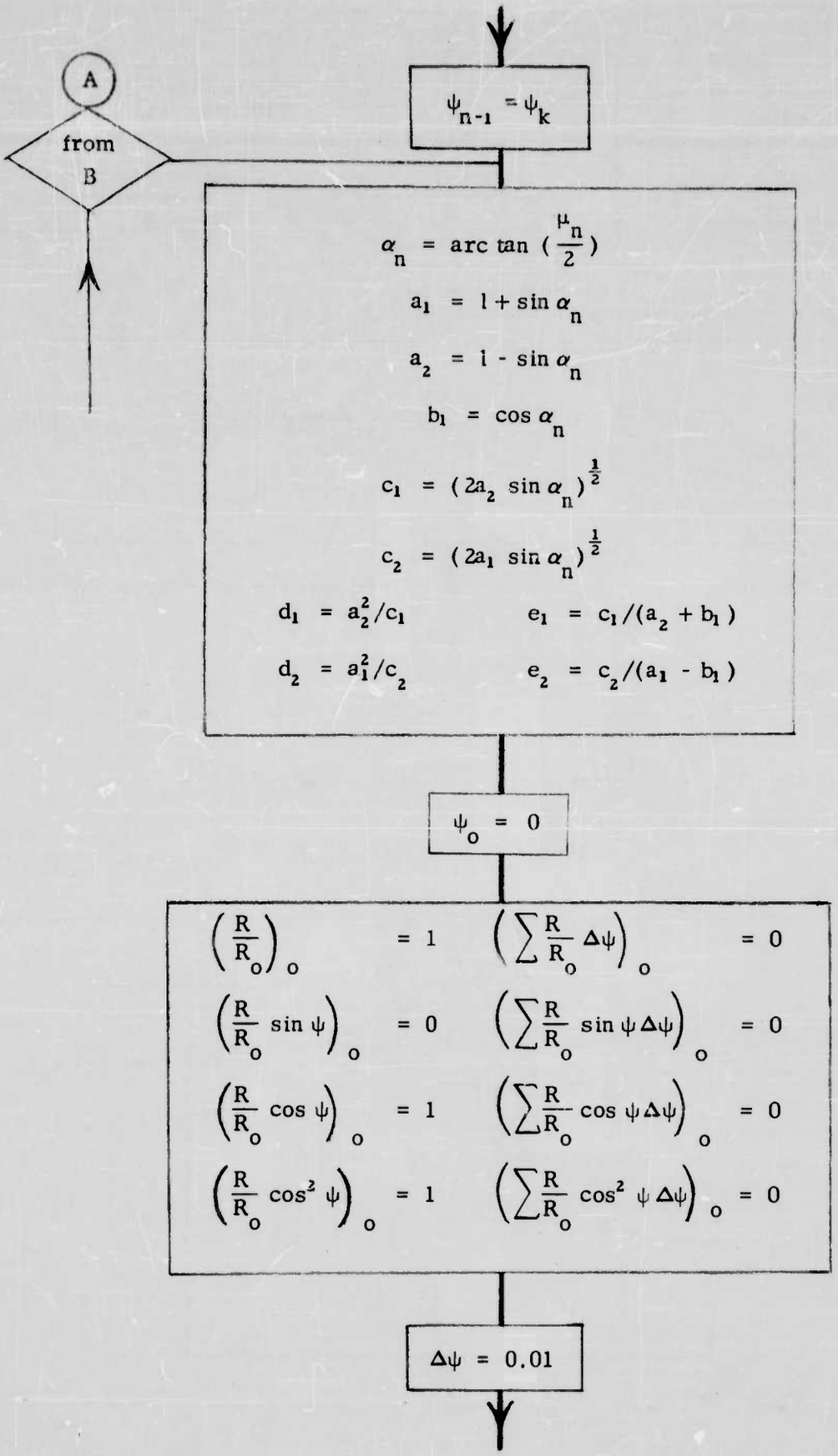
A
from B
$\psi_{n-1} = \psi_k$
$\alpha_n = \arctan\left(\frac{\mu_n}{2}\right)$
$a_1 = 1 + \sin\alpha_n$
$a_2 = 1 - \sin\alpha_n$
$b_1 = \cos\alpha_n$
$c_1 = (2a_2 \sin\alpha_n)^{\frac{1}{2}}$
$c_2 = (2a_1 \sin\alpha_n)^{\frac{1}{2}}$
$d_1 = a_2^2/c_1$
$e_1 = c_1/(a_2 + b_1)$
$d_2 = a_1^2/c_2$
$e_2 = c_2/(a_1 - b_1)$
$\psi_o = 0$
$\left(\frac{R}{R_o}\right)_o = 1$
$\left(\sum \frac{R}{R_o}\Delta\psi\right)_o = 0$
$\left(\frac{R}{R_o}\sin\psi\right)_o = 0$
$\left(\sum \frac{R}{R_o}\sin\psi\Delta\psi\right)_o = 0$
$\left(\frac{R}{R_o}\cos\psi\right)_o = 1$
$\left(\sum \frac{R}{R_o}\cos\psi\Delta\psi\right)_o = 0$
$\left(\frac{R}{R_o}\cos^2\psi\right)_o = 1$
$\left(\sum \frac{R}{R_o}\cos^2\psi\Delta\psi\right)_o = 0$
$\Delta\psi = 0.01$

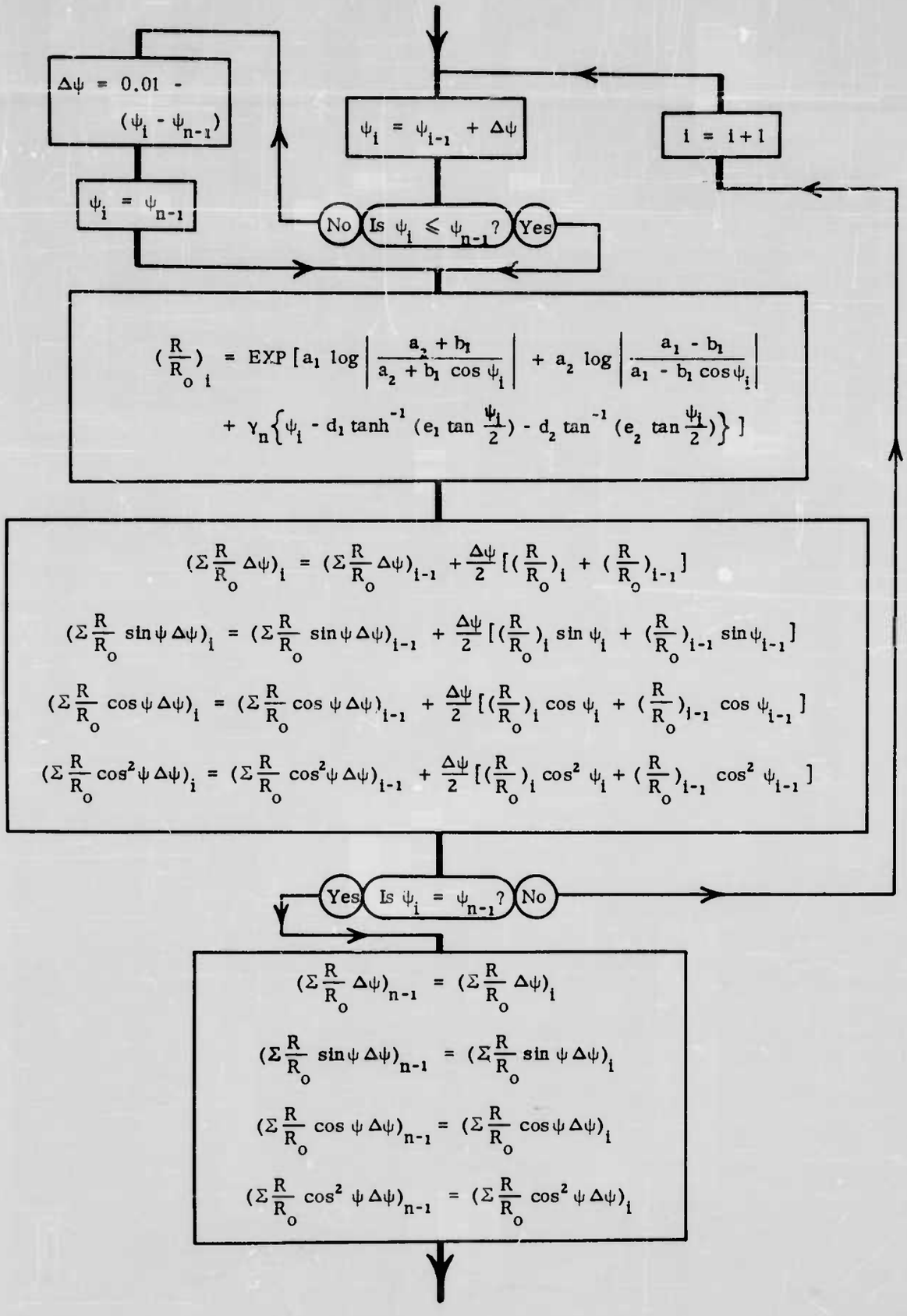
$\Delta\psi = 0.01 - (\psi_i - \psi_{n-1})$
$\psi_i = \psi_{n-1}$
$\psi_i = \psi_{i-1} + \Delta\psi$
$i = i+1$
No
Is $\psi_i \leq \psi_{n-1}$?
Yes
$(\frac{R}{R_o})_i = EXP[a_1 \log|\frac{a_2 + b_1}{a_2 + b_1 \cos\psi_i}| + a_2 \log|\frac{a_1 - b_1}{a_1 - b_1 \cos\psi_i}| + \gamma_n\{\psi_i - d_1 \tanh^{-1}(e_1 \tan\frac{\psi_i}{2}) - d_2 \tan^{-1}(e_2 \tan\frac{\psi_i}{2})\}]$
$(\Sigma\frac{R}{R_o}\Delta\psi)_i = (\Sigma\frac{R}{R_o}\Delta\psi)_{i-1} + \frac{\Delta\psi}{2}[(\frac{R}{R_o})_i + (\frac{R}{R_o})_{i-1}]$
$(\Sigma\frac{R}{R_o}\sin\psi\Delta\psi)_i = (\Sigma\frac{R}{R_o}\sin\psi\Delta\psi)_{i-1} + \frac{\Delta\psi}{2}[(\frac{R}{R_o})_i \sin\psi_i + (\frac{R}{R_o})_{i-1}\sin\psi_{i-1}]$
$(\Sigma\frac{R}{R_o}\cos\psi\Delta\psi)_i = (\Sigma\frac{R}{R_o}\cos\psi\Delta\psi)_{i-1} + \frac{\Delta\psi}{2}[(\frac{R}{R_o})_i \cos\psi_i + (\frac{R}{R_o})_{i-1}\cos\psi_{i-1}]$
$(\Sigma\frac{R}{R_o}\cos^2\psi\Delta\psi)_i = (\Sigma\frac{R}{R_o}\cos^2\psi\Delta\psi)_{i-1} + \frac{\Delta\psi}{2}[(\frac{R}{R_o})_i \cos^2\psi_i + (\frac{R}{R_o})_{i-1}\cos^2\psi_{i-1}]$
Yes
Is $\psi_i = \psi_{n-1}$?
No
$(\Sigma\frac{R}{R_o}\Delta\psi)_{n-1} = (\Sigma\frac{R}{R_o}\Delta\psi)_i$
$(\Sigma\frac{R}{R_o}\sin\psi\Delta\psi)_{n-1} = (\Sigma\frac{R}{R_o}\sin\psi\Delta\psi)_i$
$(\Sigma\frac{R}{R_o}\cos\psi\Delta\psi)_{n-1} = (\Sigma\frac{R}{R_o}\cos\psi\Delta\psi)_i$
$(\Sigma\frac{R}{R_o}\cos^2\psi\Delta\psi)_{n-1} = (\Sigma\frac{R}{R_o}\cos^2\psi\Delta\psi)_i$

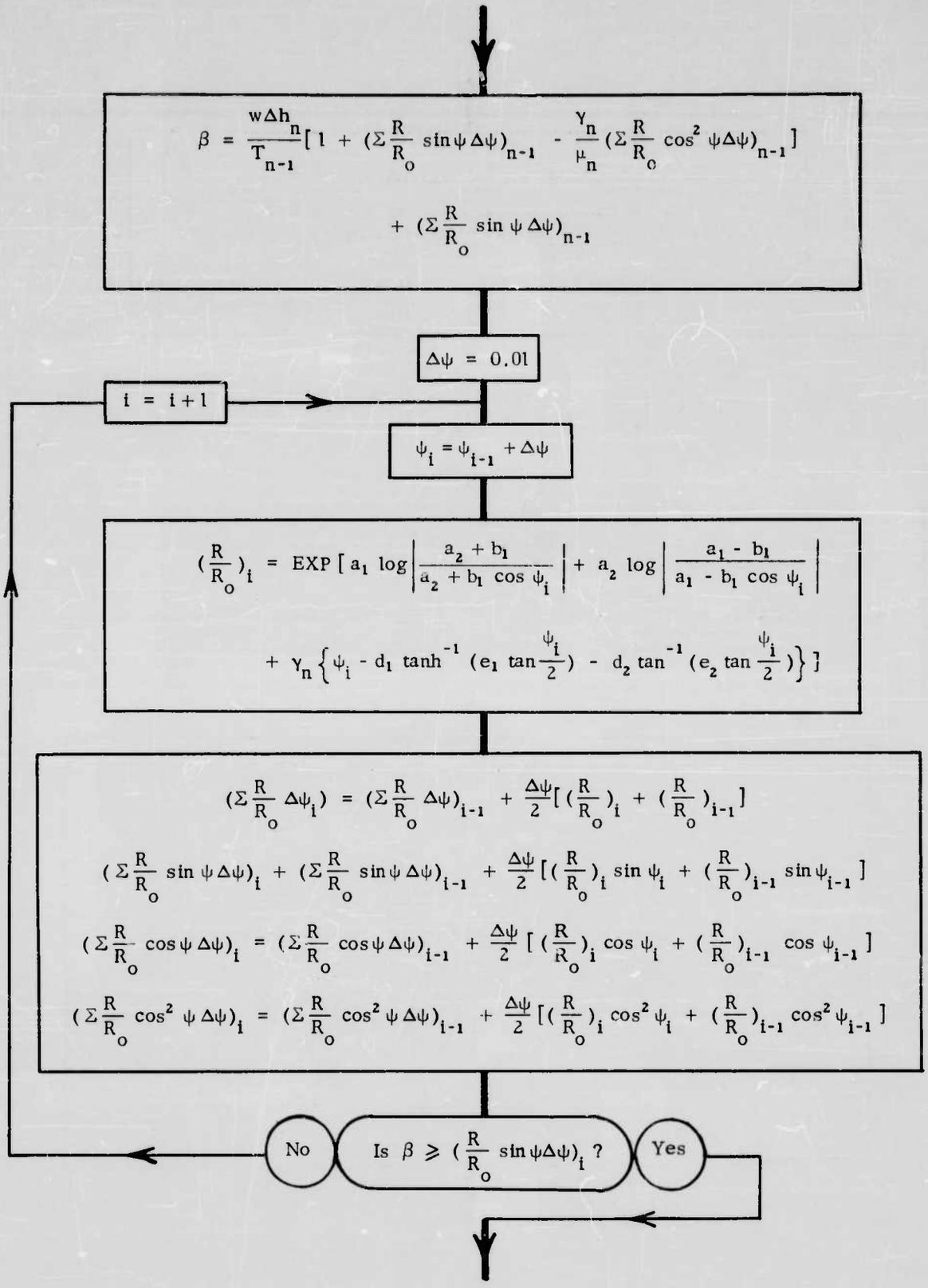
$\beta = \frac{w\Delta h_n}{T_{n-1}}[1 + (\Sigma \frac{R}{R_o} \sin\psi\Delta\psi)_{n-1} - \frac{\gamma_n}{\mu_n}(\Sigma \frac{R}{R_o} \cos^2\psi\Delta\psi)_{n-1}] + (\Sigma \frac{R}{R_o} \sin\psi\Delta\psi)_{n-1}$
$\Delta\psi = 0.01$
$i = i+1$
$\psi_i = \psi_{i-1} + \Delta\psi$
$(\frac{R}{R_o})_i = EXP[a_1 \log|\frac{a_2 + b_1}{a_2 + b_1 \cos\psi_i}| + a_2 \log|\frac{a_1 - b_1}{a_1 - b_1 \cos\psi_i}| + \gamma_n\{\psi_i - d_1 \tanh^{-1}(e_1 \tan\frac{\psi_i}{2}) - d_2 \tan^{-1}(e_2 \tan\frac{\psi_i}{2})\}]$
$(\Sigma \frac{R}{R_o} \Delta\psi_i) = (\Sigma \frac{R}{R_o} \Delta\psi)_{i-1} + \frac{\Delta\psi}{2}[(\frac{R}{R_o})_i + (\frac{R}{R_o})_{i-1}]$
$(\Sigma \frac{R}{R_o} \sin\psi\Delta\psi)_i = (\Sigma \frac{R}{R_o} \sin\psi\Delta\psi)_{i-1} + \frac{\Delta\psi}{2}[(\frac{R}{R_o})_i \sin\psi_i + (\frac{R}{R_o})_{i-1} \sin\psi_{i-1}]$
$(\Sigma \frac{R}{R_o} \cos\psi\Delta\psi)_i = (\Sigma \frac{R}{R_o} \cos\psi\Delta\psi)_{i-1} + \frac{\Delta\psi}{2}[(\frac{R}{R_o})_i \cos\psi_i + (\frac{R}{R_o})_{i-1} \cos\psi_{i-1}]$
$(\Sigma \frac{R}{R_o} \cos^2\psi\Delta\psi)_i = (\Sigma \frac{R}{R_o} \cos^2\psi\Delta\psi)_{i-1} + \frac{\Delta\psi}{2}[(\frac{R}{R_o})_i \cos^2\psi_i + (\frac{R}{R_o})_{i-1} \cos^2\psi_{i-1}]$
No
Is $\beta \geq (\frac{R}{R_o} \sin\psi\Delta\psi)_i$?
Yes

$$\epsilon_n = \frac{\beta - \left(\Sigma \frac{R}{R_o} \sin\psi\Delta\psi\right)_{i-1}}{\left(\Sigma \frac{R}{R_o} \sin\psi\Delta\psi\right)_i - \left(\Sigma \frac{R}{R_o} \sin\psi\Delta\psi\right)_{i-1}}$$

$$\left(\Sigma \frac{R}{R_o} \Delta\psi\right)_n = \left(\Sigma \frac{R}{R_o} \Delta\psi\right)_{i-1} + \epsilon_n\left[\left(\Sigma \frac{R}{R_o} \Delta\psi\right)_i - \left(\Sigma \frac{R}{R_o} \Delta\psi\right)_{i-1}\right]$$

$$\left(\Sigma \frac{R}{R_o} \sin\psi\Delta\psi\right)_n = \left(\Sigma \frac{R}{R_o} \sin\psi\Delta\psi\right)_{i-1} + \epsilon_n\left[\left(\Sigma \frac{R}{R_o} \sin\psi\Delta\psi\right)_i - \left(\Sigma \frac{R}{R_o} \sin\psi\Delta\psi\right)_{i-1}\right]$$

$$\left(\Sigma \frac{R}{R_o} \cos\psi\Delta\psi\right)_n = \left(\Sigma \frac{R}{R_o} \cos\psi\Delta\psi\right)_{i-1} + \epsilon_n\left[\left(\Sigma \frac{R}{R_o} \cos\psi\Delta\psi\right)_i - \left(\Sigma \frac{R}{R_o} \cos\psi\Delta\psi\right)_{i-1}\right]$$

$$\left(\Sigma \frac{R}{R_o} \cos^2\psi\Delta\psi\right)_n = \left(\Sigma \frac{R}{R_o} \cos^2\psi\Delta\psi\right)_{i-1} + \epsilon_n\left[\left(\Sigma \frac{R}{R_o} \cos^2\psi\Delta\psi\right)_i - \left(\Sigma \frac{R}{R_o} \cos^2\psi\Delta\psi\right)_{i-1}\right]$$

$$\Delta s_n = \frac{\Delta h_n\left[\left(\Sigma \frac{R}{R_o} \Delta\psi\right)_n - \left(\Sigma \frac{R}{R_o} \Delta\psi\right)_{n-1}\right]}{\left(\Sigma \frac{R}{R_o} \sin\psi\Delta\psi\right)_n - \left(\Sigma \frac{R}{R_o} \sin\psi\Delta\psi\right)_{n-1}}$$

$$\Delta l_n = \frac{\Delta h_n\left[\left(\Sigma \frac{R}{R_o} \cos\psi\Delta\psi\right)_n - \left(\Sigma \frac{R}{R_o} \cos\psi\Delta\psi\right)_{n-1}\right]}{\left(\Sigma \frac{R}{R_o} \sin\psi\Delta\psi\right)_n - \left(\Sigma \frac{R}{R_o} \sin\psi\Delta\psi\right)_{n-1}}$$

$$\Delta T_n = \frac{w\gamma_n \Delta h_n \left[\left(\Sigma \frac{R}{R_o} \cos^2\psi\Delta\psi\right)_n - \left(\Sigma \frac{R}{R_o} \cos^2\psi\Delta\psi\right)_{n-1}\right]}{\mu_n\left[\left(\Sigma \frac{R}{R_o} \sin\psi\Delta\psi\right)_n - \left(\Sigma \frac{R}{R_o} \sin\psi\Delta\psi\right)_{n-1}\right]}$$

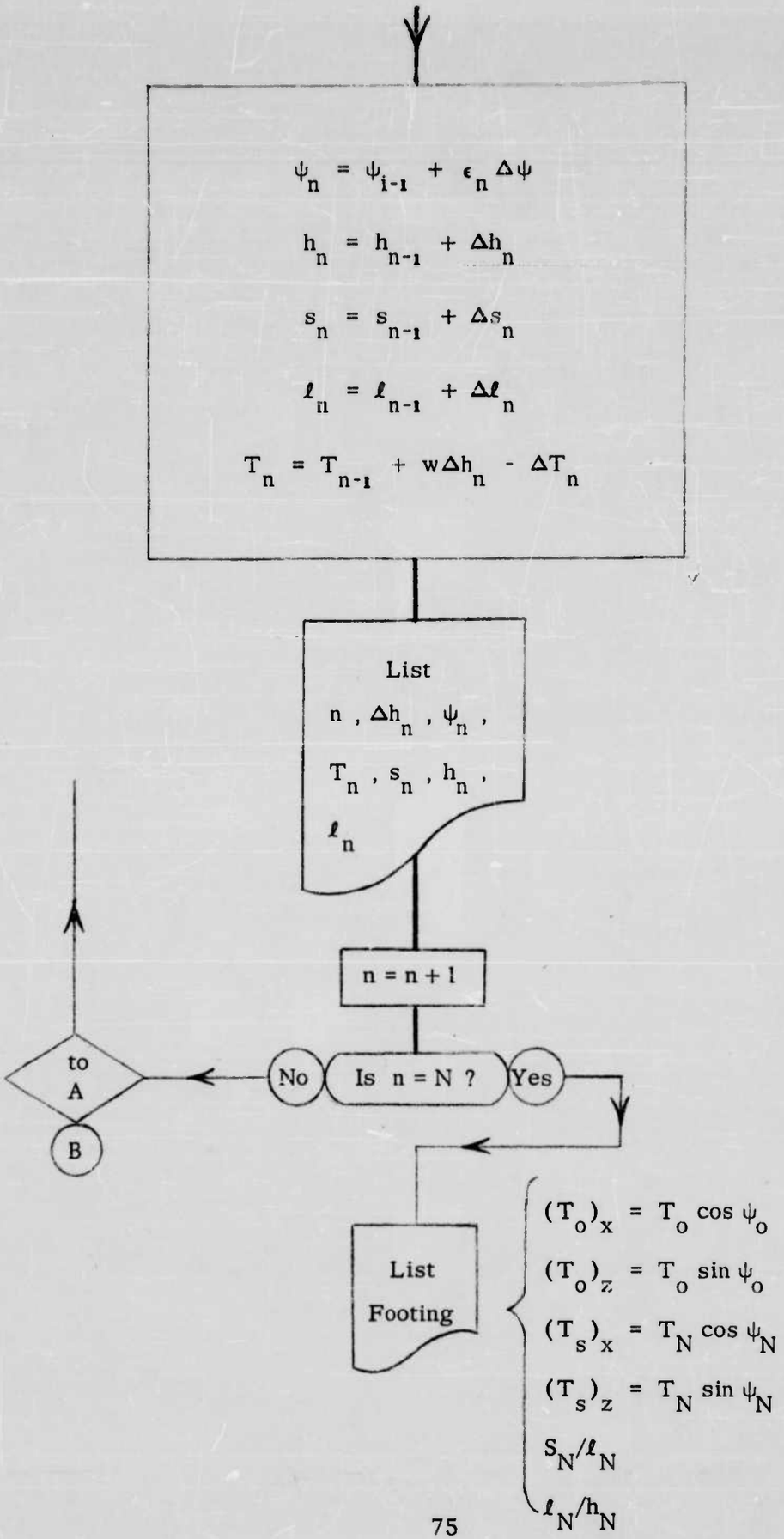
$\psi_n = \psi_{i-1} + \epsilon_n \Delta\psi$
$h_n = h_{n-1} + \Delta h_n$
$s_n = s_{n-1} + \Delta s_n$
$\ell_n = \ell_{n-1} + \Delta \ell_n$
$T_n = T_{n-1} + w\Delta h_n - \Delta T_n$
List
n , Δh_n , ψ_n ,
T_n , s_n , h_n ,
ℓ_n
$n = n + 1$
Is $n = N$?
No
Yes
to A
B
List Footing
$(T_o)_x = T_o \cos \psi_o$
$(T_o)_z = T_o \sin \psi_o$
$(T_s)_x = T_N \cos \psi_N$
$(T_s)_z = T_N \sin \psi_N$
S_N/ℓ_N
ℓ_N/h_N

LIST OF SYMBOLS

a_1, a_2	coefficients defined by Eqs. (3 i) and (3 ii)
a_n	function defined by Eq. (17 ii)
A_b	projected area of cylindrical buoy on a diametral plane incorporating the axis of the cylinder
A_d	projected area of drogue-anchor in vertical plane normal to drift
A_m	area of wetted midship cross-section of ship
A_p	transverse projected area of a ship above the water line
A_w	area of wetted surface of ship
b	function defined by Eq. 8(ii)
b_1	coefficient defined by Eq. (3 iii)
b_n	value of b at the point n on the cable [$n < k$]
B	(1) beam of a ship; (2) buoyancy of a submerged buoy
c	function defined by Eq. (8 iii)
c_1, c_2	coefficients defined by Eqs. (3 iv) and (3 v)
c_n	value of c at the point n on the cable [$n < k$]
C_1, C_2	coefficients of proportionality [Eqs. (46) and (50)]
C_D	dimensionless drag coefficient
C'_D	dimensional drag coefficient for normal flow [$= \frac{\rho_w}{2} C_D$]
C''_D	dimensional drag coefficient for tangential flow [$= \gamma C'_D$]
$[C_D]_a$	value of C_D as applicable to air flow over land
$[C_D]_w$	value of C_D as applicable to flow of water over rough plates
d	cable or rope diameter
d_1, d_2	coefficients defined by Eqs. (3 vi) and (3 vii)

D	loaded draft of a ship
D_b	diameter of cylindrical buoy
e_1, e_2	coefficients defined by Eqs. (3viii) and (3ix)
F_c	drag on a moored ship or buoy from the current flowing past it
F_d	horizontal drag on the drogue-anchor from its drift through still water
F_w	horizontal drag on a ship from a head wind
h	total water depth; also vertical projection of cable length
h_k	height of level of no-motion above sea-bed
h_N	height of upper terminal point of cable above sea-bed
Δh_n	depth of n-th fluid lamina
H	(1) holding power of an anchor (resistance to drag) over the sea-bed (2) wave height [Eq. (44)]
i	integer subscript of value 0,1,2,3...
k	integer defining level of no-motion between surface current and motionless bottom water
ℓ	horizontal projection of cable length
ℓ_k	horizontal projection of portion of cable below point k
ℓ_n	horizontal projection of portion of cable below point n
ℓ_N	horizontal projection of entire length of cable
$\Delta\ell_n$	horizontal projection of cable traversing the n-th fluid lamina
L	length of ship between perpendiculars
n	integer defining point of intersection of cable with upper boundary of fluid lamina
N	integer defining upper terminal point of cable
p	integer, particular value of i [$p < q$] for which $\psi_{p-1} < \psi_{n-1} < \psi_p$

q	integer, particular value of i [$> p$] for which $\psi_{q-1} < \psi_n < \psi_q$
R	radius of curvature at any point of a suspended cable
R_o	value of R at point where cable slope is horizontal or would be horizontal if cable were extended hypothetically
$[R]_n$	Reynolds Number for the horizontal flow round a circular cylindrical buoy, prevailing in the n-th fluid lamina.
s	distance along suspended cable from reference origin to any point
s_n	value of s to the point n on the cable
Δs_n	length of cable traversing the n-th fluid lamina
S	total length of cable suspended between two points [Fig 1]
S_N	total length of cable between terminals O and N [Fig 2]
T	(1) tension in cable at any point; (2) wave period [Eq. (44)]
T_{av}	average value of T along the length of the cable
T_1	value of T at lower terminal point or anchor [Fig 1]
T_B	value of T at the point B
T_n	value of T at any point n of the cable at upper boundary of n-th fluid lamina
T_{n-1}	value of T at point $(n - 1)$ at lower boundary of n-th fluid lamina
T_N	value of T at upper terminal point N of the cable
T_o	value of T at lower terminal point $(n = 0)$ or anchor [Fig 2]
$(T_o)_x, (T_o)_z$	components of T_o in horizontal x-direction and vertical z-direction
T_s	value of T at ship or sea-surface
ΔT_s	function defined by Eq. (7 ii)
$(T_s)_x, (T_s)_z$	components of T_s in horizontal x-direction and vertical z-direction
T_u	ultimate strength of cable; tension at failure

ΔT_n	increment of tension defined by Eq. (31 iii)
u_1	velocity of water acquired under action of wind stress
u_2	velocity of water acquired from mass transport in wave motion
U	surface wind velocity, normally considered at 10 m elevation
v	drift velocity of a ship with drogue-mooring
V	horizontal velocity of water in an ocean current
V_n	value of V prevailing in the n-th fluid lamina
V_s	value of V at the sea surface
w	weight per unit length in water of mooring cable
w_a	weight per unit length in air of mooring cable
W	displacement tonnage of a ship
W_a	weight of an anchor in water
W_c	weight of a clump in water
W_d	weight of a drogue-anchor in water
x, x'	variable horizontal distance referred to origin of reference
z, z'	variable vertical distance referred to origin of reference
α	dimensionless equivalent angle defined by Eq. (2 i)
α_n	value of α prevailing in the n-th fluid lamina
β	dimensionsionless quantity defined by Eq. (27 i)
γ	dimensionless ratio of drag coefficients $\left[= \frac{C''_D}{C'_D} \right]$
γ_n	value of γ prevailing in the n-th fluid lamina
ϵ_n	numerical fraction of $\Delta\psi$ such that $\psi_{q-1} + \epsilon_n \Delta\psi = \psi_n$
ϵ_{n-1}	numerical fraction of $\Delta\psi$ such that $\psi_{p-1} + \epsilon_{n-1} \Delta\psi = \psi_{n-1}$

ζ	factor to allow for increase of current drag on a ship from locked propellors
θ	safety factor against rope failure [= T_u/T]
μ	hydrodynamic constant defined by Eq. (2ii)
μ_n	value of μ prevailing in the n-th fluid lamina
ν	kinematic viscosity of sea water
ρ_a	mass density of air
ρ_w	mass density of sea water
τ_a	surface shear stress of wind (air) over open land
τ_w	surface shear stress of water flowing over a rough plate
ϕ	angle of latitude
ψ	variable angle of cable inclination with the horizontal [$< 90°$]
ψ_o	value of ψ at the lower terminal or anchor of the cable [Fig 2]
ψ_1	value of ψ at the anchor [Fig 1, early representation]
ψ_i	angle defined by $\psi_i = i\Delta\psi$
ψ_{i-1}	angle defined by $\psi_{i-1} = \psi_i - \Delta\psi$
ψ_k	value of ψ prevailing at the level of no-motion, k
ψ_n	value of ψ prevailing at upper boundary of n-th fluid lamina
ψ_{n-1}	value of ψ prevailing at lower boundary of n-th fluid lamina
ψ_N	value of ψ at upper terminal point of the cable
ψ_s	value of ψ at the ship or sea-surface
$\Delta\psi$	small increment of angle [= 0.01 radian]

DISTRIBUTION LIST

No. of Copies	Navy
50	Commanding Officer and Director (Principal Sponsor) David Taylor Model Basin Code 513 Washington 7, D. C.
6	Chief, Bureau of Ships Navy Department Code 312 Washington 25, D. C.
1	Commanding Officer and Director U. S. Navy Electronics Laboratory San Diego 52, California
1	Commanding Officer and Director U. S. Navy Underwater Sound Laboratory New London, Connecticut
4	Chief of Naval Research Washington 25, D. C.
3	Chief, Bureau of Yards and Docks Navy Department Washington 25, D. C.
2	Commanding Officer and Director U. S. Naval Civil Engineering Laboratory Port Hueneme, California
1	Chief, Bureau Naval Weapons Navy Department Washington 25, D. C.
1	Commander U. S. Navy Ordnance Laboratory White Oak Silver Spring, Maryland

No. of Copies	
1	Director U. S. Naval Engineering Experiment Station Annapolis, Maryland
1	Commander Boston Naval Shipyards Boston 29, Massachusetts
1	Commander Charleston Naval Shipyard Charleston, South Carolina
1	Commander Marine Island Shipyard Vallejo, California
1	Commander New York Naval Shipyard Brooklyn, New York
1	Commander Norfolk Naval Shipyard Portsmouth, Virginia
1	Commander Puget Sound Naval Shipyard Bremerton, Washington
1	Commander Pearl Harbor Naval Shipyard Navy No. 128, Fleet Post Office San Francisco, California

No. of Copies	Navy
1	Commander San Francisco Naval Shipyard San Francisco, California
1	Commander Long Beach Naval Shipyard Long Beach, California
1	U. S. Navy Hydrographer Navy Department Washington 25, D. C.
1	Department of Meteorology & Oceanography U. S. Naval Post Graduate School Monterrey, California
12	General Manager (Second Sponsor) South African Railways and Harbours Johannesburg, Union of South Africa
	Army
1	Beach Erosion Board Corps of Engineers U. S. Army 5201 Little Falls Rd., N.W. Washington 16, D. C.
1	U. S. Director Waterways Experiment Station Corps of Engineers, U. S. Army P. O. Box 637 Vicksburg, Mississippi
1	Commanding General Research and Development Division Department of the Army
1	Chief of Engineers Department of the Army Washington 25, D. C.

No. of Copies	Other Government Agencies
1	National Hydraulic Laboratory Bureau of Standards Washington 25, D. C.
1	U. S. Coast and Geodetic Survey Washington 25, D. C.
10	Commander Armed Services Technical Information Agency Arlington Hall Station Arlington 12, Virginia
1	Commandant (OAO) U. S. Coast Guard Washington 25, D. C.
1	Library of Congress Washington 25, D. C.
	Research Institutions
1	Scripps Institution of Oceanography University of California La Jolla, California
1	Woods Hole Oceanographic Institute Woods Hole, Massachusetts
1	Chesapeake Bay Institute John Hopkins University Baltimore, Maryland
1	Department of Oceanography University of Washington Seattle, Washington
1	Department of Oceanography Oregon State College Corvallis, Oregon
1	Oceanographic Institute Florida State University Tallahassee, Florida

No. of Copies	Research Institutions
1	Department of Meteorology and Oceanography New York University University Heights New York, New York
1	Lamont Geological Observatory Columbia University Palisades, New York
1	Lake Research Institute University of Michigan Ann Arbor, Michigan
1	Coastal Engineering Laboratory University of Florida Gainsville, Florida
3	National Engineering Science Company 511 South Fair Oaks Avenue Pasadena, California
1	Department of Civil Engineering Princeton University Princeton, New Jersey
1	Hydrodynamics Laboratory California Institute of Technology Pasadena, California
1	Department of Civil Engineering University of Illinois Urbana, Illinois
1	Experimental Towing Tank Stevens Institute Technology Hoboken, New Jersey
1	Department of Naval Architecture and Marine Engineering Massachusetts Institute of Technology Cambridge 39, Massachusetts
1	Department of Naval Architecture University of Michigan Ann Arbor, Michigan
1	Hydrodynamics Laboratory Massachusetts Institute of Technology Cambridge, Massachusetts
1	Institute of Engineering Research University of California Berkeley, California
1	St. Anthony Falls Hydraulic Laboratory University of Minnesota Minneapolis, Minnesota
1	Southwest Research Institute 8500 Culebra Road San Antonio, Texas
1	Engineering Society Library 29 West 39th Street New York 18, New York
1	Dr. Louis Landweber Iowa Inst. of Hydraulic Research University of Iowa Iowa City, Iowa
1	Dr. Leonard Pode Voi-Shan Electronics 13259 Sherman Way North Hollywood, California
1	Dr. Thomas E. Stelson Head, Department of Civil Engineering Carnegie Institute of Technology Pittsburg 13, Pennsylvania

No. of Copies	Research Institutions
1	National Institute Oceanography Wormley, nr. Godalming Kent, England
1	Hydraulic Research Station Howbery Park Wallingford, Berks, England
2	Texas A & M Research Foundation College Station, Texas
10	Department of Oceanography and Meteorology A. & M. College of Texas College Station, Texas Cushing Library Engineers Library Galveston Marine Laboratory

Technical Report No. 204-3

ERRATA

p. 51 Problem No. 1, line (iii)
"displacemtn" should read "displacement"

p. 53 Table VIII, Column 4
Add + in front of 20%

p. 58 Second line from bottom
Insert 3 in $\Psi_o = 53^{\circ} \pm 0.5$

p. xi Address of National Engineering Science Company should read:
711 South Fair Oaks Avenue
Pasadena, California

Dept. of Oceanography and Meteorology, Agricultural and Mechanical College of Texas (Texas A & M Research Foundation), Tech. Report No. 204-3 and 204-3A (Ref. 61-1T).
CHARACTERISTICS OF DEEP-SEA ANCHOR-CABLES IN STRONG OCEAN CURRENTS by Basil W. Wilson
March, 1961, 80 pp. (204-3); 266 pp. (204-3A).

UNCLASSIFIED

This report and its companion (Table of Values) investigate the deep-sea mooring of ships and objects in steady ocean currents (with or without collinear winds) that are non-uniform with the depth, taken nominally as 12,000 ft. The characteristics of steel wire and nylon rope mooring cables of various sizes in strong currents such as the Gulf Stream are evaluated in tabular form. Examples are given of the use of the tables in solution of mooring problems.

1. Ships - Mooring - Theory
2. Mooring Cables - Hydrodynamic characteristics - Mathematical analysis
3. Ocean currents

I. Wilson, Basil W.

Dept. of Oceanography and Meteorology, Agricultural and Mechanical College of Texas (Texas A & M Research Foundation), Tech. Report No. 204-3 and 204-3A (Ref. 61-1T).
CHARACTERISTICS OF DEEP-SEA ANCHOR-CABLES IN STRONG OCEAN CURRENTS by Basil W. Wilson
March, 1961, 80 pp. (204-3); 266 pp. (204-3A).

UNCLASSIFIED

This report and its companion (Table of Values) investigate the deep-sea mooring of ships and objects in steady ocean currents (with or without collinear winds) that are non-uniform with the depth, taken nominally as 12,000 ft. The characteristics of steel wire and nylon rope mooring cables of various sizes in strong currents such as the Gulf Stream are evaluated in tabular form. Examples are given of the use of the tables in solution of mooring problems.

1. Ships - Mooring - Theory
2. Mooring Cables - Hydrodynamic characteristics - Mathematical analysis
3. Ocean currents

I. Wilson, Basil W.

Dept. of Oceanography and Meteorology, Agricultural and Mechanical College of Texas (Texas A & M Research Foundation), Tech. Report No. 204-3A (Ref. 61-1T).
CHARACTERISTICS OF DEEP-SEA ANCHOR-CABLES IN STRONG OCEAN CURRENTS by Basil W. Wilson
March, 1961, 80 pp. (204-3); 266 pp. (204-3A).

UNCLASSIFIED

This report and its companion (Table of Values) investigate the deep-sea mooring of ships and objects in steady ocean currents (with or without collinear winds) that are non-uniform with the depth, taken nominally as 12,000 ft. The characteristics of steel wire and nylon rope mooring cables of various sizes in strong currents such as the Gulf Stream are evaluated in tabular form. Examples are given of the use of the tables in solution of mooring problems.

1. Ships - Mooring - Theory
2. Mooring Cables - Hydrodynamic characteristics - Mathematical analysis
3. Ocean currents

I. Wilson, Basil W.

Dept. of Oceanography and Meteorology, Agricultural and Mechanical College of Texas (Texas A & M Research Foundation), Tech. Report No. 204-3 and 204-3A (Ref. 61-1T).
CHARACTERISTICS OF DEEP-SEA ANCHOR-CABLES IN STRONG OCEAN CURRENTS by Basil W. Wilson
March, 1961, 80 pp. (204-3); 266 pp. (204-3A).

UNCLASSIFIED

This report and its companion (Table of Values) investigate the deep-sea mooring of ships and objects in steady ocean currents (with or without collinear winds) that are non-uniform with the depth, taken nominally as 12,000 ft. The characteristics of steel wire and nylon rope mooring cables of various sizes in strong currents such as the Gulf Stream are evaluated in tabular form. Examples are given of the use of the tables in solution of mooring problems.

1. Ships - Mooring - Theory
2. Mooring Cables - Hydrodynamic characteristics - Mathematical analysis
3. Ocean currents

I. Wilson, Basil W.

Dept. of Oceanography and Meteorology, Agricultural and Mechanical College of Texas (Texas A & M Research Foundation), Tech. Report No. 204-3 and 204-3A (Ref. 61-1T).
CHARACTERISTICS OF DEEP-SEA ANCHOR-CABLES IN STRONG OCEAN CURRENTS by Basil W. Wilson
March, 1961, 80 pp. (204-3); 266 pp. (204-3A).

UNCLASSIFIED

This report and its companion (Table of Values) investigate the deep-sea mooring of ships and objects in steady ocean currents (with or without collinear winds) that are non-uniform with the depth, taken nominally as 12,000 ft. The characteristics of steel wire and nylon rope mooring cables of various sizes in strong currents such as the Gulf Stream are evaluated in tabular form. Examples are given of the use of the tables in solution of mooring problems.

1. Ships - Mooring - Theory
2. Mooring Cables - Hydrodynamic characteristics - Mathematical analysis
3. Ocean currents

I. Wilson, Basil W.

Dept. of Oceanography and Meteorology, Agricultural and Mechanical College of Texas (Texas A & M Research Foundation), Tech. Report No. 204-3 and 204-3A (Ref. 61-1T).
CHARACTERISTICS OF DEEP-SEA ANCHOR-CABLES IN STRONG OCEAN CURRENTS by Basil W. Wilson
March, 1961, 80 pp. (204-3); 266 pp. (204-3A).

UNCLASSIFIED

This report and its companion (Table of Values) investigate the deep-sea mooring of ships and objects in steady ocean currents (with or without collinear winds) that are non-uniform with the depth, taken nominally as 12,000 ft. The characteristics of steel wire and nylon rope mooring cables of various sizes in strong currents such as the Gulf Stream are evaluated in tabular form. Examples are given of the use of the tables in solution of mooring problems.

1. Ships - Mooring - Theory
2. Mooring Cables - Hydrodynamic characteristics - Mathematical analysis
3. Ocean currents

I. Wilson, Basil W.

Dept. of Oceanography and Meteorology, Agricultural and Mechanical College of Texas (Texas A & M Research Foundation), Tech. Report No. 204-3A (Ref. 61-1T).
CHARACTERISTICS OF DEEP-SEA ANCHOR-CABLES IN STRONG OCEAN CURRENTS by Basil W. Wilson
March, 1961, 80 pp. (204-3); 266 pp. (204-3A).

UNCLASSIFIED

This report and its companion (Table of Values) investigate the deep-sea mooring of ships and objects in steady ocean currents (with or without collinear winds) that are non-uniform with the depth, taken nominally as 12,000 ft. The characteristics of steel wire and nylon rope mooring cables of various sizes in strong currents such as the Gulf Stream are evaluated in tabular form. Examples are given of the use of the tables in solution of mooring problems.

1. Ships - Mooring - Theory
2. Mooring Cables - Hydrodynamic characteristics - Mathematical analysis
3. Ocean currents

I. Wilson, Basil W.

Dept. of Oceanography and Meteorology, Agricultural and Mechanical College of Texas (Texas A & M Research Foundation), Tech. Report No. 204-3 and 204-3A (Ref. 61-1T).
CHARACTERISTICS OF DEEP-SEA ANCHOR-CABLES IN STRONG OCEAN CURRENTS by Basil W. Wilson
March, 1961, 80 pp. (204-3); 266 pp. (204-3A).

UNCLASSIFIED

This report and its companion (Table of Values) investigate the deep-sea mooring of ships and objects in steady ocean currents (with or without collinear winds) that are non-uniform with the depth, taken nominally as 12,000 ft. The characteristics of steel wire and nylon rope mooring cables of various sizes in strong currents such as the Gulf Stream are evaluated in tabular form. Examples are given of the use of the tables in solution of mooring problems.

1. Ships - Mooring - Theory
2. Mooring Cables - Hydrodynamic characteristics - Mathematical analysis
3. Ocean currents

I. Wilson, Basil W.